

**MECHANICS OF SPASTIC MUSCLE AND EFFECTS OF
TREATMENT TECHNIQUES: ASSESSMENTS WITH
INTRA-OPERATIVE AND ANIMAL EXPERIMENTS**

by

Filiz Ateş

B.Sc., Electronics Engineering, İstanbul University, 2003

M.Sc., Biomedical Engineering, Boğaziçi University, 2005

Submitted to the Institute of Biomedical Engineering

in partial fulfillment of the requirements

for the degree of

Doctor

of

Philosophy

Boğaziçi University

2013

**MECHANICS OF SPASTIC MUSCLE AND EFFECTS OF
TREATMENT TECHNIQUES: ASSESSMENTS WITH
INTRA-OPERATIVE AND ANIMAL EXPERIMENTS**

APPROVED BY:

Assoc. Prof. Dr. Can Ali Yücesoy
(Thesis Advisor)

Prof. Dr. Cengizhan Öztürk

Prof. Dr. Mehmed Özkan

Prof. Dr. Muharrem İnan

Assoc. Prof. Dr. Umut Akgün

DATE OF APPROVAL: 23 January 2013

ACKNOWLEDGMENTS

It is with immense gratitude that I acknowledge the support and help of my supervisor Assoc. Prof. Dr. Can A. Yücesoy. This thesis would not have been possible without his great efforts.

I wish to thank Prof. Dr. Peter Huijing for his guidance and valuable suggestions and also Guus Baan for his continual and precious help during animal surgery.

I owe my sincere thanks to Prof. Dr. Cengizhan Öztürk and Prof. Dr. Mehmed Özkan for being in the thesis progress committee and for the helpful suggestions during this period.

It gives me great pleasure in acknowledging the support and help of Prof. Dr. Mustafa Karahan and his team in Marmara University, Medical School, Department of Orthopedics and Traumatology, and also Assoc. Prof. Dr. Umut Akgün, who made incredible contributions.

I am indebted to our collaborators Prof. Dr. Yener Temelli, and his team in Istanbul University, Istanbul Medical School, Department of Orthopedics and Traumatology and also Assoc. Prof. Ekin Akalan for their helps during the collaboration.

I would like to thank Adnan Kurt for designing novel instruments for our experiments and solving the problems in setup with his incredible talent. I also wish to thank Renan Mert Özel for the helps during data processing.

I wish to thank the members of the crew of Biomechanics Laboratory; Ahu Nur Türkoğlu, Uluç Pamuk, Sevgi Umur, Alper Yaman, Önder Emre Arıkan, Selen Ersoy, Rana N. Özdeşlik, Gülay Hocaoğlu, Arda Arpak, F. Oya Aytürk, Zeynep Susam, Begüm Anlar, Y. Turgay Ertugay, Gizem Sarıbaş, Ferah İlhan, Zeynep Şeref Ferlencez,

Bora Yaman. “*Once a biomechanics lab member, always a biomechanics lab member*”

I owe special thanks to my friends Nermin Topalođlu, Adu Nur Tırkođlu, Murat Tümer, Ayşe Sena Kabaş Sarp, Didar Talat, Burcu Tunç, Muhammed Avşar, Sevinç Mutlu, Mehmet Kocatürk, Eda Çapa, Bora Büyüksaraç, Özlem Özmen Okur, Esin Karahan, Meltem Sevgi, Özgür Tabakođlu, Mehmet Yumak, Mustafa Kemal Ruhi, Engin Baysoy with whom we crossed paths at the Institute of Biomedical Engineering.

I warmly thank to my friends Selcan Çınar, Şule Süzük, Özüm Seda Duran, Özge Özyılmaz, Sergül Aydore, Merve Arkan, Burçin Duan, Gülay Tezgel for making life more bearable.

This thesis would not have been possible unless the support and love of Ateş family; my parents Nimet and Adem, my siblings Ali Murat, Fatih, Mehmet Yavuz, my sister in law Özlem, and my nephews Atahan, Alper Kaan.

Abstract

MECHANICS OF SPASTIC MUSCLE AND EFFECTS OF TREATMENT TECHNIQUES: ASSESSMENTS WITH INTRA-OPERATIVE AND ANIMAL EXPERIMENTS

Present thesis is focused on mechanics of spastic human muscles and the effects of widely used treatment methods in the context of the determinant role of epimuscular myofascial force transmission (EMFT). A novel intra-operative method was developed to measure human Gracilis (GRA) muscle isometric forces with respect to knee angle. In healthy subjects, GRA was shown to have very large operational length range. For spastic cerebral palsy patients on the other hand, GRA muscle did not show “abnormal” mechanical characteristics: (i) Length range was not narrowed and (ii) high flexion forces were not available. Such abnormality occurred if its antagonist vastus medialis is activated simultaneously. Therefore, EMFT mechanism through inter-antagonistic interaction was suggested to determine human muscle characteristics in spasticity. Effects of treatment methods were investigated in animal experiments: (1) Muscle lengthening surgery was shown to affect (i) proximal and distal sides differentially and (ii) non-operated neighboring muscle as well. (2) Botulinum Toxin Type-A (BTX-A) administration was shown to change the mechanics of not only the injected but also non-injected muscles in conditions close to in vivo. Additional to active force reductions (i) the narrowed length range of force exertion and (ii) pronounced passive force increase contradictory to the aim were shown. EMFT mechanism was concluded to be determinant for the treatment methods as well.

Keywords: Epimuscular myofascial force transmission, spastic cerebral palsy, intra-operative human experiments, rat anterior crural compartment, muscle lengthening surgery, aponeurotomy, botulinum toxin type-A.

ÖZET

SPASTİK KAS MEKANİĞİNİN VE TEDAVİ YÖNTEMLERİNİN ETKİLERİNİN İNTRA-OPERATİF DENEYLER VE HAYVAN DENEYLERİ İLE İNCELENMESİ

Bu tez, epimüsküler miyobağdokusal kuvvet iletimi (EMKİ) çerçevesinde spastik kas mekaniğine ve yaygın kullanılan tedavi yöntemlerine odaklanmıştır. İnsan gracilis (GRA) kası izometrik kuvvetini diz açısının fonksiyonu olarak ölçmek üzere yeni bir yöntem geliştirilmiştir. Sağlıklı deneklerin GRA kasının geniş bir operasyonel boy aralığı olduğu gösterilmiştir. Spastik serebral palsili hastaların GRA kasının ise anomali göstermediği bulunmuştur: (i) kasın boy aralığı daralmamıştır ve (ii) yüksek fleksiyon kuvvetleri gözlenmemiştir. Bu tür bir anomali antagonisti vastus medialis ile eş zamanlı uyarıldığında ortaya çıkmıştır. Bu nedenle, EMKİ mekanizmasının inter-antagonist etkileşim üzerinden spastisite durumunda insan kası karakteristiğini belirleyici olduğu önerilmiştir. Tedavi yöntemlerinin etkileri ise hayvan deneyleri ile incelenmiştir: (1) Kas uzatma ameliyatının (i) proksimal ve distalde değişken etkileri olduğu ve (ii) opere edilmeyen komşu kasları da etkilediği gösterilmiştir. (2) Botulinum Toksin Tip-A (BTX-A) uygulamasının in vivo ya yakın koşullarda hem enjekte edilen hem edilmeyen kasları etkilediği gösterilmiştir. Aktif kuvvet düşüşlerinin yanı sıra uygulamanın hedefiyle çelişen (i) aktif kuvvet etkime boy aralığında daralma ve (ii) belirgin pasif kuvvet artışı görülmüştür. EMKİ mekanizmasının tedavi yöntemlerinde de belirleyici olduğu sonucuna varılmıştır.

Anahtar Sözcükler:Epimüsküler miyobağdokusal kuvvet iletimi, spastik beyin felci, insanda intra-operatif deneyler, sıçan anterior krural kompartmanı, kas uzatma operasyonu, aponevroz gevşetme, botulinum toksin tip-A.

Contents

| | |
|--|------|
| ACKNOWLEDGMENTS | iii |
| Abstract | v |
| ÖZET | vi |
| List of Figures | xi |
| List of Tables | xiii |
| LIST OF SYMBOLS | xiv |
| LIST OF ABBREVIATIONS | xv |
| 1. GENERAL INTRODUCTION | 1 |
| 1.1 Muscle Force-Length Characteristics and Transmission of Forces | 1 |
| 1.2 Myofascial Force Transmission | 2 |
| 1.3 Mechanics of Spastic Muscle | 3 |
| 1.4 Clinical and Surgical Interventions to Correct Impaired Joint Function | 3 |
| 1.5 Goals and Overview of Dissertation | 5 |
| 2. INTRAOPERATIVE MEASUREMENT OF HUMAN GRACILIS MUSCLE ISOMETRIC FORCES AS A FUNCTION OF KNEE ANGLE | 7 |
| 2.1 Introduction | 7 |
| 2.2 Methods | 8 |
| 2.2.1 Subjects | 8 |
| 2.2.2 Methods | 8 |
| 2.2.3 Processing of Data | 11 |
| 2.3 Results | 12 |
| 2.3.1 Peak GRA forces and inter-subject variability | 12 |
| 2.3.2 Knee joint angle-GRA force characteristics | 12 |
| 2.3.3 Length history effects | 13 |
| 2.4 Discussion | 13 |
| 2.4.1 Intraoperative experiments and our present approach | 13 |
| 2.4.2 Functional joint range of motion | 16 |
| 2.4.3 Length history effects do occur in human muscle | 17 |
| 2.4.4 Limitations and implications | 18 |

| | | |
|---------|---|----|
| 2.4.4.1 | Lack of passive force data | 18 |
| 2.4.4.2 | Implications of EMFT | 18 |
| 3. | HUMAN SPASTIC GRACILIS MUSCLE ISOMETRIC FORCES AS A FUNCTION OF KNEE ANGLE SHOW NO ABNORMAL MUSCULAR MECHANICS | 21 |
| 3.1 | Introduction | 21 |
| 3.2 | Methods | 22 |
| 3.2.1 | Patients | 22 |
| 3.2.2 | Methods | 24 |
| 3.2.3 | Processing of data | 26 |
| 3.2.3.1 | Clinical Measures | 26 |
| 3.2.3.2 | Experimental measures | 26 |
| 3.2.3.3 | Clinical and experimental measures compared | 28 |
| 3.3 | Results | 29 |
| 3.3.1 | Clinical Measures | 29 |
| 3.3.2 | Experimental measures | 29 |
| 3.3.3 | Clinical vs. experimental measures | 31 |
| 3.4 | Discussion | 32 |
| 3.4.1 | The intraoperative measurement method | 32 |
| 3.4.2 | Experimental data show no abnormal mechanical characteristics for spastic GRA muscle | 33 |
| 3.4.3 | Mechanisms which may be responsible with the present findings | 35 |
| 4. | SIMULTANEOUS AGONISTIC-ANTAGONISTIC STIMULATION CAUSES PARALLELISM BETWEEN MECHANICS OF SPASTIC GRACILIS MUSCLE AND THE PATIENTS' MOVEMENT LIMITATION | 40 |
| 4.1 | Introduction | 40 |
| 4.2 | Methods | 41 |
| 4.2.1 | Patients | 41 |
| 4.2.2 | Methods | 42 |
| 4.2.3 | Processing of Data | 44 |
| 4.3 | Results | 46 |
| 4.3.1 | Clinical Data | 46 |

| | | |
|-------|--|----|
| 4.3.2 | Experimental Data | 47 |
| 4.4 | Discussion | 50 |
| 4.4.1 | Joint range of motion | 51 |
| 4.4.2 | Availability of high muscle force | 52 |
| 5. | MUSCLE LENGTHENING CAUSES DIFFERENTIAL ACUTE MECHANICAL EFFECTS IN BOTH TARGETED AND NON-TARGETED SYNERGISTIC MUSCLES | 54 |
| 5.1 | Introduction | 54 |
| 5.2 | Methods | 55 |
| 5.2.1 | Surgical procedures and preparation for experiments | 55 |
| 5.2.2 | Experimental conditions and procedure | 56 |
| 5.2.3 | Experimental protocol | 57 |
| 5.2.4 | Processing of experimental data and statistics | 57 |
| 5.3 | Results | 59 |
| 5.4 | Discussion | 62 |
| 6. | BTX-A ADMINISTRATION TO THE TARGET MUSCLE AFFECTS FORCES OF ALL MUSCLES WITHIN AN INTACT COMPARTMENT | 70 |
| 6.1 | Introduction | 70 |
| 6.2 | Methods | 72 |
| 6.2.1 | Surgical procedures | 73 |
| 6.2.2 | Experimental set-up | 74 |
| 6.2.3 | Experimental conditions and procedures | 74 |
| 6.2.4 | Processing of experimental data and statistics | 76 |
| 6.3 | Results | 78 |
| 6.4 | Discussion | 83 |
| 6.5 | Conclusions | 90 |
| 7. | EFFECTS OF BTX-A ON NON-INJECTED BI-ARTICULAR MUSCLE INCLUDE A NARROWER LENGTH RANGE OF FORCE EXERTION AND INCREASED PASSIVE FORCE | 91 |
| 7.1 | Introduction | 91 |
| 7.2 | Methods | 93 |
| 7.2.1 | Assessment of the effects of BTX on muscular mechanics | 93 |

| | | |
|--|---|-----|
| 7.2.2 | Surgical Procedures | 93 |
| 7.2.3 | Experimental set-up | 96 |
| 7.2.4 | Experimental conditions and procedures | 96 |
| 7.2.5 | Assessments of the effects of BTX-A on intramuscular connective tissue content | 97 |
| 7.2.6 | Data processing and statistics | 98 |
| 7.3 | Results | 100 |
| 7.3.1 | Effects of BTX-A on the TA and EHL muscles | 100 |
| 7.3.2 | Effects of BTX-A after proximal lengthening of the EDL | 101 |
| 7.3.3 | Effects of BTX-A after distal lengthening of the EDL | 105 |
| 7.3.4 | Distal vs. proximal lengthening condition | 105 |
| 7.3.5 | Effects of BTX-A on intramuscular connective tissue content | 107 |
| 7.4 | Discussion | 107 |
| 8. | GENERAL DISCUSSION AND CONCLUSIONS | 116 |
| 8.1 | Mechanics of Human Spastic Muscles, Limitations, and Future Directions | 116 |
| 8.2 | Treating Spastic Cerebral Palsy, Limitations, and Future Directions | 119 |
| 8.2.1 | Muscle lengthening surgery | 119 |
| 8.2.2 | BTX-A Application | 120 |
| Appendix A. PRECONDITIONING REMOVES LENGTH HISTORY EFFECTS AND ENSURES SUCCESSIVE FORCE-LENGTH MEASUREMENTS | | 122 |
| A.1 | Introduction | 122 |
| A.2 | Methods | 123 |
| A.2.1 | Surgical procedures | 123 |
| A.2.2 | Experimental conditions and procedure | 123 |
| A.2.3 | Processing of data and statistics | 124 |
| A.3 | Results | 126 |
| A.3.1 | EDL | 126 |
| A.3.2 | TA+EHL | 128 |
| A.4 | Discussion | 128 |
| REFERENCES | | 129 |

List of Figures

| | | |
|------------|---|-----|
| Figure 2.1 | Apparatus for intra-operative muscle mechanics experiments in the lower extremities. | 10 |
| Figure 2.2 | Typical examples of force-time traces for GRA muscle. | 13 |
| Figure 2.3 | The isometric GRA muscle knee angle-force characteristics. | 14 |
| Figure 2.4 | Effects of previous activity at high length on muscle force. | 15 |
| Figure 3.1 | Usage of buckle force transducer and the apparatus for intra-operative muscle mechanics experiments in the lower extremities. | 23 |
| Figure 3.2 | Typical examples of force-time traces for spastic GRA muscle. | 29 |
| Figure 3.3 | The isometric KA-FGRA characteristics for spastic GRA muscle. | 30 |
| Figure 4.1 | Usage of buckle force transducer and stimulation electrodes. | 43 |
| Figure 4.2 | Typical examples of force-time traces for spastic GRA muscle. | 46 |
| Figure 4.3 | The isometric KA-FGRA characteristics of spastic GRA muscle. | 48 |
| Figure 5.1 | Schematic view of the experimental setup. | 58 |
| Figure 5.2 | The isometric muscle force-length curves of target EDL muscle. | 61 |
| Figure 5.3 | Forces exerted by non-operated TA and EHL muscles. | 63 |
| Figure 6.1 | The experimental set-up. | 75 |
| Figure 6.2 | Typical examples of force time traces measured at tendons of muscles of the anterior crural compartment. | 77 |
| Figure 6.3 | The effects BTX-A injection to TA muscle on its isometric muscle force-length characteristics. | 79 |
| Figure 6.4 | The effects of BTX-A injection to TA muscle on the EDL forces as a function of increasing TA muscle length. | 81 |
| Figure 6.5 | The effects of BTX injection to TA muscle on the EHL forces as a function of increasing TA muscle length. | 82 |
| Figure 7.1 | Schematic view of the experimental setup. | 95 |
| Figure 7.2 | Sample histological sections of anterior crural muscles stained using PAS for glycogen. | 102 |
| Figure 7.3 | Forces of the TA and EHL muscles as a function of increasing EDL muscle length. | 103 |

| | | |
|------------|---|-----|
| Figure 7.4 | EDL force-length characteristics obtained after proximal lengthening. | 104 |
| Figure 7.5 | EDL force-length characteristics obtained after distal lengthening. | 106 |
| Figure 7.6 | Sample histological sections of anterior crural muscles stained using Trichrome Gomori for collagen. | 107 |
| Figure A.1 | The experimental set-up. | 125 |
| Figure A.2 | Force-length characteristics of (a) EDL distal, (b) EDL proximal, and (c) TA+EHL muscles obtained after distal lengthening. | 127 |

List of Tables

| | | |
|-----------|--|----|
| Table 2.1 | Anthropometric data, peak GRA forces and peak GRA tendon stresses | 9 |
| Table 3.1 | Patient parameters | 25 |
| Table 3.2 | Clinical measures characterizing motion limitation and experimental measures | 27 |
| Table 4.1 | Patient Parameters | 44 |
| Table 4.2 | Clinical measures characterizing motion limitation and experimental measures | 49 |

LIST OF SYMBOLS

| | |
|-----------------|-------------------|
| ° | Degree |
| C | Celcius |
| cm | Centimeter |
| Hz | Hertz |
| <i>kg</i> | Kilogram |
| mA | Milli Amper |
| ml | Milliliter |
| mm ² | Square Millimeter |
| MPA | Mega Pascal |
| ms | Milli second |
| N | Newton |
| p | Probability Value |

LIST OF ABBREVIATIONS

| | |
|-----------------|--|
| Δl_{mt} | Muscle-tendon Length |
| ANOVA | Analysis of Variance |
| ACL | Anterior Cruciate Ligament |
| AFO | Ankle Foot Orthosis |
| AT | Aponeurotomy |
| BTX-A | Botulinum Toxin Type - A |
| CC | Control Contractions |
| $c_{mid-thigh}$ | Mid-thigh Circumference |
| CP | Cerebral Palsy |
| ECM | Extracellular Matrix |
| EDL | Extensor Digitorum Longus |
| EHL | Extensor Hallicus Longus |
| EMFT | Epimuscular Myofascial Force Transmission |
| F_a | Active Force |
| FEM | Finite Element Modeling |
| F_{GRA} | Gracilis Muscle Force |
| FL | Force Length |
| F_p | Passive Force |
| F_t | Total Force |
| FT | Force Transducer |
| GMFCS | Gross Motor Functional Classification System |
| GRA | Gracilis |
| HAA | Hip Abduction Angle |
| KA | Knee Angle |
| Lambda | Tonic Stretch Reflex Threshold |
| l_{leg} | Leg Length |
| l_{opt} | Optimum Length |
| l_{range} | Leg Range |

| | |
|-------------|---|
| l_{ref} | Reference Length |
| l_{thigh} | Thigh Length |
| MFT | Myofascial Force Transmission |
| MRI | Magnetic Resonance Imaging |
| PA | Popliteal Angle |
| PAS | Periodic acid-Schiff |
| PD | Preparatory Dissection |
| ρ | Spearman's Rank Correlation Coefficient |
| ROM | Range of Motion |
| SD | Standard Deviation |
| SE | Standard Error |
| TA | Tibialis Anterior |
| US | Ultrasound |
| VM | Vastus Medialis |

1. GENERAL INTRODUCTION

1.1 Muscle Force-Length Characteristics and Transmission of Forces

Forces generated by skeletal muscle fibers and transmitted to the bones cause joint motion. Force-length characteristics representing the maximal force with respect to the length shows functional potential of muscle independent from velocity and activation parameters such as stimulation frequency or amplitude [e.g. 1]. One of the determinants of such potential is muscle architecture defined with muscle length, fiber length, pennation angle, fiber type distribution, and number of sarcomeres in series and in parallel [2]. Muscle length denoting muscle excursion determines the joint range of motion [3-4] and it is typically associated with fiber length [5] i.e., number of sarcomeres in series mostly related with velocity of movement with pennation angle and fiber type distribution [6-8]. Number of sarcomeres in parallel on the other hand translates to the muscle cross sectional area and it is directly related to force production capacity with also pennation angle [4, 9-11].

Additional to such architectural properties, as part of structural and morphological features of muscles, transmission mechanisms of the forces are other determinants of muscle function. Myotendinous junctions having specialized morphological features are one of the paths of force transmission [12]: forces generated by sarcomeres in a muscle fiber are transmitted to the bone through aponeurosis and tendon attached to the bone. Myotendinous connections are very important for joint motion; however, they are not exclusive pathways. Force transmission shown to have more complicated mechanism includes also lateral pathways: transmission of forces from sarcomeres to the extracellular matrix via special proteins [13-14]. Considering the continuity of extracellular matrix with epimysium and collagen rich fascial structures, such lateral pathways transmit forces to the neighboring fibers, muscles, and non-muscular structures.

1.2 Myofascial Force Transmission

Transmission of forces from myofiber to its extracellular matrix composed of collagen fibers is called intramuscular myofascial force transmission (MFT) [15-17]. Such transmission may occur along the endomysial perimeter of muscle fiber having tightly arranged collagen layers [18]. In addition to intramuscular MFT, forces are also transmitted from extracellular matrix of a muscle to the adjacent muscle's extracellular matrix. It is referred to as intermuscular MFT [19-20] if it is through the direct connections between the muscles. Transmission of force from the extracellular matrix of a muscle to surrounding non-muscular structures and bone is referred to as extramuscular MFT [15, 20-22]. Since inter- and extramuscular connections constitute an integral system and cannot be distinguished they are defined as epimuscular myofascial force transmission (EMFT) [23].

Myofascial loads representing the amount of EMFT were quantified as the difference between muscle forces measured from proximal and distal tendons at specific muscle lengths. Such myofascial loads shown to be prominent [15, 22, 24] indicates the important role of inter- and extramuscular connections. If a muscle is not isolated, shape of the force-length curve representing its characteristics changes drastically due to EMFT [23, 25]. Another indicator of myofascial loads are force alterations measured due to the relative positional differences between muscles even their lengths are fixed [26-27]. The muscle model developed with finite element modeling (FEM) method [28] also revealed the effects of intra-, inter-, and extramuscular connections: Sarcomere length heterogeneity with stress distribution along fiber bundles was shown as an evidence of EMFT determining muscle force production capacity [25].

Consequently, muscles do not act as independent actuators. These previous findings showing how EMFT modifies muscle force-length characteristics did suggest the functional role of this transmission mechanism in health and also in pathology.

1.3 Mechanics of Spastic Muscle

Cerebral palsy (CP) is a neuromuscular disorder caused by damage of the developing brain. Most of the cerebral palsy patients suffer from spasticity which is a form of hypertonia [29-31] characterized by velocity dependent exaggerated reflexes [31-34]. Continuously activated muscles remain at low lengths and adapt to the immobilization at shortened position [35-37]. Thus, in long term, contracture formation [38-42] with muscle and soft tissue shortening [39] accompanies to spasticity even anti-spastic treatments are applied [43-44]. Contracture as a reason or a consequence is associated with decreased joint range of motion thus impaired function such as flexed hips, knees and equines deformity at the ankles [40, 45-48].

Many architectural changes due to spasticity were reported: muscle shortening [49-51], decrease in muscle volume [51-54] and cross-sectional area [52, 55-56], increased stiffness [57-59], fiber type alterations and increased amount of extracellular collagen [59]. Even many structural changes for spastic muscles were found and the impaired function is known to be related with these changes, no previous study revealed the relationship between joint range and specific muscle function.

On the other hand, EMFT occurs also for CP patients [60-61] and known to have important role for spasticity [62-63] in consistent with the increased stiffness, implications of this knowledge needs further examinations.

1.4 Clinical and Surgical Interventions to Correct Impaired Joint Function

There are various methods for the treatment of spastic cerebral palsy from physical therapy to neuromuscular surgical interventions applied depending on the severity of the symptoms. To reduce spasticity injection of botulinum toxin type A (BTX-A) causing muscle paralysis by inhibiting acetylcholine release [64-65] is used.

The effects of BTX-A have been widely studied by quantifying the area of paralysis [66], compound muscle action potential [67] and electromyography [68]. However, reports on mechanical parameters, e.g., twitch and tetanic force have been limited to selected muscle lengths or joint positions [e.g. 67, 69]. Even it is well known that BTX-A injected to the muscles spread through the fascia [70] and affects neighboring muscles [71-72], the effects of BTX-A on the mechanical characteristics of targeted and non-targeted neighboring muscles are not known.

Surgical interventions are performed on the patients having severe impairments due to contracture formation. Remedial surgery known as muscle recession [73-74], muscle release [75], muscle lengthening [76-80], and aponeurotomy (AT) [81] involves cutting of an intramuscular aponeurosis transversely to its longitudinal direction. Limited effects of aponeurotomy per se were shown previously even a discontinuity occurring. However, subsequent rupturing of intramuscular connections denoting the removal of intramuscular MFT had major effects on force-length characteristics [82]. Following studies pronounced the altering role of extramuscular MFT on the effects of AT [83-84]. Such results evoke a question if most of the epimuscular connections are intact similar to in vivo condition how aponeurotomized muscle and its neighbors are affected.

1.5 Goals and Overview of Dissertation

Present thesis is focused on spastic muscle mechanics and the treatment methods used in the context of the determinant role of epimuscular myofascial force transmission (EMFT). The goals of the study and the publications addressed in sequence in the following chapters are

Chapter 2 aimed at developing an intra-operative method to measure human muscle isometric forces directly with respect to joint angle and measure human gracilis (GRA) muscle characteristics in health. It is published as

Yucesoy, C.A., Ateş, F., Akgün U., Karahan M., "Measurement of human gracilis muscle isometric forces as a function of knee angle, intraoperatively," J Biomechanics, Vol. 43, p. 2665-71, 2010.

Chapter 3 aimed at measuring the forces of activated spastic GRA muscle as a function of knee joint angle and to test the following hypotheses: (i) The muscle's joint range of force exertion is narrow and (ii) High muscle forces are available at flexed joint positions. It is published as

Ateş, F., Temelli, Y., and Yucesoy, C.A., "Human spastic Gracilis muscle isometric forces measured intraoperatively as a function of knee angle show no abnormal muscular mechanics," Clin Biomech (Bristol, Avon), 2012

Chapter 4 aimed at measuring spastic GRA muscle characteristics during simultaneous stimulation with its antagonist and to test (i) if the joint range of force exertion is narrow and (ii) if GRA muscle has higher force exertion capacity at low lengths.

Chapter 5 aimed at revealing the effects of muscle lengthening surgery on rat muscles and test the following hypotheses: (i) Effects of AT on the target muscle are different at distal and proximal tendons, (ii) forces of non-targeted synergistic muscles

are affected as well, and (iii) preparatory dissection performed to reach the target aponeurosis is responsible from some of these effects. It is submitted as

Ateş, F., Huijing P.A., Yucesoy, C.A., 2013. Muscle lengthening surgery causes differential acute mechanical effects in both targeted and non-targeted synergistic muscles, *Journal of Electromyography and Kinesiology*, in revision.

Chapter 6 aimed at testing the effects of BTX-A on (i) not only the injected but also the non-injected rat muscles and also (ii) EMFT mechanism. It is published as

Yucesoy, C.A., Arıkan Ö.E., Ateş F., 2012. BTX-A Administration to the Target Muscle Affects Forces of All Muscles Within an Intact Compartment and Epimuscular Myofascial Force Transmission, *Journal of Biomechanical Engineering*, 134:111002-1-9.

Chapter 7 aimed at testing the effects of BTX-A on (i) the active contribution of bi-articular neighboring muscle as well as (ii) the passive forces for both proximal and distal joints it spans. It is submitted as

Ateş, F., Yucesoy, C.A., 2013. Effects of BTX-A on non-injected bi-articular muscle include a narrower length range of force exertion and increased passive force, *Muscle & Nerve*, in revision.

2. INTRAOPERATIVE MEASUREMENT OF HUMAN GRACILIS MUSCLE ISOMETRIC FORCES AS A FUNCTION OF KNEE ANGLE

2.1 Introduction

Muscle force-length characteristics comprise one of the most important elements of muscular mechanics. Such characteristics have been widely studied using highly standardized experimental procedures in numerous animals [e.g., 85, 86]. In contrast, although to an appreciable extent, the main goal of the research conducted is to understand the function of human muscles, data available are mostly obtained from indirect approaches including cadaver studies [87], joint torque measurements [88-89], modeling [89] and use of dynamometry and ultrasound [90]. In only a limited number of studies, direct measurement of human muscle forces was performed during activities in vivo [91]. Direct measurements of isometric force-length characteristics in human muscles were also rare and limited to the upper extremities [60, 92-93]. Improved understanding of human muscle functioning in health and disease necessitates collection of data that relates isometric muscle force to joint angle, directly.

Recent experiments in the rat have shown that previous activity at high (over optimum) muscle lengths causes considerable active force changes (predominantly a decrease) at lower lengths [15, 62]. Such length history effects present importance: they comprise a distinct muscle mechanics phenomenon with unclear mechanisms and implications. However, their occurrence has not been shown in human muscle.

The goals of this study were (1) to measure intraoperatively the previously unstudied isometric forces of activated human Gracilis (GRA) muscle as a function of knee joint angle and (2) to test our hypothesis that length history effects substantiate also in human muscle. Experiments were conducted during anterior cruciate ligament (ACL) reconstruction surgery.

2.2 Methods

Surgical and experimental procedures, in strict agreement with the guidelines of Helsinki declaration were approved by a Committee on Ethics of Human Experimentation at Marmara University, Istanbul. University, Istanbul.

2.2.1 Subjects

Seven male and one female patients (mean age 25 years, range 19-32, standard deviation 4.7 years) undergoing ACL reconstruction surgery; however, with no former musculoskeletal pathology were included in the study. Prior to surgery, (1) after a full explanation of the purpose and methodology of the experiments, the subjects provided their informed consent and (2) subject anthropometric data were collected.

2.2.2 Methods

Subjects were under general anesthesia but no muscle relaxants were used. All intraoperative experiments were performed after routine incisions to reach the distal GRA tendon and before any other surgical procedures of ACL reconstruction.

Using a scalpel blade (number 10), 2 cm oblique skin incision was made parallel to the GRA tendon palpated 1 cm below the tuberosity of the tibia and 3 cm below the medial joint gap. Sartorial fascia covering hamstring tendons was cut to expose the GRA tendon with two incisions: (i) parallel to GRA tendon and (ii) parallel to longitudinal axis of the tibia. Subsequently, a buckle force transducer (NK Biotechnical Engineering Co., Minneapolis, Minnesota, USA, for further details [94] was mounted over the tendon. Note that prior to each experiment, the force transducer was (i) calibrated using bovine tendon strips (with rectangular cross section, dimensions approximating 7 x 2 mm, similar to human GRA distal tendon) and (ii) sterilized (using dry gas at maximally 50⁰ C).

Table 2.1
Anthropometric data, peak GRA forces and peak GRA tendon stresses

| Subject | Height (cm) | Mass (kg) | Thigh length (cm) | Mid-thigh circumference (cm) | Peak G force (N) | Optimal knee angle (°) | Tendon cross-sec. area (mm ²) | Peak GRA tendon stress (MPa) |
|---------|-------------|-----------|-------------------|------------------------------|------------------|------------------------|---|------------------------------|
| A | 172 | 70 | 43.0 | 53.0 | 183.1 | 60 | 7.54 | 24.27 |
| B | 167 | 68 | 41.0 | 50.5 | 121.5 | 60 | 4.52 | 26.87 |
| C | 176 | 78 | 43.0 | 55.5 | 196.0 | 90 | 7.78 | 25.16 |
| D | 157 | 55 | 40.0 | 49.5 | 92.0 | 30 | 3.79 | 24.21 |
| E | 184 | 77 | 46.0 | 53.5 | 139.0 | 120 | 7.24 | 19.19 |
| F | 179 | 80 | 44.0 | 59.5 | 17.2 | 0 | 11.45 | 1.50 |
| G | 180 | 77 | 44.0 | 58.0 | 27.8 | 60 | 7.46 | 3.72 |
| H | 185 | 83 | 44.0 | 56.0 | 490.5 | 120 | 7.06 | 69.4 |

Isometric GRA force was measured at various muscle lengths imposed by manipulating the knee joint angle. Starting at 120° (i.e., knee joint at maximal experimentally attainable flexion, as limited by the surgery table), GRA length was increased progressively by extending the knee with 30° increments, until full knee extension (i.e., GRA force was measured at 120°, 90°, 60°, 30° and 0°). An apparatus with two functional components (Figure 2.1) was designed: (1) knee angle adjustor allows setting the knee angle and restraining it during the contractions. This component is a compound structure including i) an ankle foot orthosis (AFO), ii) a spatial locator and iii) a height adjustor. A fixture with adjustable tightness interconnects all there elements at the ankle. The spatial locator at the other end fits in the slot of the surgery table which allows a horizontal position adjustment when not restrained fully with a separate fixture. (2) leg holder (also fits in the slot of the surgery table) allows fixing the hip angle (to 0° both in the sagittal and frontal planes) and restraining the upper leg.

A pair of gel-filled skin electrodes (EL501, BIOPAC Systems, CA, USA) were placed on the skin, over GRA muscle belly. Using a custom made constant current high voltage source (cccVBioS, TEKNOFIL, Turkey) the muscle was stimulated supramaximally (transcutaneous electrical stimulation with a bipolar rectangular signal, 140 mA,

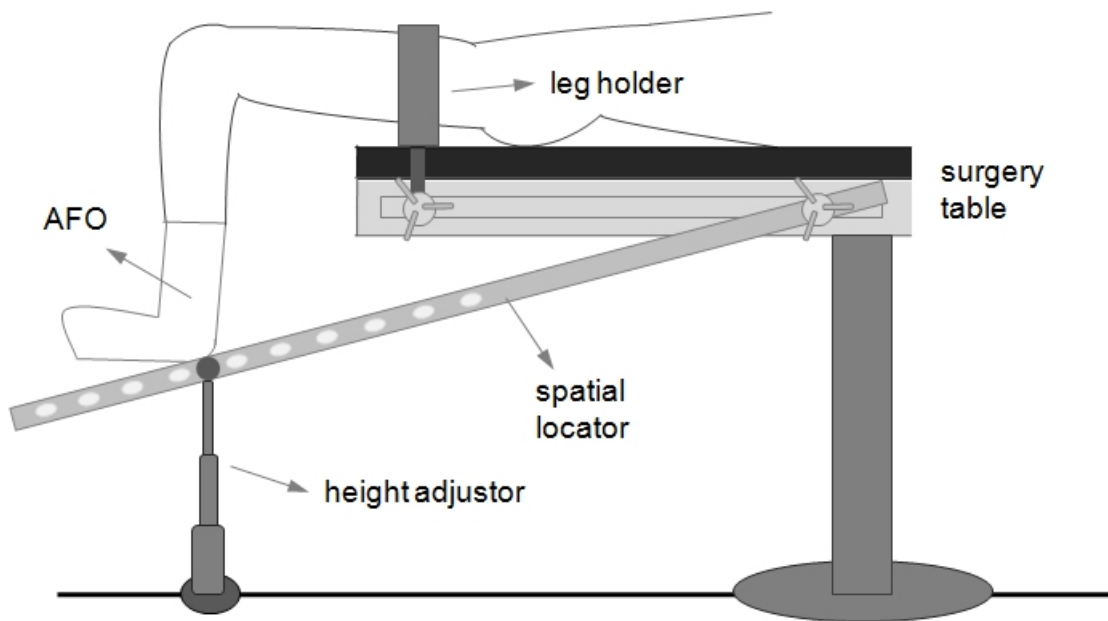


Figure 2.1 Apparatus for intra-operative muscle mechanics experiments in the lower extremities. Setting of the knee angle and restraining it during the contractions is achieved using the knee angle adjustor, a compound structure including i) an ankle foot orthosis (AFO), ii) a spatial locator and iii) a height adjustor. The leg holder allows fixing the hip joint angle (to 0° both in the sagittal and frontal planes) and restraining the upper leg. Note that the spatial locator and the leg holder were manufactured to fit in the slot of the surgery table.

50Hz): two twitches were evoked (100 ms apart) which after 300 ms were followed by a pulse train for 1000 ms to induce a tetanic contraction (see Figure 2.1 for superimposed examples of force-time traces for GRA muscle at five knee angles).

Note that: (1) a pilot study ($n=1$) had confirmed that 140 mA ensures a maximal activation: randomized use of current amplitudes of 130 mA, 140 mA, 150 mA and 160 mA at knee angles of 90° and 60° yielded (i) no systematic force increase as a result of increasing current amplitude and (ii) no appreciable force variation (standard deviations of forces measured were limited to 5.2% and 8.9% of the mean GRA force for knee angles of 90° and 60° , respectively). (2) Active GRA forces measured during a 500 ms period in the middle of the tetanus were averaged to obtain the muscle force. A data acquisition system (MP150WS, BIOPAC Systems, CA, USA, 16-bit A/D converter, sampling frequency 40 KHz) was used with an amplifier for each transducer (DA100C, BIOPAC Systems, CA, USA). After each contraction, the muscle was allowed to recover for 2 minutes at a flexed knee posture.

Subsequent to collection of a complete set of knee joint angle-force data, control measurements were performed at lower GRA length (corresponding to 90° knee angle) in order to test if previous activity at high length (imposed by full knee extension) had any effect on the force exerted. All experimental preparations and data collection were completed within 20 min, the maximal study duration allowed by the ethical committee. Diagnostic upper leg MRI images of the subjects were used to determine GRA muscle tendon cross-sectional areas: using the built in software of the Picture Archiving and Communication System, area of tendon cross-section marked in an image slice located distally, approximately where force transducers were mounted were determined as number of pixels in the marked area x pixel area.

2.2.3 Processing of Data

(1) Peak GRA forces as well as GRA tendon stresses (Peak GRA force/tendon cross-sectional area) and the corresponding optimal knee angles were studied. Pearson's correlation coefficient was calculated to quantify inter-subject variability between the peak force and stress values and subject (i) weight (ii) mid-upper leg perimeter and (iii) upper leg length. Correlations were considered significant at $p < 0.05$.

(2) Knee joint angle-GRA muscle force characteristics were studied separately for each subject: operational portion of the force-length characteristics were characterized.

(3) Effects of previous activity at high length on muscle force exerted at lower lengths were assessed: control force for each subject measured at 90° knee angle was compared to the force measured at identical knee angle during collection of knee angle-GRA muscle force data. Existence of a correlation between optimal knee angle and history effect was assessed: Pearson's correlation coefficient was calculated using absolute values of % force changes. Correlation was considered significant at $p < 0.05$.

2.3 Results

2.3.1 Peak GRA forces and inter-subject variability

Table 1 shows the key anthropometric parameters of the subjects as well as the magnitude and the corresponding knee joint angle for the peak GRA forces measured. Peak GRA forces show a sizable inter-subject variability: peak force (mean = 178.5 ± 270.3 N) ranges between 17.2 N and 490.5 N. Mean peak GRA tendon stress equals 24.4 ± 20.6 MPa. Optimal knee angles (mean = $67.5 \pm 41.7^\circ$) include all angles studied.

Only a limited correlation was found between peak GRA force and subject mass as well as mid-thigh perimeter (correlation coefficient equals 0.34 and -0.17, respectively) whereas, almost no correlation was found between peak GRA force and thigh length (correlation coefficient equals 0.02). None of these correlations were statistically significant. Similarly, correlations between peak GRA tendon stress and subject mass, mid-thigh perimeter and thigh length (correlation coefficient equals 0.14, -0.24, and -0.06, respectively) were insignificant.

2.3.2 Knee joint angle-GRA force characteristics

Knee joint angle-GRA force characteristics (Figure 2.3) for only two subjects (E and H) indicate that GRA muscle may operate in the descending limb of its force-length characteristics. In contrast, for a majority of the subjects, such operational range includes parts of both ascending and descending limbs. Nevertheless, even for those subjects Figure 2.3 shows sizable inter-subject variability presenting itself as shape differences in knee joint angle-GRA force characteristics.

An important finding is that for none of the knee angles studied, GRA muscle was at active slack length indicating that this length corresponds to a knee flexion over 120° .

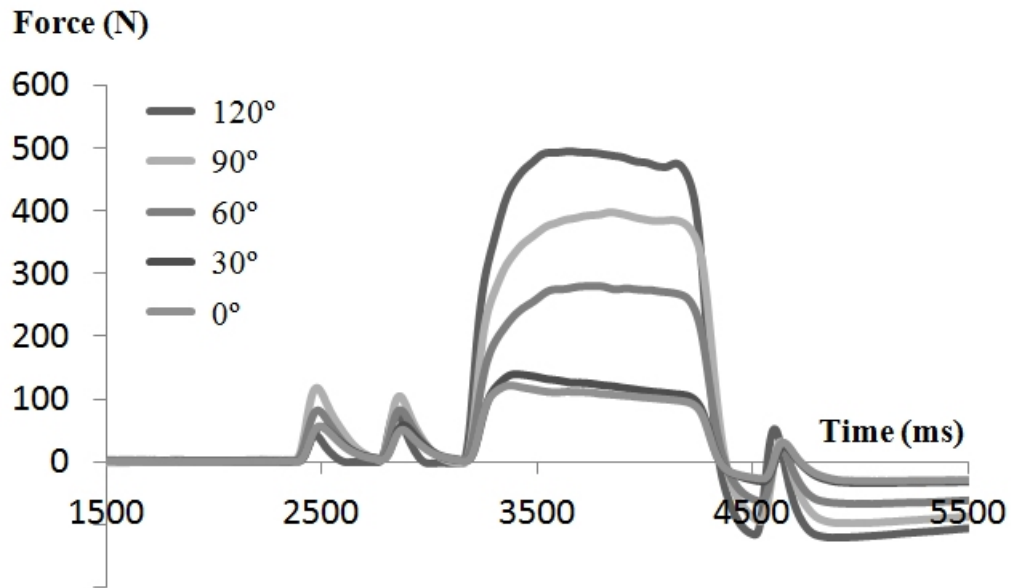


Figure 2.2 Typical examples of force-time traces for GRA muscle. Superimposed traces recorded for GRA muscle at five knee angles studied are shown. Note that the negative forces measured after the tetanus was ceased originate from the buckling of the tendon during unloading and are not representative of the passive state of the muscle.

2.3.3 Length history effects

Figure 2.4 shows that previous activity during collection of a complete set of knee angle-force data caused G force at reference joint angle to change considerably: a significant correlation was found between optimal knee angle and % force change (correlation coefficient equals 0.88). Note that except for two of the subjects (B and F) GRA muscle control forces were than those measured during collection of knee joint-force data (minimally 12.4% for E and maximally 42.3% for G).

2.4 Discussion

2.4.1 Intraoperative experiments and our present approach

Studies measuring directly human isometric muscle force are very rare: (1) Ralston et al. [95] reported force-length data of human arm muscle. (2) Freehafer et al [92] and Lacey et al [96] measured intraoperatively force-length characteristics of human

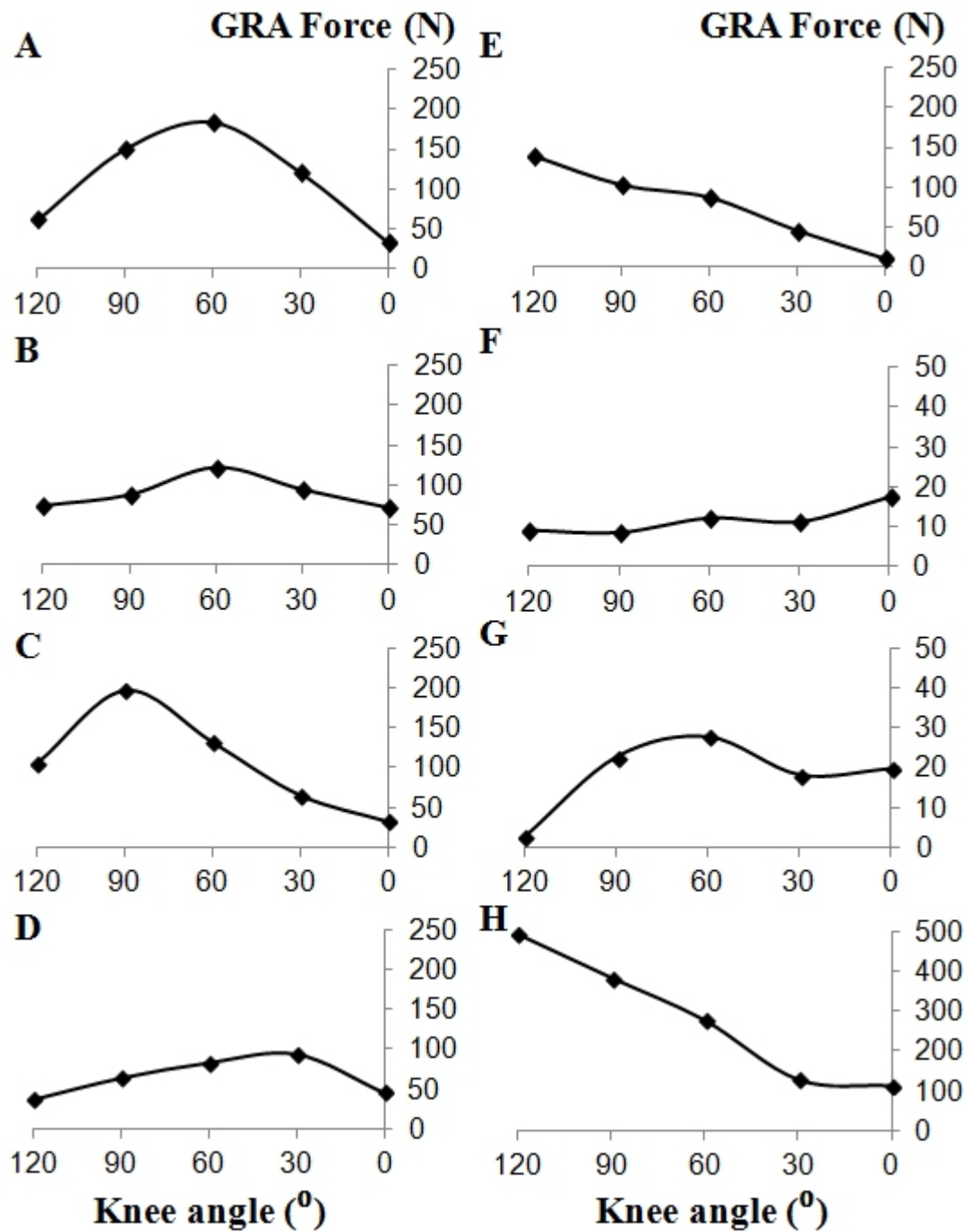


Figure 2.3 The isometric GRA muscle knee angle-force characteristics. Data is shown separately for each subject (panels A to H). Isometric GRA muscle forces were measured at five knee angles: 0° i.e., knee extended maximally, 30°, 60°, 90° and 120°.

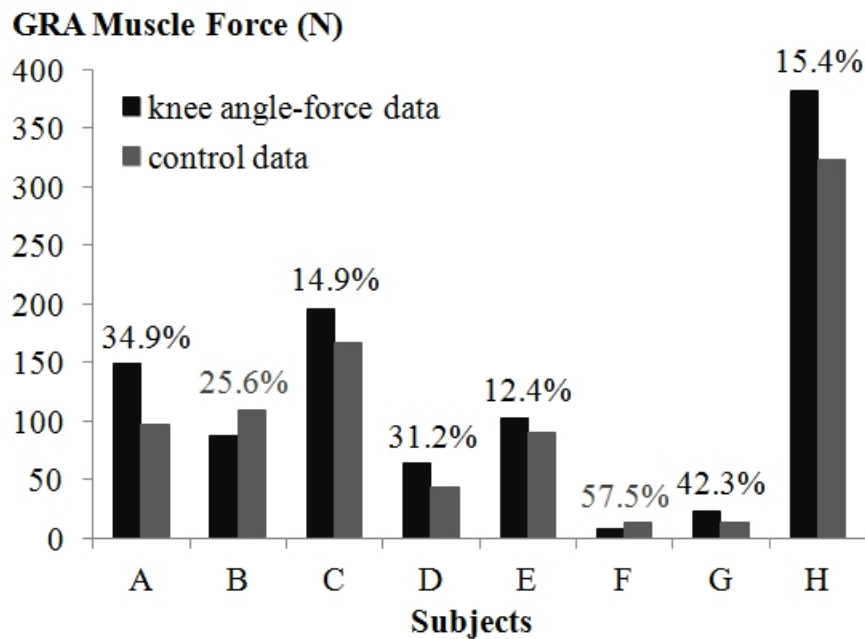


Figure 2.4 Effects of previous activity at high length on muscle force. Data shown separately for each subject compares the control forces measured at knee angle = 90° with the force measured at identical knee angle during collection of knee angle-GRA muscle force data. Note that percent differences shown for each subject in gray characters indicate a force increase (for subjects B and F) whereas; the remainder indicate a force decrease.

lower arm muscles. Despite such pioneering contributions, the experimental setup of those authors was not capable of avoiding all movement artifacts of the arm. (3) A systematic set of studies reporting intraoperatively measured human flexor carpi ulnaris muscle force-length data were published recently by Smeulders, Kreulen and colleagues [e.g. 61, 93, 97]. Using well designed experimental procedures and setup, these authors were able to remove limb movement artifacts and standardize their approach. They therefore, made a major contribution not only to intraoperative experimentation but also to our understanding of human muscle mechanics.

Our present intraoperative approach features to the same capacity, the ability to ensure the isometric nature of experiments. Moreover, data, more representative of the situation in vivo can be obtained: the buckle force transducers allow measuring (1) after minimal tissue interventions and (2) muscle force directly as a function of joint angle. The latter yields simultaneous length changes of all muscular and non-muscular structure as it occurs in vivo.

2.4.2 Functional joint range of motion

Our results show that human GRA muscle is capable of producing non-zero active forces even for the shortest length studied hence, at least for a joint range between 0° to 120° . This finding is in concert with those of Ward et al. [98] who showed that G is among the lower extremity muscles that feature the greatest excursion. Note that, for fundamental motions like walking and sit-to-stand, maximal knee flexion was shown to equal 110° [99] and 103° [100], respectively. Our results show that GRA muscle is capable of contributing to knee flexor moment also for such joint positions.

In isometric experiments performed in animal [e.g. 23] and human muscles [e.g. 61], in situ data produced include typically both ascending and descending limbs of muscle force-length characteristics. However, studies inferring to in vivo condition have reported that muscle functional joint range does not correspond fully to such in situ length range of active force exertion. For example, Lieber and coworkers [101-103] showed that synergistic extensor carpi radialis brevis and longus muscles function in the descending limb of their force-length characteristics. In contrast, human gastrocnemius muscle was reported to operate within the ascending limb [89, 104]. Our present results suggest in agreement with these studies that human GRA muscle does not operate within the entire length range of force exertion. However, for a majority of the subjects (except subjects E and H) it appears to function in both of the ascending and descending limbs. Nevertheless, even for those subjects inter-subject variability is considerable: the knee angle-muscle force curves show shape differences as well as different optimal knee angles. Moreover, data of subjects E and H indicate that their GRA muscles operate within the descending limb, exclusively. Therefore, we conclude that the functional joint range of motion for human GRA muscle is at least as wide as full knee extension to 120° of knee flexion, however; the portion of the knee angle-muscle force relationship operationalized is not unique but individual specific.

2.4.3 Length history effects do occur in human muscle

Our results confirmed our hypothesis that length history effects [e.g. 15, 105] do occur also in human muscle. The exact mechanism is not immediately apparent; however, due to the cyclic testing nature (increasing muscle lengths and shortening before control measurements), one may consider hysteresis as a determinant. Our recent findings do indicate such viscoelastic intra- and epimuscular tissue role [106]: (i) a second control contraction after a longer recovery period (15 min) showed even greater history effects however, (ii) interfering surgically with the fascial connections of muscle caused history effects to decrease.

Nevertheless, such energy dissipation mechanism is expected to cause a force reduction. Although, for a majority of the present and previously reported data this is the case, there are remarkable exceptions with possibly important messages: (1) Previous activity of a muscle at high length was shown to cause a certain force increase in its restrained synergistic [106] or even antagonistic [107] muscles. (2) For two of the present subjects, our results show such force increase also for the target muscle. Activity specifically over muscle optimum length has been argued to cause force reducing length history effects [62]. Accordingly, knee angle-force characteristics of subject F (Figure 2.2 F) suggest that GRA muscle was not activated over optimum length even for maximal knee extension. However, the considerably increased control force for subject B is clearly exceptional: knee angle-force characteristics indicate strongly that for maximal knee extension, GRA muscle was at a higher length than optimum length. Note that unlike the previous animal experiments reporting such history effects, muscle lengths were manipulated presently by altering the joint angle. Moment arms that could vary among subjects and differences in position of the target muscle relative to its neighboring muscular and nonmuscular structures (nontargetted muscles were restrained in animal experiments) may affect the lengths of the tissues involved. Muscle relative position reported as a key determinant of epimuscular myofascial force transmission [26-27, 108-109] was shown to alter muscular mechanics substantially [e.g. 27, 108]. Nevertheless, the exceptional results discussed here suggest that time dependent material properties may not be the exclusive cause for the history effects indicating

more complex mechanisms involving also the contractile elements. Possible history dependent role played by the active and passive components of muscle tissue [e.g., 110] should be considered and addressed in specifically planned new studies.

2.4.4 Limitations and implications

2.4.4.1 Lack of passive force data. Both prior and subsequent to the tetanus, measurement of passive force was not possible: (1) the amplitude of the twitches evoked before the tetanus appears to be not high enough to remove the GRA tendon slack. (2) Since the tendon buckles during unloading, the force transducers working on a principle of torque measurement [94] measure negative forces, not representative of the passive state after the tetanus was ceased. In new studies, successful passive data collection could be possible by either increasing the twitch current amplitude or by measuring passive force-joint angle relationship separately.

2.4.4.2 Implications of EMFT . Our research groups have shown that due to myofascial force transmission [111] occurring epimuscularly [23] forces produced in neighboring synergistic rat muscles can be integrated with the force of the agonist and exerted onto the bone from its tendon [22]. Moreover, experimentally manipulating such force transmission pathways (e.g., dissection of connective tissues at muscle bellies or removal of synergistic muscles) has been shown to change the magnitude of muscle force exerted at the same lengths, explained by sarcomere length changes [23, 25]. Therefore, due to epimuscular myofascial force transmission, the shape of the muscle length–force characteristics was shown to change as a function of different mechanical conditions in which the muscle functions.

We expect important implications of this mechanism:

(1) Harvesting the distal tendon of GRA muscle often together with semitendinosus (ST) muscle is a common technique in ACL reconstruction. Although, such direct

impairment of the myotendinous force transmission path implies post-operative knee flexion deficiency, several studies reported only a small reduction in peak knee flexion moment after recovery, if any [e.g., 112, 113-115]. Accordingly, such post-operatively unchanged peak knee flexion moment may be ascribable, at least in part, to epimuscular myofascial force transmission from GRA and ST muscles to the knee joint via neighboring hamstrings muscles.

(2) Epimuscular myofascial force transmission may be an important factor responsible at least in part with the inter-subject variability shown presently: (i) plausible differences in the mechanical properties of the muscle's epimuscular connections among different subjects are conceivable to cause shape differences in their knee angle-muscle force relationships and hence, lead to functional portions of this relationship to be individual specific. Smeulders et al. [61] reported data indicating effectiveness of myofascial force transmission in human muscles and ascribed apparent inter-subject variability to such mechanism additional to spasticity related differences in muscle properties. (ii) Note that although care was taken presently to stimulate the targeted GRA muscle exclusively, unintentional marginal stimulation of also the neighboring hamstrings was not completely impossible due to the surface electrodes used. In such a situation, additional force transmitted via myofascial pathways from a neighboring muscle onto GRA muscle may also be responsible with some of the inter-subject variability.

For a broader consideration of muscle-tendon biomechanical function and inter-subject variability, tendon stress is a valuable parameter. Addressing bone, muscle and tendon stresses across species, importance of biomechanical consequences of scaling was reviewed extensively by Biewener [116]. In specific studies e.g., on kangaroo rat locomotion [117-118] determining how stress scales with force yielded important insights allowing relating animal size and motion strategies. It should be noted that presently much less inter-subject variability was shown for peak GRA tendon stresses. Nevertheless, a surprising finding was that tendon cross-sectional area of subject F was the largest and tendon of subject H was not oversized. Therefore, there was no fully consistent scaling of tendon size and force. This suggests that certain inter-subject variability should originate from differential force production capacity of the muscle

which implies much higher contribution of the GRA muscle to knee flexion moment for some individuals which is likely to have consequences post-operatively. New studies are indicated to study simultaneously the knee angle-force characteristics of also other hamstrings in order to (1) assess the effects of epimuscular myofascial force transmission and (2) determine the relative contribution of GRA, ST and e.g. semimembranosus muscles to knee moment. The lack of correlation shown between typical subject anthropometrics and peak muscle force and even stress indicates the difficulty of estimation of the contribution of human muscles to joint moments for different individuals using such indirect measurements.

In conclusion, mean peak GRA force, mean peak GRA tendon stress and optimal knee angle equaled 178.5 ± 270.3 N, 24.4 ± 20.6 MPa and $67.5 \pm 41.7^\circ$, respectively. A substantial inter-subject variability was found and our results indicate that typical subject anthropometrics cannot be used as predictors. The functional joint range of motion for human GRA muscle was at least as wide as full knee extension to 120° of knee flexion. However; the portion of the knee angle-muscle force relationship operationalized by GRA muscle is not unique but individual specific. Previous isometric activity of a human muscle at high length was shown for the first time to affect muscle forces measured at lower lengths causing for most of the subjects a decrease.

3. HUMAN SPASTIC GRACILIS MUSCLE ISOMETRIC FORCES AS A FUNCTION OF KNEE ANGLE SHOW NO ABNORMAL MUSCULAR MECHANICS

3.1 Introduction

Cerebral palsy is a movement disorder caused by damage of the developing brain. Skeletal muscle spasticity is the central aspect of such disorders associated with exaggerated stretch reflexes caused by diminished inhibition [32, 34]. Due to that, if the spastic muscle is stretched rapidly, it will resist lengthening actively and, therefore, remain at low length. Such increased resistance to stretch leads to a long lasting, shortened condition of the muscle often followed by structural changes [e.g., 39, 119]. Contractures [38-39, 42] and muscle hypertonicity [29-31] that commonly occur in the lower extremities cause children suffering from spastic cerebral palsy to walk with the hips and knees flexed and with equines deformity at the ankles.

We should be able to show that the mechanics of the spastic muscle are representative of the functional deficiencies clearly apparent in the joints. The limited joint range of motion of the patients suggests that spastic muscle may not be capable of exerting force for the entire range of joint angles attainable from a flexed joint position to full extension. The fact that the joint is forcefully kept in a flexed position suggests that the spastic muscle should be capable of exerting high forces at lower muscle lengths. In order to demonstrate such characteristics, it is necessary to collect data that relate isometric muscle force to joint angle, directly. Measurements of spastic muscle forces of this nature are rarely done in the upper extremities [61, 93] and, to our knowledge, never in the lower extremities.

In the present study, using our recently developed methods [120], we measured the forces of activated spastic Gracilis (GRA) muscle as a function of knee joint angle during remedial surgery. Our goal was to test the following hypotheses: (1) the muscle's

joint range of force exertion is narrow. (2) High muscle forces are available at flexed joint positions corresponding to low muscle lengths.

3.2 Methods

Surgical and experimental procedures, in strict agreement with the guidelines of the Helsinki declaration, were approved by a Committee on Ethics of Human Experimentation at Istanbul University, Istanbul.

3.2.1 Patients

Seven patients (four male and three female: at the time of surgery, mean age 8 years, range 5-18, standard deviation 4.6 years) diagnosed with spastic cerebral palsy, however with no prior remedial surgery, were included in the study.

The Gross Motor Functional Classification System (GMFCS) [121-122] was used to classify the mobility of the patients. Those who were included in the study attained scores of level II or higher, indicating the severity of their limited mobility (Table 1). In short, all patients tested were in need of physical assistance for walking (in order to avoid a fall and rapid buildup of fatigue) and also a support was necessary for sitting and standing (level II). For some patients, additional aids including a wheelchair or a body support walker were needed for mobility (level III and IV). Additional patient classification was done based on popliteal angle [the angle between hip and knee at hip in 90° flexion, see 123] and hip abduction angle measured when the hip is in extended position [124] (Table 2). Clinical tests led to a decision that all patients required remedial surgery including release of hamstrings and hip adductors.

All patients were operated on bilaterally. For three of the patients, separate experiments were performed on both legs, whereas for the remainder, only one leg was experimented on due to time limitations imposed by subsequent multilevel surgery.

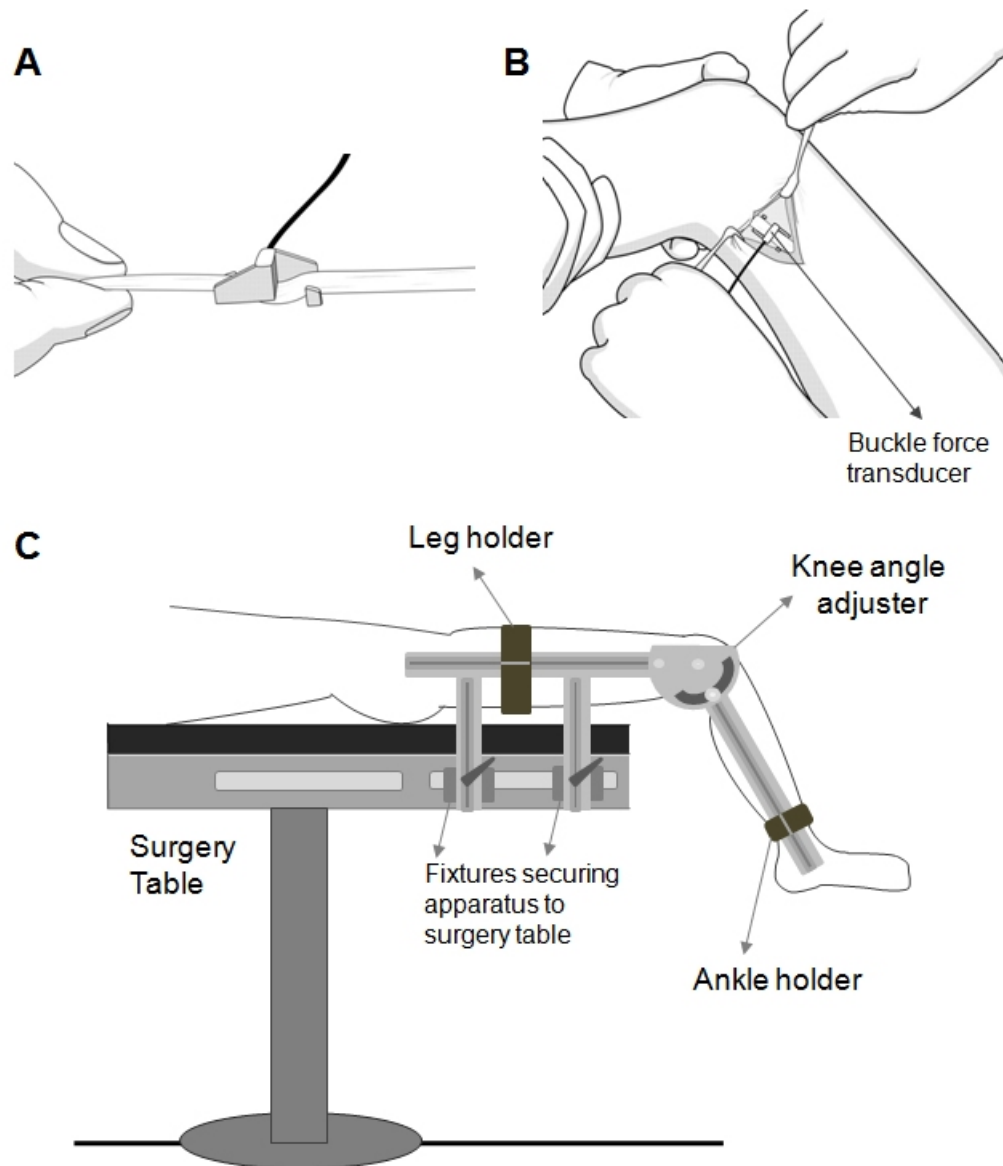


Figure 3.1 Usage of buckle force transducer and the apparatus for intra-operative muscle mechanics experiments in the lower extremities. Illustrations of how the buckle force transducer is mounted over (a) tendon strips, and (b) over the GRA distal tendon for measurements of muscle force are shown. (c) The apparatus designed is comprised of three components. (i) The Upper leg component incorporating a leg holder allows fixing the hip angle (to 0° both in the sagittal and frontal planes). This component is secured to the slot of the surgery table. (ii) The Lower leg component incorporating an ankle holder supports the lower leg. (iii) The knee angle adjuster that links together the upper and lower leg components and allows setting the knee angle and fixing it during a contraction.

Therefore, a total of ten knee angle-GRA muscle force data sets were collected. Prior to surgery, (1) after a full explanation of the purpose and methodology of the experiments, the patients or their parents provided their informed consent, and (2) patient anthropometric data were collected.

3.2.2 Methods

The patients received general anesthesia and no muscle relaxants or tourniquet was used. All intraoperative experiments were performed after routine incisions to reach the distal GRA tendon and before any other surgical procedures of muscle lengthening surgery.

Using a scalpel blade (number 18), a longitudinal skin incision of 2.5cm was made immediately above the popliteal fossa. After cutting the adipose tissue and the fascia lata, the distal GRA tendon was exposed. Subsequently, a buckle force transducer (S-shape, dimensions: width=12mm length=20mm and height=9mm, TEKNOFIL, Turkey) was mounted and fixed over the tendon. Note that prior to each experiment, the force transducer was (i) calibrated using bovine tendon strips (with rectangular cross section, dimensions 7x2mm² representative of that of the GRA distal tendon) and (ii) sterilized (using dry gas at maximally 50⁰ C). See Figure 3.1a and b, respectively, for illustrations of how a buckle force transducer is mounted over tendon strips and over the GRA distal tendon for measurements of muscle force.

An apparatus comprised of three components (Figure 3.1c) was designed: (1) the upper leg component was secured with two fixtures to the slot of the surgery table and the leg holder, which had an adjustable position on it that allowed supporting the upper leg and fixing the hip angle (to 0° both in the sagittal and frontal planes); (2) the knee angle adjustor combining the upper and lower leg components allowed setting the knee angle and fixing it during the contractions; (3) the lower leg component with an ankle holder that had an adjustable position on it allowing support of the lower leg. Isometric spastic GRA muscle force was measured at various muscle lengths imposed

Table 3.1
Patient parameters

| Patient | Age (years) | Limb | L_{leg} (cm) | L_{thigh} (cm) | $c_{mid-thigh}$ (cm) | GMFCS |
|---------|----------------|------|----------------|------------------|----------------------|-------|
| 1 | 6 | A | 48.0 | 24.0 | 33.0 | II |
| 1 | 6 | B | 48.0 | 24.0 | 32.5 | II |
| 2 | 6 | C | 56.0 | 28.0 | 30.0 | III |
| 3 | 7 | D | 47.0 | 23.0 | 23.0 | IV |
| 3 | 7 | E | 45.0 | 23.0 | 23.5 | IV |
| 4 | 9 | F | 57.5 | 28.5 | 34.0 | III |
| 5 | 5 | G | 45.0 | 24.0 | 28.0 | II |
| 6 | 6 | H | 47.0 | 24.0 | 30.0 | II |
| 7 | 18 | I | 77.5 | 38.5 | 49.0 | II |
| 7 | 18 | J | 78.0 | 38.0 | 47.0 | II |

by manipulating the knee joint angle. Starting at a highly flexed knee (120°), muscle length was increased progressively by extending the knee by 30° increments, until full knee extension (i.e., muscle force was measured at 120° , 90° , 60° , 30° and 0°). Seven patients (four male and three female: at the time of surgery, mean age 8 years, range 5-18, standard deviation 4.6 years) diagnosed with spastic cerebral palsy, however with no prior remedial surgery, were included in the study.

A pair of gel-filled skin electrodes (EL501, BIOPAC Systems, CA, USA) was placed on the skin, over the GRA muscle belly. Using a custom made, constant current high voltage source (cccVBioS, TEKNOFIL, Istanbul, Turkey) the muscle was stimulated supramaximally (transcutaneous electrical stimulation with a bipolar rectangular signal, 160 mA, 50Hz): a twitch was evoked which after 300 ms was followed by a pulse train for 1000 ms to induce a tetanic contraction and a subsequent twitch (see Figure 3.2 for superimposed examples of force-time traces for spastic GRA muscle at the five knee angles). The GRA muscle forces measured during a 500 ms period in the middle of the tetanus were averaged to obtain the muscle force.

A data acquisition system (MP150WS, BIOPAC Systems, CA, USA, 16-bit A/D converter, sampling frequency 40 KHz) was used with an amplifier for each transducer (DA100C, BIOPAC Systems, CA, USA). After each contraction, the muscle was al-

lowed to recover for 2 minutes in a flexed knee posture.

All experimental preparations and data collection were completed within 30 minutes, the maximal study duration allowed by the ethics committee.

3.2.3 Processing of data

3.2.3.1 Clinical Measures. The popliteal and hip abduction angles for each limb were normalized for the values of these angles representing the most severe limitations to joint motion among our patients using equations (1) and (2):

$$PA_{normalized} = \frac{PA}{PA_{max}} \quad (1)$$

where, PA and $PA_{normalized}$ are the actual and normalized popliteal angle for a particular limb, respectively. PA_{max} is the maximal popliteal angle value measured among the limbs studied.

$$HAA_{normalized} = \frac{HAA}{HAA_{max}} \quad (2)$$

where, HAA and $HAA_{normalized}$ are the actual and normalized hip abduction angle for a particular limb, respectively. HAA_{max} is the maximal hip abduction angle value measured among the limbs studied. The GRA muscle is a flexor of the knee as well as an adductor of the hip. Therefore, summed $PA_{normalized}$ and $HAA_{normalized}$ represented a *limb score for limited range of motion* (ROM) (Table 2).

3.2.3.2 Experimental measures. Using a least squares criterion, data for total GRA muscle force (FGRA) in relation to knee joint angle (KA) were fitted with a polynomial function

$$F_{GRA} = a_0 + a_1KA + a_2KA^2 + \dots + a_nKA^n$$

Table 3.2
Clinical measures characterizing motion limitation and experimental measures

| Limb | Clinical examination data | | | Experimental data | | | |
|------|---------------------------|--------|----------------------------|--|---------------------------|--------------------------------|------------------------------|
| | PA (°) | HAA(°) | Limb score for limited ROM | KA _{F_{GRA} peak} (°) | F _{GRA peak} (N) | % F _{GRA peak} 120° | % F _{GRA peak} 0° |
| A | 85 | 30 | 128 | 34 | 126.9 | 26.3 | 88.5 |
| B | 85 | 25 | 134 | 65 | 10.4 | 66.0 | 67.6 |
| C | 55 | 40 | 0.86 | 16 | 82.6 | 47.8 | 96.1 |
| D | 90 | 35 | 129 | 0 | 86.5 | 22.4 | 100.0 |
| E | 60 | 30 | 1.00 | 66 | 26.5 | 74.6 | 61.6 |
| F | 90 | 10 | 2.00 | 63 | 34.4 | 79.1 | 73.9 |
| G | 80 | 40 | 1.14 | 0 | 10.5 | 38.4 | 100.0 |
| H | 65 | 35 | 1.01 | 0 | 10.8 | 34.6 | 100.0 |
| I | 65 | 15 | 1.39 | 43 | 13.6 | 66.2 | 89.7 |
| J | 80 | 15 | 1.56 | 0 | 13.8 | 41.2 | 100.0 |

$a_0, a_1 \dots a_n$ are coefficients determined in the fitting process. The lowest order of the polynomials that still added a significant improvement to the description of changes of KA and F_{GRA} data were selected using a one-way analysis of variance (ANOVA) [125]. The fitted KA-F_{GRA} characteristics of the patients were studied separately for each limb for characterization of the mechanics of the spastic GRA muscle.

Experimentally obtained measures were used for an objective assessment of our hypotheses based on (i) joint range of muscle force exertion and (ii) availability of high muscle force at low muscle length. We considered that a narrow joint range together with the availability of the peak muscle force at the lowest muscle length studied would provide an ideal match between the clinically diagnosed impaired joint motion and the experimentally determined KA-F_{GRA} characteristics. Therefore, we first studied our data to see if the spastic GRA muscle operates within the descending portion of its KA-F_{GRA} curve, exclusively. For KA-F_{GRA} curves other than that, the following procedures were followed.

Measures based on joint range of muscle force exertion

If the peak GRA muscle force (F_{GRA_{peak}}) was attained within the knee joint

range studied such that the increase trend of the force ceased before full knee extension, the spastic GRA muscle was concluded to operate within both the ascending and descending portions of its KA-F_{GRA} curve. Therefore, the joint range of muscle force exertion is not as narrow as for the ideal match. The proximity of the KA at which F_{GRApeak} was exerted (KA_{F_{GRApeak}}) to the maximal knee flexion angle studied indicates how narrow the joint range of force exertion of each limb is. If, on the other hand, F_{GRApeak} was attained only at KA=0°, such that the increase trend of the force was not ceased, the spastic GRA muscle was concluded to operate exclusively within the ascending portion of its KA-F_{GRA} curve. Therefore, such curves were considered not to represent a narrow joint range, and hence not representative of the compromised joint motion regarding this measure. In order to distinguish those limbs, the slope of the KA-F_{GRA} curve for KA=5° to 0° range was calculated. The steepest slope was considered to represent the widest joint range of force exertion among the limbs studied. Additionally, KA-F_{GRA} curves were extrapolated to determine the KA corresponding to muscle active slack length (i.e., the shortest length at which the muscle can still exert non-zero force).

Measures based on the availability of muscle force

Even for the limbs that do not show a narrow knee joint range of GRA muscle force exertion, we considered that the availability of high muscle force at knee flexion represents characteristics of spastic muscle. In order to quantify that, the percentage of F_{GRApeak} exerted at KA=120° (%F_{GRApeak/120°}) was calculated. Additionally, the availability of high muscle force at full knee extension was assessed. In order to quantify that, the percentage of F_{GRApeak} exerted at KA=0° (%F_{GRApeak/0°}) was calculated.

3.2.3.3 Clinical and experimental measures compared. Spearman's Rank correlation coefficient was calculated to test if limb scores for limited ROM are correlated with the key determinants of KA-F_{GRA} characteristics, i.e., (i) KAF_{GRApeak}, (ii) %F_{GRApeak/120°} and, (iii) %F_{GRApeak/0°}. Correlations were considered significant at P<0.05.

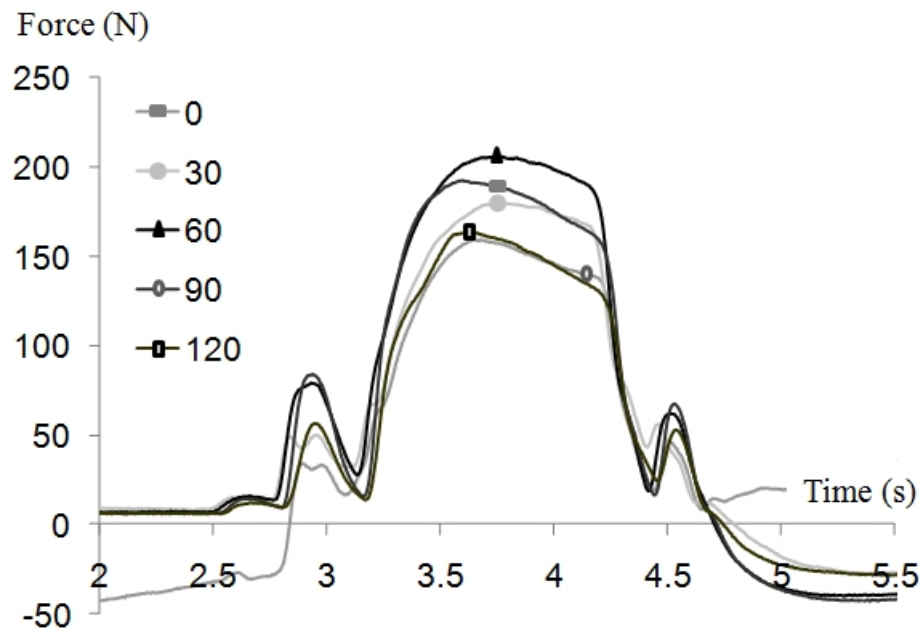


Figure 3.2 Typical examples of force-time traces for spastic GRA muscle. Superimposed traces recorded for GRA muscle at the five knee angles studied are shown

3.3 Results

3.3.1 Clinical Measures

Table 2 shows popliteal angle mean 75.50° (SD 13.01°) and hip abduction angle mean 27.50° (SD 10.87°) values for the limbs tested. Limb scores for limited ROM showed that limb F and limb C, respectively, are the ones that have the most and least pronounced effects of limitations in joint motion.

3.3.2 Experimental measures

Figure 3.3 shows the $KA-F_{GRA}$ characteristics. F_{GRA} peak (mean $41.59N$ (SD $41.76N$)) range between $10.4N$ (limb B) and $126.9N$ (limb A).

Remarkably, for none of the limbs studied, did the spastic GRA muscle operate within the descending portion of its $KA-F_{GRA}$ curve, exclusively. This shows that for none of the limbs studied is there an ideal match between the clinically diagnosed

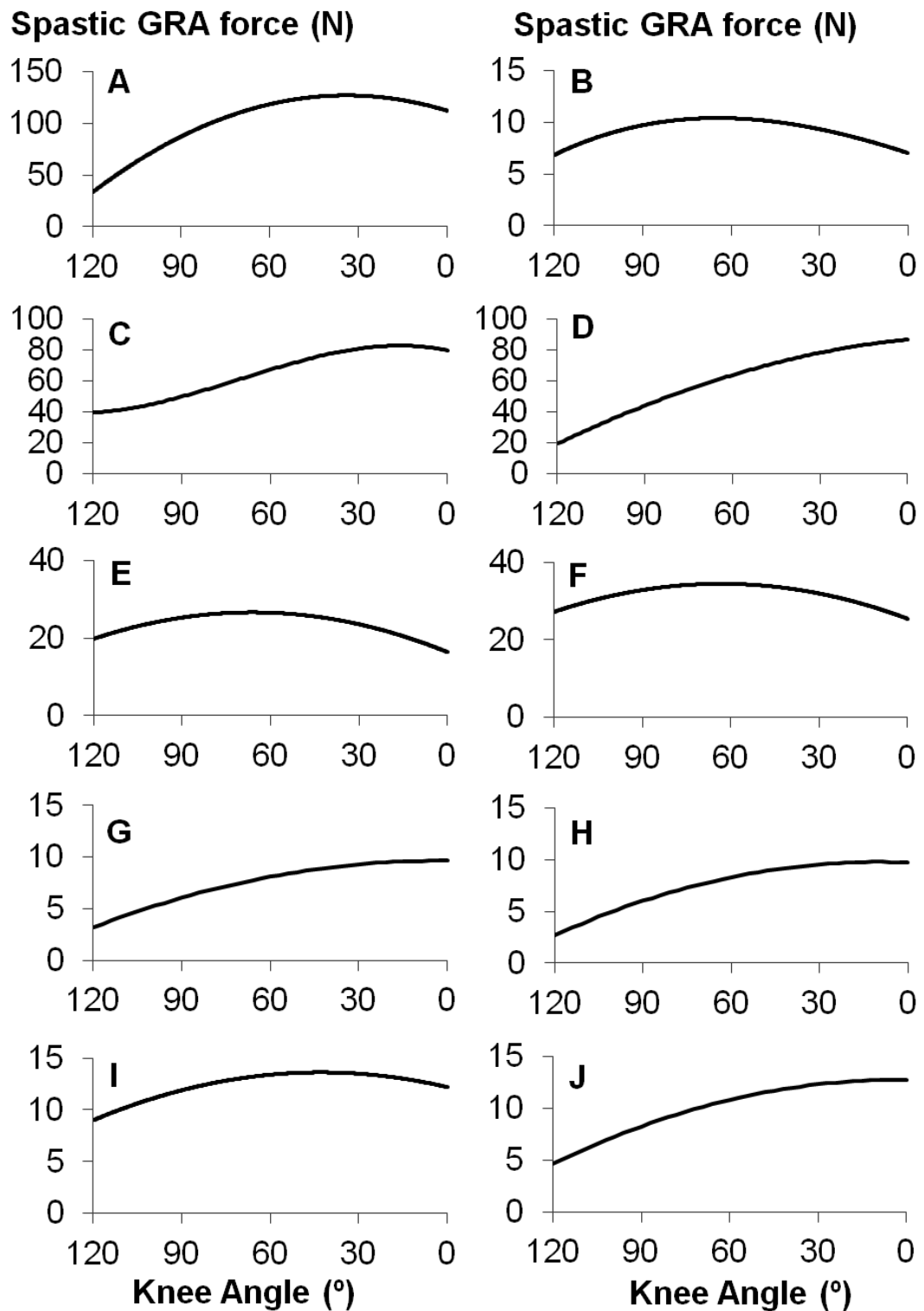


Figure 3.3 The isometric KA-FGRA characteristics for spastic GRA muscle. Data are shown separately for each limb (panels A to J) experimented. Isometric GRA muscle forces were measured at five knee angles: 0° i.e., maximal extension of knee, 30°, 60°, 90° and 120°.

decreased mobility and the experimentally determined KA- F_{GRA} characteristics.

Measures based on joint range of muscle force exertion

For all limbs and for all the knee angles studied, non-zero muscle forces were measured. This indicates that the GRA muscle's operational joint range of muscle force exertion includes the entire joint range studied. Therefore, the muscle's active slack length corresponds to a knee flexion of over 120° (minimally 134° for limb A, as determined using extrapolated data). For only 6 limbs (A, B, C, E, F and I), was it possible to determine the KAF $_{GRA}$ peak within the knee joint range studied (Table 2). The operational joint range of force exertion for limb E (KAF $_{GRApeak} = 66^\circ$) was found to be the narrowest. For the remaining 4 limbs (D, G, H and J), the operational joint range of force exertion was shown to include exclusively the ascending portion of their KA- F_{GRA} curves. The steepest slope at KA= 0° of these curves was calculated for limb D, indicating the widest operational joint range of force exertion.

Measures based on availability of muscle force

Table 2 shows that as much as 79.1% and 74.6% of $F_{GRApeak}$ are available at the lowest muscle length studied respectively for limbs F and E. For the remainder of the limbs, maximally 66.2% (limb I) and minimally 22.4% (limb D) of $F_{GRApeak}$ were available at such low length. The GRA muscle was capable of exerting high forces even at the highest length studied: minimally for limb E $\%F_{GRApeak/0^\circ} = 61.6$ (Table 2).

3.3.3 Clinical vs. experimental measures

No significant correlations were found between limb scores for limited ROM and the key determinants of KA- F_{GRA} characteristics: Spearman's rank correlation coefficients were only 0.03 ($p = 0.93$), 0.24 ($p = 0.48$), and 0.02 ($p = 0.96$), respectively, for a comparison with respect to KAF $_{GRApeak}$, $\%F_{GRApeak/120^\circ}$ and, $\%F_{GRApeak/0^\circ}$.

3.4 Discussion

3.4.1 The intraoperative measurement method

Clinical measures of the GMFCS as well as popliteal and hip abduction angles indicated decreased mobility of all of our patients requiring multilevel surgery involving lengthening of the GRA muscle. The purpose of this study was to test our hypotheses to demonstrate that the mechanics of the spastic GRA muscle are representative of such impaired joint motion.

Prior to any routine surgical procedures, except for the incisions required for exposing the distal GRA tendon, the muscle forces were measured using buckle force transducers. This avoids any dissection of the muscle belly and therefore any potential damage to innervation and blood supply to the muscle. An important advantage of our methods is that the difficulty of matching muscle forces and corresponding joint angles is eliminated by measuring muscle forces directly as a function of knee joint angle. Therefore, the experimental conditions were the closest possible to those attainable in vivo. To our knowledge, such data for spastic GRA muscle are presented for the first time.

Before discussing the implications of the results obtained, it is important to consider some of the limitations of this study: (I) Measurement of passive force was not possible: (1) prior to the tetanus, the twitches did not always remove the GRA tendon slack entirely; (2) After the tetanus was ceased, since the tendon buckles during unloading, the force transducers working on a principle of torque measurement [94] measure negative forces, not representative of the passive state. Due to that, our results are not capable of reflecting on high passive tissue stiffness considered to characterize spastic muscle in general [57-58] and spastic GRA muscle in particular [59]. (II) Although the availability of muscle force data per joint angle allows for making clinically relevant interpretations, because the moment arm lengths of muscles vary with varying joint angles [e.g. 126, 127], relating the changes in knee joint angle to actual muscle length change is not possible. To our knowledge no study is available that

reports such relationship for spastic GRA muscle. Therefore, presently the arguments on spastic GRA forces measured are based on our assumptions that flexion of the knee joint causes GRA muscle length to decrease. Intuitively, this is a tenable assumption. However, the measurement of muscle force-length characteristics can allow for a more direct addressing of muscle length related issues, e.g., the availability of high muscle force at low muscle length. After being modified, our methods can be used for such measurements, e.g., by attaching a regular force transducer to the tendon and measuring isometric muscle forces subsequent to altered position of the transducer as done in animal experiments [e.g. 23]. However, in order for this to be possible, the distal GRA tendon has to be transected, which is not included in the allowable procedures of muscle lengthening surgery. Medical imaging modalities may be used in relating the changes in knee joint angle to actual muscle length change. New studies are indicated to address this issue.

3.4.2 Experimental data show no abnormal mechanical characteristics for spastic GRA muscle

Spasticity is a motor disorder characterized by a velocity-dependent resistance to stretch [31]. The feature central to spastic muscle is hypertonia [39, 128]. Such increased muscle tone originates in part from increased stretch reflex activity [34]. However, methods (e.g., injection of botulinum-toxin) to suppress the problem are not fully effective [44]. Therefore, this is not likely to be the sole cause of increased muscle tone due to which spastic muscle tissue is considered typically as stiffened. A suggestion is that there is a passive component to the stiffening of spastic muscle tissue [30, 58]. Chronic activation of the affected muscle causes acute muscle shortening [39], and an adaptation to such state is referred to as contracture. Contractured muscle in the clinics is considered to limit the ROM around a joint even in the absence of any active force exertion [129].

Presently, we evaluated for each limb the outcome of clinical examinations performed in the passive state. A popliteal angle greater than 50° in age groups of 5

years and older was shown to indicate abnormal knee flexor tightness [123]. For all limbs studied presently, this limit was exceeded. Also hip abduction of less than 40° was shown to indicate abnormality [75, 130]. Limb C was at the limit of such abnormality, which was exceeded for all other limbs. Therefore, the pre-operative clinical examinations performed presently did indicate a severely limited range of knee and hip joint motion suggesting strongly an occurrence of muscle contracture. However, our experimental results show for all limbs tested that the activated spastic GRA muscle is capable of exerting non-zero forces at all of the joint angles studied. This shows that the functional joint ROM for spastic GRA muscle is at least as wide as a full knee extension to 120° of knee flexion. Using the same methods, we tested recently the GRA muscle of healthy adults undergoing anterior cruciate ligament reconstruction surgery [120]. Obviously, at least because those patients were of a different age group, sizable differences in muscle force data are to be expected. Yet, there is full qualitative agreement between our present and previous results that functional joint ROM is as wide for spastic GRA muscle as for healthy GRA muscle. Our present finding suggesting that muscle optimum length corresponds to a high muscle length does not show any particular dissimilarity to the mechanical characteristics of healthy muscle. Therefore, we conclude that the KA-FGRA characteristics of spastic GRA muscle are not representative of the limited ROM the patients are suffering and reject our first hypothesis. Moreover, our results showed that the limb scores for limited ROM and the key determinants of KA-FGRA characteristics are not correlated. Therefore, although muscle contracture alone is known to limit joint ROM, our present findings indicate that it may not affect joint angle-muscle force characteristics for activated muscle.

During daily life, joint ROM may be limited by the muscle's active resistance capacity, rather than by its passive resistance. A parameter that could objectively characterize this was the availability of high force at low length: even if the spastic muscle was capable of exerting muscle force for a ROM that appears wide enough for daily activities, high muscle forces exerted at low length may prevent the operationalization of the remainder of the ROM and cause movement disorder.

Our results show that for none of the limbs tested was the highest muscle force

available at the lowest muscle length studied. For limbs E and F, a sizable portion of the peak muscle force (as high as 79%) was measured at low GRA muscle length. This suggests for these limbs that the shape of the KA-FGRA curve may be in reasonable agreement with an expected shape for spastic muscle. However, for limbs B and I approximately 66%, and for the remainder of the limbs less than only 50% of the peak muscle force was available at low length. Moreover, muscle forces for some limbs, including E and F, appear to be low. Our methods were confirmed to stimulate the muscle maximally [120]. However, a decrease in neuronal drive in cerebral palsy patients [131-132] is possible. A decreased muscle size is also likely [51, 53]. Such factors may have caused the muscle to be “weakened”. In sum, no supreme active resistance capacity of spastic GRA muscle to stretch was shown presently. This contradicts an expectation that spastic muscle is a source of high forces that cause movement limitation at the joint. Therefore, also our second hypothesis can be rejected.

3.4.3 Mechanisms which may be responsible with the present findings

In a recent study on the muscles important for propulsion in hemiplegic subjects, Riad et al. [133] reported that muscle volumes assessed using magnetic resonance imaging (MRI) analyses were decreased compared to the noninvolved side, with an exception for the GRA muscle. This may suggest that the GRA muscle is relatively spared in hemiplegic cerebral palsy. However, in another recent study, Smith et al. [59] reported increased collagen content and increased stiffness for the extracellular matrix of GRA muscle of subjects with cerebral palsy. The existence of such adaptation of intramuscular connective tissues indicates that this muscle also is affected in children with spastic cerebral palsy. Yet, two issues should be considered: GRA muscle (1) in healthy subjects was shown to have long fibers [134] and large excursion [98], and (2) is not a primary knee flexor. The former suggests that this muscle may operate over very large joint flexions even if it suffers from contracture secondary to cerebral palsy. This could be responsible for the lack of the narrow operational joint range of force exertion shown presently. The latter suggests that the dominant source of high forces that cause movement limitation at the joint may be the hamstrings. It was shown that the fiber

length of the semimembranosus and biceps femoris muscles are three to four times shorter than that of the GRA muscle [134]. Therefore, it may be more likely to find a relationship between contracture magnitude and active force-joint angle relationships in such muscles with shorter fibers. Note that Makihara et al. [134] showed that also the semitendinosus muscle has long muscle fibers comparable to those of the GRA muscle. However, in children with cerebral palsy, the results of Oberhofer et al. [51] obtained by using MRI analyses and anatomically-based modeling techniques are not in full agreement with the expectations related to muscle architecture in relation to tissue adaptation: these authors showed that the semimembranosus was shortened together with the much longer fibered semitendinosus, whereas the biceps femoris was not shortened significantly. Additionally, after analyzing crouch gait with a graphic-based model accompanied by 3D kinematic data, Delp et al. [135] showed that only for a minority of their subjects were the lengths of hamstring muscles shorter than normal. These findings do not seem to indicate univocally that the present findings are due to the particular muscle architecture of the GRA muscle. However, new studies are indicated in which hamstrings are tested.

Adaptation to a prolonged shortened state of muscle is considered as a characteristic spasticity-related effect yielding a reduction in the number of sarcomeres within muscle fibers and shortened muscle fibers [136]. Studies using ultrasound imaging [50, 137] show no evidence for fascicle length change in spastic gastrocnemius muscle. Nevertheless, it is believed that sarcomere numbers within fascicles may change in the spastic muscle even though fascicle lengths may not change [59]. Therefore, one parameter which has been used to assess the effects of a contracture is increased sarcomere length. Dr. Lieber's group developed elegant measurement techniques and reported that sarcomere lengths are indeed higher in spastic muscle [59, 138-139]. Smith et al. [59] concluded that the increased sarcomere length shown for spastic GRA muscle is an indicator of spastic muscle being under higher passive stress, and hence plays an important role in contracture formation. However, an additional consequence of increased sarcomere length is that this would favor the production of active force at shorter muscle lengths. The present findings are not capable of showing whether spastic GRA muscle forces measured at the flexed knee position are higher than those of typically

developing subjects. Nevertheless, the data showing that no particularly high muscle force is measured at knee flexion do not strongly support the expectation of favored production of active force at shorter muscle lengths. On the other hand, increased sarcomere length of spastic muscle also suggests that at high muscle lengths, sarcomeres should be overstretched. Presently, even at full knee extension, the spastic GRA muscle was capable of exerting high forces (on average 87.7% of FGRA peak). This implies that sarcomeres are not at very high lengths, unfavorable for force production. However, due to the unavailability of passive muscle forces, studying active muscle forces and hence inferring sarcomere lengths at high muscle length is not possible. Nevertheless, Smeulders et al. [97] did show a contrasting finding to the expectation of existence of overstretched sarcomeres indirectly: a majority of the maximum active force of the spastic flexor carpi ulnaris muscle was available at maximal extension of the wrist, indicating abundant overlap of the sarcomeres at high muscle length and hence no sarcomere overstressing. Moreover, these authors also reported that at high flexor carpi ulnaris lengths, the passive force measured was not exceptionally high. Therefore, considering increased sarcomere length as a determinant for the effects of a contracture does not seem to explain the present findings consistently.

The present experiments were performed at hip angle fixed to 0° . As the GRA muscle is also a hip flexor, any added flexion of the hip to the test position plausibly would have caused the muscle to be shortened proximally. This suggests that the spastic GRA muscle may have been tested at even lower lengths than presently studied for the same maximal knee flexion tested. As one of the key goals of the present study was to assess the muscle's force at lower muscle lengths, this may be seen as a limitation. However, an added proximal shortening imposed with a flexed hip position is expected to lead to even lower %FGRA peak | 120° values to be measured. In contrast, introducing certain added hip extension to the test position may allow measurement of higher %FGRA peak | 120° values. It is important to note that both modifications were not feasible due to limitations by the surgery table as well as the surgical procedures. On the other hand, the testing of hamstrings in the present experimental conditions may have caused these hip extensors to be tested at lower lengths for the same maximal knee flexion tested. If possibilities can be created, these alternatives should be tested

in new studies.

Based on our findings and the mechanisms considered above, considering the question “what could be the origin of high forces within the spastic paretic limb?” posed recently [62] may contribute to this discussion. This question was posed because in the characteristic joint positions (e.g., flexed knee) of cerebral palsy patients, the spastic muscle is at low length. For healthy muscle, this means a low capacity for active force exertion. Confirming Huijing’s implicit assumption, our results showed that this is not particularly different for spastic muscle. Dr. Huijing proposed that the source of forces high enough to generate moments that keep the joint in the particular position is the antagonistic muscles which are at higher length, favorable for higher force exertion. He hypothesized that forces generated within sarcomeres of an antagonistic muscle by epimuscular myofascial force transmission (EMFT) [for a review of key concepts see 63, 140] can be exerted at the distal tendon of the spastic muscle.

Note that unlike the animal experiments on healthy muscles [e.g. 107], there is no direct evidence for antagonistic EMFT to occur in cerebral palsy. However, Kreulen et al. [60] did show that epimuscular connections (i.e., EMFT pathways) comprised of e.g., neurovascular tracts and compartmental boundaries [for pictures, see 20, 63] play a mechanical role in spastic muscle: subsequent to the tenotomy of flexor carpi ulnaris muscle, they tested whether dissecting the muscle’s epimuscular connections affects the muscle length: i) in the neutral wrist position and ii) on passively moving the wrist. In the neutral wrist position, tenotomy alone (no dissection of the epimuscular connections done) caused a minor shortening of the passive muscle and only a limited further shortening was found after the muscle was tetanized. In contrast, after partial dissection of the muscles’ epimuscular connections its shortening increased substantially in both passive and active conditions. On passively moving the wrist, the authors showed that muscle excursions measured in intact condition and after tenotomy alone were very similar. However, dissection caused a dramatic decrease in the muscles’ excursion. These results suggest that the EMFT mechanism plays a role in muscle spasticity.

In the present experimental conditions, epimuscular connections were intact. However, among others, an important difference of the test conditions to those of daily activities in which several muscles are activated simultaneously is that solely the target GRA muscle was activated. Therefore, although the mechanical interaction of the spastic GRA muscle with its surrounding structures was probable, no EMFT of active antagonistic force was possible. This may be responsible at least in part for the “normal” function of the spastic muscle shown presently, and supports Huijing’s hypothesis implicitly.

On the other hand, myofascial loads acting on the muscle fibers are expected to make the force balance determining the length of a sarcomere much more involved than that determined solely by the interaction of the sarcomeres arranged in series within the same fiber [141]. This can cause distribution of lengths of sarcomeres [22, 25, 109], a major effect of EMFT. Using MRI, such loads that may originate from stretching epimuscular connections were shown to cause substantial deformations within lengthened as well as restrained human calf muscles, *in vivo* [142]. In the case of the simultaneous activation of muscles within a limb, much enhanced myofascial loads are conceivable to cause sizable sarcomere length heterogeneity. This may have two relevant implications: (1) overstretched sarcomeres may be found locally, but this may not necessarily be a general effect within the entire spastic muscle, (2) major shape changes shown to occur in muscle force-length characteristics [23, 25] due to altered sarcomere length heterogeneity may yield joint angle-muscle force characteristics that are more representative of the movement disorder.

In conclusion, the knee angle-muscle force characteristics of the spastic GRA muscle are not representative of the pathological condition occurring at the joint, indicating no abnormal muscular mechanics. An explanation for this may be activation of the muscle alone.

4. SIMULTANEOUS AGONISTIC-ANTAGONISTIC STIMULATION CAUSES PARALLELISM BETWEEN MECHANICS OF SPASTIC GRACILIS MUSCLE AND THE PATIENTS' MOVEMENT LIMITATION

4.1 Introduction

Many cerebral palsy, multiple sclerosis, and stroke, patients suffer from spasticity which is a form of hypertonia characterized by velocity dependent exaggerated reflexes [31, 33]. In long term, even anti-spastic treatments are applied [43-44] contracture formation with muscle and soft tissue shortening [39] accompanies spasticity [40-41]. Decreased joint range of motion and impaired function [40, 45-48] is associated with contracture.

Due to spastic CP, previous studies showed muscle shortening for gastrocnemius [49-50], for semitendinosus, semimembranosus [51], and a decrease in muscle volume for gastrocnemius [54], hamstrings [51], adductors [53], and anterior muscles [52]. However, such changes in muscles and muscle groups shown with ultrasound (US) or magnetic resonance imaging (MRI) modalities were not linked with the joint function. On the other hand, Smith et al. [59] reported increased collagen content and stiffness for the extracellular matrix for the spastic gracilis (GRA) muscle whereas an MRI study [133] showed that in contrast to other muscles, the decrease in GRA muscle volume was not significant.

Our previous study [143] reporting spastic GRA muscle's isometric forces as a function of knee joint angle for the first time in the literature showed no abnormality for GRA muscle characteristics: in contrast to the clinically pathological function of the knee joint, spastic GRA muscle (i) showed no narrow operational joint range of force exertion and (ii) active resistance capacity of this muscle was not supreme at low

lengths. Such results showing qualitative similarity with previous ones we reported for healthy GRA [120] suggest that stimulation electrically of solely the target GRA muscle in the experiments and in contrast to the typical in vivo conditions which involve simultaneous contraction of several muscles may be the reason of such normal mechanics. This condition limits epimuscular myofascial force transmission (EMFT) [62, 107], which has been shown to change the magnitude of muscle force and how it is related to muscle length [16, 111, 140-141]. Therefore, we hypothesized that the knee joint angle-muscle force curves of spastic GRA muscle activated simultaneously with its antagonist vastus medialis (VM) show abnormal mechanics representative of joint movement disorder.

4.2 Methods

Surgical and experimental procedures, in strict agreement with the guidelines of the Helsinki declaration, were approved by a Committee on Ethics of Human Experimentation at Istanbul University, Istanbul.

4.2.1 Patients

Six patients (four male and two female: at the time of surgery, mean age 10.7 years, range 6-16, standard deviation 3.6 years) diagnosed with spastic cerebral palsy, however with no prior remedial surgery, were included in the study. The Gross Motor Functional Classification System (GMFCS) [121-122] was used to classify the mobility of the patients. Those who were included in the study attained scores of level II to IV, indicating the severity of their limited mobility (Table 4.1). Additional patient classification was done based on popliteal angle [the angle between hip and knee at hip in 90° flexion, see 123] and abduction angle measured when the hip is in extended position [124] (Table 4.2). Clinical tests led to a decision that all patients required remedial surgery including release of hamstrings and hip adductors.

All patients were operated on bilaterally. For four of the patients, separate experiments were performed on both legs, whereas for the remainder, only one leg was experimented on due to time limitations imposed by subsequent multilevel surgery. Therefore, a total of ten knee angle-GRA muscle force data sets were collected. Prior to surgery, (1) after a full explanation of the purpose and methodology of the experiments, the patients' parents provided their informed consent, and (2) patient anthropometric data were collected (Table 4.1).

4.2.2 Methods

The patients received general anesthesia and no muscle relaxants or tourniquet was used. All intraoperative experiments were performed after routine incisions to reach the distal GRA tendon and before any other surgical procedures of muscle lengthening surgery. Using a scalpel blade (number 18), a longitudinal skin incision of 2.5cm was made immediately above the popliteal fossa. After cutting the adipose tissue and the fascia lata, the distal GRA tendon was exposed. Subsequently, a buckle force transducer (Figure 4.1A) (S-shape, dimensions: width=12mm length=20mm and height=9mm, TEKNOFIL, Turkey) was mounted and fixed over the tendon. Note that prior to each experiment, the force transducer was (i) calibrated using bovine tendon strips (with rectangular cross section, dimensions 7x2 mm² representative of that of the GRA distal tendon) and (ii) sterilized (using dry gas at maximally 50°C).

Two pairs of gel-filled skin electrodes (EL501, BIOPAC Systems, CA, USA) were placed on the skin, over the GRA and VM muscle belly (Figure 4.1B). Using a custom made, constant current high voltage source (cccVBioS, TEKNOFIL, Istanbul, Turkey) the muscles were stimulated supramaximally (transcutaneous electrical stimulation with a bipolar rectangular signal, 160 mA, 50Hz): two twitches were evoked which after 300 ms was followed by a pulse train for 1000 ms to induce a tetanic contraction and a subsequent twitch.

During isometric force measurements, subject's hip was fixed to 0° both in the



Figure 4.1 Usage of buckle force transducer and stimulation electrodes. Illustrations of how (A) the buckle force transducer is mounted over tendon strips, and (B) the skin electrodes are mounted over the GRA and VM muscles are shown.

sagittal and frontal planes and the ankle was immobilized. GRA muscle isometric forces were measured (i) at 120° and 90° of knee angle by stimulating GRA muscle exclusively, afterwards (ii) from 120° , a highly flexed knee, to full extension with 30° increments (at 120° , 90° , 60° , 30° and 0°) by stimulating GRA and VM muscles simultaneously. Note that, some patients were not capable of extending their knee fully (0°). Therefore, for the limbs that full KA range was not feasible, the last force measurement was performed at the most possible extended position of knee. A data acquisition system (MP150WS, BIOPAC Systems, CA, USA, 16-bit A/D converter, sampling frequency 40 KHz) was used with an amplifier for each transducer (DA100C, BIOPAC Systems, CA, USA). After each contraction, the muscle was allowed to recover for 2 minutes in a flexed knee posture. Data collection was completed within 30 min, the maximal study duration allowed by the ethics committee.

A data acquisition system (MP150WS, BIOPAC Systems, CA, USA, 16-bit A/D converter, sampling frequency 40 KHz) was used with an amplifier for each transducer (DA100C, BIOPAC Systems, CA, USA). After each contraction, the muscle was allowed to recover for 2 minutes in a flexed knee posture. Data collection was completed within 30 min, the maximal study duration allowed by the ethics committee.

Table 4.1
Patient Parameters

| Patient | Limb | Sex | Age | l_{leg} (cm) | l_{thigh} (cm) | $C_{mid-thigh}$ (cm) | GMFCS |
|---------|------|-----|-----|----------------|------------------|----------------------|-------|
| A | 1 | M | 16 | 86 | 40 | 44.2 | II |
| B | 2 | M | 10 | 68 | 33 | 35 | II |
| C | 3 | F | 8 | 53 | 24 | 27 | II |
| C | 4 | F | 8 | 54 | 24 | 28.5 | II |
| D | 5 | M | 6 | 54.5 | 24 | 29 | IV |
| D | 6 | M | 6 | 54 | 24.5 | 27 | IV |
| E | 7 | F | 13 | 73 | 35 | 29 | II |
| E | 8 | F | 13 | 73 | 35 | 29 | II |
| F | 9 | M | 11 | 73 | 36 | 34.5 | IV |
| F | 10 | M | 11 | 73 | 36 | 34.5 | IV |

4.2.3 Processing of Data

Clinical Examination Data Since the GRA muscle is a flexor of the knee as well as an adductor of the hip, the sum of popliteal and hip abduction angles normalized for their most severe case among our patients with the equation (1) represented the limb score for limited range of motion (ROM).

$$\text{Limb Score for Limited ROM} = \frac{PA}{PA_{max}} + \frac{HAA_{min}}{HAA} \quad (1)$$

where, PA and HAA are the actual popliteal and hip abduction angles for a particular limb, respectively. PA_{max} is the maximal popliteal angle and HAA_{min} is the minimum hip abduction angle measured among the limbs studied. Both represent the most severe cases.

Experimental data Each raw GRA force-time data was filtered with Savitzky-Golay smoothing filter (see Figure 4.2 for superimposed examples of filtered force-time traces for spastic GRA muscle at the five knee angles).

The GRA muscle forces measured during a 100 ms period in the middle of the tetanus were averaged to obtain the muscle total force. Using a least squares criterion, data for total GRA muscle force (FGRA) in relation to knee joint angle (KA) were fitted with a polynomial function

$$F_{GRA} = a_0 + a_1KA + a_2KA^2 + \dots + a_nKA^n$$

$a_0, a_1 \dots a_n$ are coefficients determined in the fitting process. The lowest order of the polynomials that still added a significant improvement to the description of changes of KA and The lowest order of the polynomials that still added a significant improvement to the description of changes of KA and FGRA data were selected using a one-way analysis of variance (ANOVA) [125]. The fitted KA- F_{GRA} characteristics of the patients were studied separately for each limb for characterization of the mechanics of the spastic GRA muscle. Experimentally obtained measures were used for an objective assessment of our hypotheses based on (i) joint range of muscle force exertion and (ii) availability of high muscle force at low muscle length.

Joint range of muscle force exertion If the peak GRA muscle force ($F_{GRApeak}$) was attained within the knee joint range studied such that the increase trend of the force ceased before full knee extension, the spastic GRA muscle was concluded to operate within both the ascending and descending limbs of its KA- F_{GRA} characteristics. If a local minimum defined as the minimum force measured inside the range of KAs scanned appeared, maximum force measured before that point was considered as F_{peak} .

The proximity of the KA at which F_{GRA} peak was exerted ($KAF_{GRApeak}$) to the maximal knee flexion angle studied indicates how narrow the joint range of force exertion of each limb is. Therefore, the curves including local minimum or $KAF_{GRApeak}$ closed to flexion were considered to represent a narrow joint range, and hence representative of the compromised joint motion.

The availability of muscle force The availability of high muscle force at knee flexion was considered to represent a typical characteristic of spastic muscle. In order to

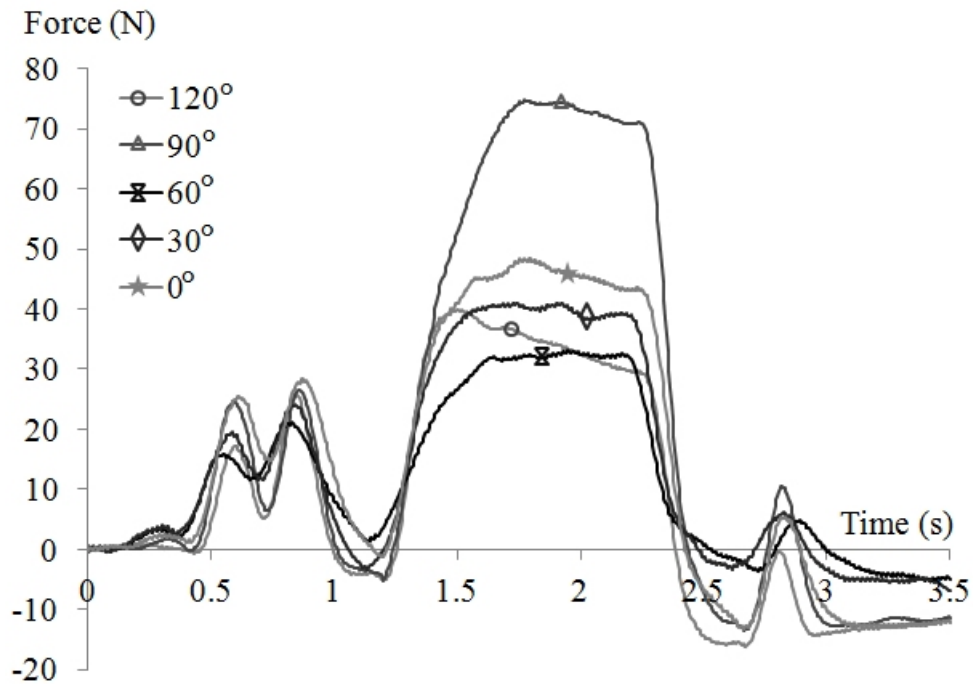


Figure 4.2 Typical examples of force-time traces for spastic GRA muscle. Superimposed traces recorded for GRA muscle at the five knee angles studied are shown.

quantify high forces, the following were done: (i) The percentage of $F_{GRApeak}$ exerted at $KA=120^\circ$ ($\%F_{GRApeak/120^\circ}$) was calculated. (ii) The percentage of $F_{GRApeak}$ exerted at $KA=0^\circ$ or at local minimum if occurred ($\%F_{GRApeak/0^\circ\text{or min}}$) was calculated. (iii) GRA muscle isometric forces measured at $KA=120^\circ$ and 90° (1) after stimulation of GRA muscle exclusively and (2) after stimulation of GRA and VM muscles simultaneously were compared.

4.3 Results

4.3.1 Clinical Data

Table 4.2 shows popliteal angle (mean \pm SD = $85.50^\circ \pm 7.98^\circ$) and hip abduction angle (mean \pm SD = $31.00^\circ \pm 6.58^\circ$) values for the limbs. Limb scores for limited ROM showing values between 1.39 and 2.00 indicated that all the limbs tested have severe knee flexion and hip abduction limitations.

4.3.2 Experimental Data

Figure 3 shows the KA- F_{GRA} characteristics. FGRA peak (mean \pm SD = 47.92N \pm 22.08N) ranges between 12.70N (limb 2) and 84.61N (limb 4).

Joint range of muscle force exertion

Limbs with full KA range feasible: For six of the limbs (limbs 1-4, 7, and 9) non-zero muscle forces were measured for all KAs studied. This suggests that GRA muscle's operational joint range of muscle force exertion includes the entire joint range studied. However, although for limbs 1, 7 and 9 this seems to hold true, the remainder of the limbs deserves further attention. Limbs 2-4 show a very notable property that the KA- F_{GRA} curves include a local minimum (KAF_{min} at KA= 74°, 22°, and 55° for limbs 2, 3 and 4, respectively), which is followed by an increase of GRA total force. For limbs 3 and 4, the KA- F_{GRA} curves include an ascending and a subsequent descending portion, and KAF_{min} is attained after the descending portion. A tenable explanation for this is that with knee extension, the muscle is stretched to a length unfavorable for active force exertion and that the total muscle force increase shown is ascribable to increasing passive force. For limb 2, KAF_{min} appears to succeed only the descending portion of the KA- F_{GRA} curve.

Limbs with full KA range not feasible: For four of the limbs, muscle force measurements had to be ceased at certain knee extension position (for limbs 5-6 at KA= 30°, for 8, and 10 at 10° and 20°, respectively) as full knee extension could not be achieved.

For limb 5, also KAF_{min} was attained (KA= 75°). KA- F_{GRA} curves of limbs 6 and 10 include both ascending and descending portions whereas, that of limb 8 appears to have only the former.

Availability of muscle force For two of the limbs (2 and 5), were the highest muscle forces available at the maximal knee flexion angle studied. For limbs 6, 7 and

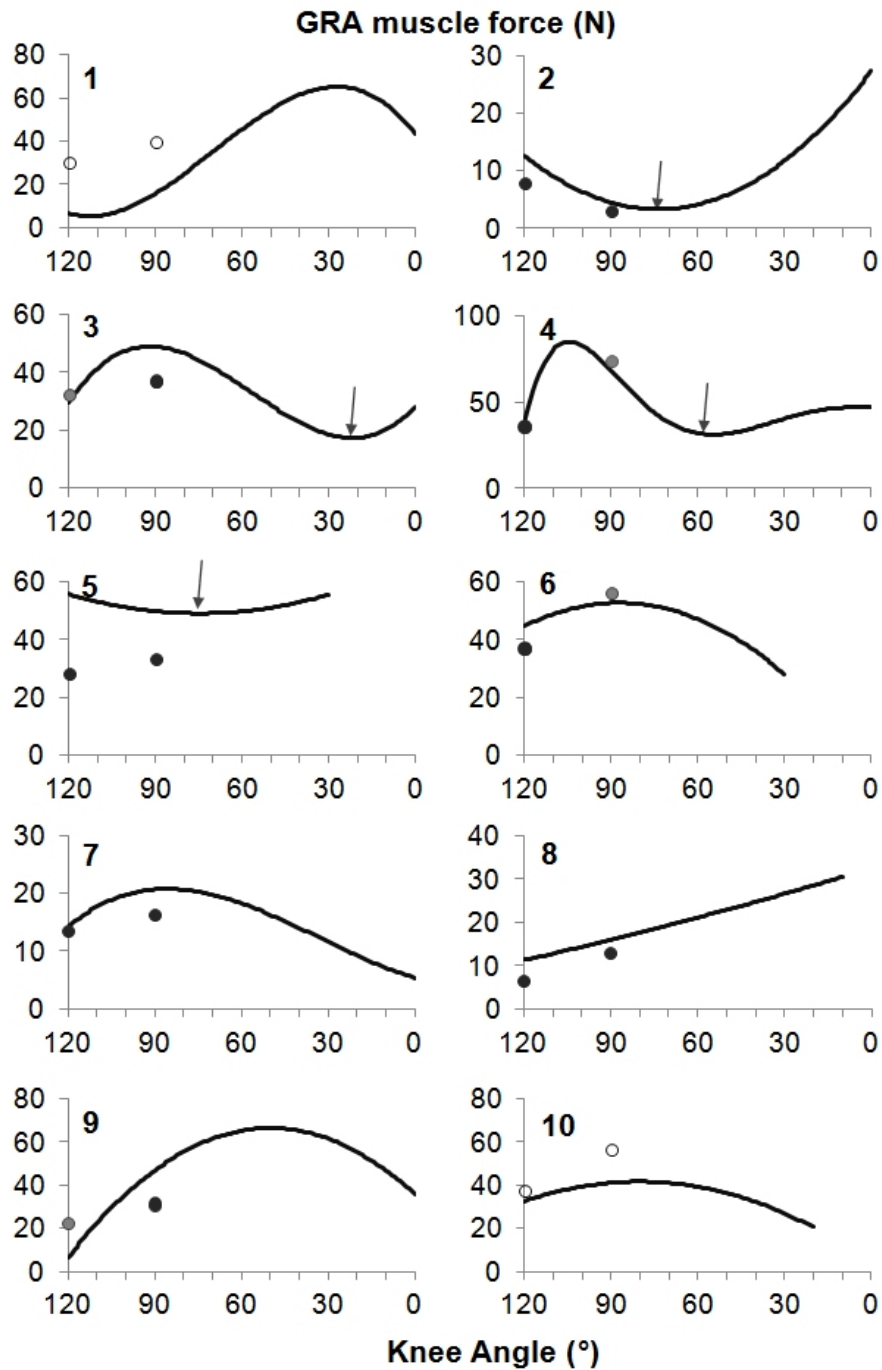


Figure 4.3 The isometric KA-FGRA characteristics of spastic GRA muscle. Data are shown separately for each limb (panels 1 to 10) experimented. Isometric GRA muscle forces were measured during exclusive stimulation at 120° and 90°, and simultaneous stimulation with VM at 120°, 90°, 60°, 30°, and 0° of knee angles. Arrows indicate existence of a local minimum point within the curve as a remarkable finding. Hollow circles show higher forces, dark grey circles show lower forces, and light grey circles show higher forces only for one of the angles studied.

Table 4.2
Clinical measures characterizing motion limitation and experimental measures

| Limb | Clinical Examination Data | | | Experimental Data | | | |
|------|---------------------------|---------|----------------------------|---------------------|------------------------|--------------------------|-------------------------------|
| | PA (°) | HAA (°) | Limb score for limited ROM | $F_{GRA\ peak}$ (N) | KA $F_{GRA\ peak}$ (°) | % $F_{GRA\ peak}$ 120° | % $F_{GRA\ peak}$ 0° or min |
| 1 | 90 | 20 | 2.00 | 65.16 | 27 | 10.15 | 10.15 |
| 2 | 65 | 30 | 1.39 | 12.70 | 120 | 100.00 | 26.35 |
| 3 | 85 | 35 | 1.52 | 48.98 | 92 | 60.11 | 35.24 |
| 4 | 80 | 35 | 1.46 | 84.61 | 104 | 44.51 | 36.69 |
| 5 | 90 | 25 | 1.80 | 55.74 | 120 | 100.00 | 87.99 |
| 6 | 90 | 25 | 1.80 | 52.71 | 87 | 84.78 | 53.11 |
| 7 | 85 | 40 | 1.44 | 20.78 | 86 | 68.95 | 25.73 |
| 8 | 90 | 40 | 1.50 | 30.55 | 10 | 36.99 | 100.00 |
| 9 | 90 | 30 | 1.67 | 66.33 | 50 | 9.79 | 54.05 |
| 10 | 90 | 30 | 1.67 | 41.61 | 80 | 78.26 | 49.37 |

10, the percentage of $F_{GRA\ peak}$ exerted at KA=120° ($\%F_{GRA\ peak/120^\circ}$) was quite high: 84.8%, 69.0%, and 78.3%, respectively. For limbs 3-4, $\%F_{GRA\ peak/120^\circ}$ was lower (60.1% and 44.5%, respectively). However, the proximity of the KA at which $F_{GRA\ peak}$ was measured to 120° (92° and 104°, respectively for limbs 3 and 4) suggests that active resistance capacity of the GRA muscle to stretch is still substantial at flexed joint angles. In contrast, for the remainder of the limbs (1 and 8-9) availability of force at flexed knee positions is not appreciable. At high lengths, the GRA muscle was capable of exerting high forces only for the limbs 5 and 8 (87.99% and 100% of its $\%F_{GRA\ peak/0^\circ\text{ or min}}$, respectively). For the remainder of the limbs, maximally 54.05% (limb 9) and minimally 10.15% (limb 1) of FGRA peak were available (Table 2).

Exclusive vs simultaneous stimulation at low lengths Simultaneous stimulation of VA muscle caused GRA muscle isometric forces to increase for the limbs 2, 5, 7, and 8 both at 120° and 90° of knee angles (Fig. 2). Force enhancement due to simultaneous stimulation occurred only at maximal flexion (120°) for the limbs 4 and 6. For the limbs 3 and 9, such effects were shifted to a less flexed knee position (90°). For the

limbs 1 and 10 on the other hand, simultaneous stimulation did cause force reduction at both positions.

In conclusion, (i) local minima for the limbs 2, 3, 4, and 5, (ii) the proximity of the KA at which FGRA peak was measured to 120° for all of the limbs except 1, 8, and 10, (iii) low forces at extended knee positions, and (iv) force enhancement at flexion for most of the limbs showed that simultaneous stimulation caused length range of GRA muscle to be narrowed and active resistance of muscle to increase at flexed knee positions. Therefore, our hypothesis is confirmed for the majority of the limbs tested.

4.4 Discussion

EMFT defines the transmission of muscle forces to the neighboring muscular and non-muscular structures through the epimysium. This is because the muscles' epimysium is continuous with myofascial structures [23, 140]. Such transmission of force was shown with earlier animal experiments to occur between antagonist muscles [107, 144]. Moreover, its functional role in vivo was also proved for human lower leg muscles [142]. Such mechanism is important also for surgical treatments [83]. On the other hand, there is no direct evidence for occurrence of inter-antagonistic EMFT for spastic muscles. However, Kreulen et al. [60] did show that the epimuscular connections for flexor carpi ulnaris muscle of cerebral palsy patients play a substantial mechanical role. Since an increase in stiffness of the spastic muscles [30, 57-58] and their connective tissues [59] have been reported, we may expect that the role of EMFT mechanism for the spastic limbs may even be more pronounced than in health. Our previous results showing no abnormal mechanics for spastic GRA muscle which was stimulated alone may support that idea implicitly because even though the muscle compartment with almost all of its connective tissues was intact, no other muscle was activated. In this study, we tested whether the spastic GRA muscle characteristics change to represent better a characteristic that can be expected from a spastic muscle if it is stimulated simultaneously with its antagonist VM. Our hypotheses on both narrowing length range

and higher force exertion at flexion are confirmed for the majority of the limbs tested.

Before discussing the probable mechanisms causing such results, it should be noted, in the present study, the pre-operative clinical examinations showing (i) CP patients had GMFCS values indicating decreased mobility and causing a decision for lengthening surgery on GRA muscle as well and (ii) popliteal angles greater than 50° [123] and hip abduction angles lower than or equal to 40° [75, 130] indicated severe knee joint problem. Since the popliteal angle measures under anesthesia were shown not to differ from clinic [145], we may accept that these limbs have permanent and prominent contractures in daily life. Additionally, (iii) four of the limbs tested (5, 6, 8, and 10) showed lacking full knee extension. Therefore, all the limbs experimented had GRA muscle contracture and severe joint impairment passively.

4.4.1 Joint range of motion

Present results showed a narrowing for length range of spastic GRA muscle. Healthy GRA has long fibers [134] and large excursion [98], thus its length range of force production is expected to be wide comparably. Our previous results showed that the operational joint range was at least as wide as 120° from the most flexed position of the knee tested to the full extension for both healthy [120] and spastic GRA muscle [143] if they are stimulated alone. Presently, mean KAFGRA peak value was 78° and 7 of the limbs tested produced their peak forces at more flexed position than 80° . Compared to the previous results [143] showing peak forces produced between 66° and 0° of knee angles (mean 29°) for exclusive stimulation of spastic GRA, the proximity of the KA at which FGRA peak was measured to 120° and thus, a shift of KAFGRA peak to more flexed positions occurred. Therefore, such present results indicated that if stimulated simultaneously with VM, spastic GRA muscle operational range is narrowed.

Two of the limbs (2 and 5) operational only at the descending portion and three of the remaining limbs (6, 7, 10) mostly at the descending portion of their KA-FGRA characteristics indicated that at least for half of the limbs, simultaneous stimulation

of antagonist VM changed the characteristics of spastic GRA majorly and supported our hypothesis on narrowing range as well. Considering that the maximum ankle torque previously shown to be at more plantar flexion for CP patients than normal children [146] our results indicate that narrowed range of GRA muscle represents the abnormality at the joint.

Additionally, %48 shown for mean %FGRA peak | 0° or min indicated a major force reduction for most of the limbs at knee extension. This ratio relating peak forces to the forces produced at high muscle lengths was about half of the previous ones shown for the exclusively stimulated GRA muscle [143]. More interestingly, the increasing trend of the KA-FGRA curve shown after decreasing for four of the limbs (2, 3, 4, and 5) resembles to the ideal force-length characteristics of a muscle having all sarcomeres at high lengths and no extra capacity for active force production. Thus, the passive force increase being responsible from such high forces is compatible with the narrowing of length range with simultaneous stimulation.

No previous study reported the force production capacity of VM with respect to its length or knee joint angle. However, for stable standing and walking, it is probable that VM with other quadriceps produces quite amount of forces at extended knee positions. Compromised force production with general weakness due to cerebral palsy is also probable [147-148]. Nevertheless, considering that the spastic GRA having increased stiffness with its extramuscular structures due to CP may serve a probable path for inter-antagonistic force transmission.

4.4.2 Availability of high muscle force

Our results showing (i) active resistance capacity of the GRA muscle at flexion with the exception of limbs 1, 8-9 and (ii) force enhancement during simultaneous activity of VM with the exception of limbs 1 and 10 indicated availability of high flexion forces. It should be noted that antagonistic muscle activity occurs at many multi-joint movements in daily life [149-150]. Such co-contraction is reported to be even higher in

spasticity [151-153]. Thus, the effects of antagonistic muscle activation not only for joint function but also for spastic flexors are conceivable. On the contrary, joint weakness [147-148, 154] as well as changes causing muscle weakness [50, 52, 54] were reported for spastic CP. Therefore, lower forces produced and transmitted by either flexor or its antagonist corresponding to such low joint torques may be expected. Nevertheless, our results reported considerable effects due to inter-antagonistic interaction with high flexion forces for most of the limbs.

In conclusion, simultaneous stimulation of antagonistic VM muscle causes (i) spastic GRA muscle peak forces to shift to the more flexed positions, (ii) operational range of GRA muscle to be narrowed and (iii) operational portion of knee angle-muscle force curve to shift to the flexion. Thus, our hypothesis on narrowed joint range of motion is verified. High flexion forces measured due to simultaneous activity confirmed our second hypothesis as well. It is suggested that inter-antagonistic interaction imposes myofascial loads on muscles through epimuscular connections stiffened due to spasticity. Such loads cause intramuscular alterations on spastic GRA muscle: Sarcomeres are lengthened at flexion and thus, excessive lengthening occurs at knee extension. Therefore, flexion forces increase and length range decreases. Such probable mechanism should be tested with spastic muscle model and also by adding histological examinations to our experimental method improved to measure passive forces.

5. MUSCLE LENGTHENING CAUSES DIFFERENTIAL ACUTE MECHANICAL EFFECTS IN BOTH TARGETED AND NON-TARGETED SYNERGISTIC MUSCLES

5.1 Introduction

In remedial surgery, known under various names (muscle recession [73-74], muscle release [155], muscle lengthening [76-80], aponeurotomy (AT) [81] involves cutting of an intramuscular aponeurosis transversely. Preparatory dissection (PD) is performed first to reach the target muscle [156], AT is used for correction of problems of range of movement and joint position in spastic paresis. The most important acute effect allowing lengthening of muscle is creation of a gap within the muscle. Enhancing the compromised joint range of motion is a primary goal [157], but reduction of muscle force to correct imbalances of force between antagonistic muscles [158] are additional clinical aims.

The myotendinous junction is widely considered as the main [159] or implicitly even the sole site [many studies in biomechanics e.g. 160] for transmission of forces generated within sarcomeres onto the tendon and from there to bone. However, force transmission is possible also via trans-sarcolemmal proteins connecting muscle fibers along their full periphery of their length to the collagen reinforced extracellular matrix (ECM) [for a review see 161]. As a consequence, muscle fibers have been shown to interact mechanically with the ECM and with each other with a bundle [162-163]. Later, for whole muscle, such transmission has been named, myofascial force transmission (MFT) [111].

Moreover, muscle functioning within its normal context of connective tissues is connected to surrounding muscles and non-muscular structures and epimuscular myofascial force transmission (EMFT) occurs via such connections [e.g. 63, 140]. EMFT has been shown to cause asymmetric effects at muscle's origin and insertion and depen-

dency of muscle characteristics on mechanical conditions within which it functions [140, 164]. Evidence for EMFT is accumulating for human muscles in vivo [142, 165-167].

It is quite conceivable that PD (e.g. opening of the compartment) may affect MFT within a compartment and because of mechanical interaction between muscles, also acute mechanical effects of AT could be present in muscles other than those on which the main surgical intervention was performed. Post operative effects of AT were investigated at the joint level by using e.g., gait analysis [157, 168]. However, effects on the target and non-targeted muscles were not studied explicitly.

Therefore, we designed the present study to test for such effects of MFT and test the following hypotheses for muscles within the anterior crural compartment of the rat: (1) effects of muscle lengthening surgery on the target muscle are different at distal and proximal tendons, (2) forces of non-targeted synergistic muscles are affected as well, and (3) PD is responsible from some of these effects.

5.2 Methods

5.2.1 Surgical procedures and preparation for experiments

Surgical and experimental procedures were approved by the Committee on Ethics of Animal Experimentation at Boğaziçi University. Young adult male Wistar rats ($n = 8$, mean body mass 327.0 g (SD 18.4 g)) anaesthetized using intraperitoneal injection of urethane (1.2 ml/100 g body mass). Additional doses were given, if necessary (maximally 0.5 ml). The animals were placed on a heated pad (Harvard Apparatus) during surgery and data collection. Left hind limb skin and biceps femoris muscle were removed and the anterior crural compartment, containing extensor digitorum longus (EDL), tibialis anterior (TA) and extensor hallucis longus (EHL) muscles was exposed. Only limited distal fasciotomy was performed to remove the retinaculae, leaving fully intact connective tissues at the muscle. At a reference position selected (knee and ankle joint angles of 90° and 100° respectively), the four distal tendons of

EDL muscle were tied together using silk thread. Matching markers were placed on distal tendons of EDL, TA and EHL muscles, as well as on the lower leg. Subsequently, the distal tendons of EDL, as well as TA and EHL were cut as distally as possible. The proximal EDL tendon was cut from the femur, with a small piece of the lateral femur condyle still attached. To allow connection to force transducers, Kevlar threads were sutured to all cut tendons. Within the femoral compartment, the sciatic nerve was dissected and cut as proximal as possible. All its branches to muscles of that compartment were cut.

5.2.2 Experimental conditions and procedure

The rat was mounted in the experimental set-up (Fig. 1). The femur and foot were clamped, such that the knee was kept at 90° and the ankle in maximal plantar flexion (180°) to allow for free passage of Kevlar threads. Each Kevlar thread was connected to a force transducer (BLH Electronics Inc., Canton MA). The distal end of the sciatic nerve was placed on a bipolar silver electrode. Room temperature was kept at 26° C. Muscle and tendon tissues were irrigated regularly by isotonic saline to prevent dehydration during the experiment.

Markers on EDL proximal tendon and distal tendons of TA and EHL were kept in their reference positions at all times. EDL length was changed by moving its distal force transducer (in steps of 1 mm), until 2 mm over distal optimum length, and EDL length-force data were collected at proximal and distal EDL tendons. Distal forces of TA and EHL were measured.

Muscles were activated maximally by supramaximal stimulation of the sciatic nerve at a constant current of 2 mA (Biopac Systems stimulator, STMISOC: square pulse width 0.1 ms, pulse train 400 ms, stimulation frequency 100 Hz). After setting EDL to a new length, two twitches were evoked and the muscles were tetanized 300 ms after the second twitch. At 200 ms after cessation of stimulation, another twitch was evoked. After these contractions, muscles were allowed to recover for 2 min. (EDL at

low length, others at l_{ref}).

5.2.3 Experimental protocol

Before acquiring data, muscle-tendon complexes and their epimuscular connections were preconditioned by isometric contractions, alternatingly at high and low EDL lengths, until forces at low EDL length were reproducible (i.e. effects of previous activity at high length [169] are removed).

Three conditions were studied: (1) Control with an intact anterior crural compartment. (2) After preparatory dissection (Post PD), performed to gain access to the target muscle. Laterally, a probe was inserted from proximally into the anterior crural compartment between EDL and TA until the middle of the compartment was reached by the probe tip (i.e., approximately for 12 mm). Using a micro scissor, half of the anterior crural compartmental fascia was cut (partial fasciotomy). Intermuscular connections between EDL and TA along half of EDL length were removed by blunt dissection (using a cotton swab). (3) Post-AT EDL proximal aponeurosis was transected at its middle, perpendicular to its longitudinal direction using a scalpel blade (Surgeon, number 11).

Subsequently, muscles were activated with EDL at optimum length (of control condition). This causes tearing of the ECM along muscle fibers located below the site of AT. Effects of PD, AT and subsequent tearing of the ECM together are referred to as cumulative effects of muscle lengthening surgery.

5.2.4 Processing of experimental data and statistics

Muscle passive isometric forces were measured at 100 ms after the second twitch before the tetanus. The mean total force during the tetanic plateau was calculated for an interval of 200 ms starting after 150 ms of tetanic stimulation.

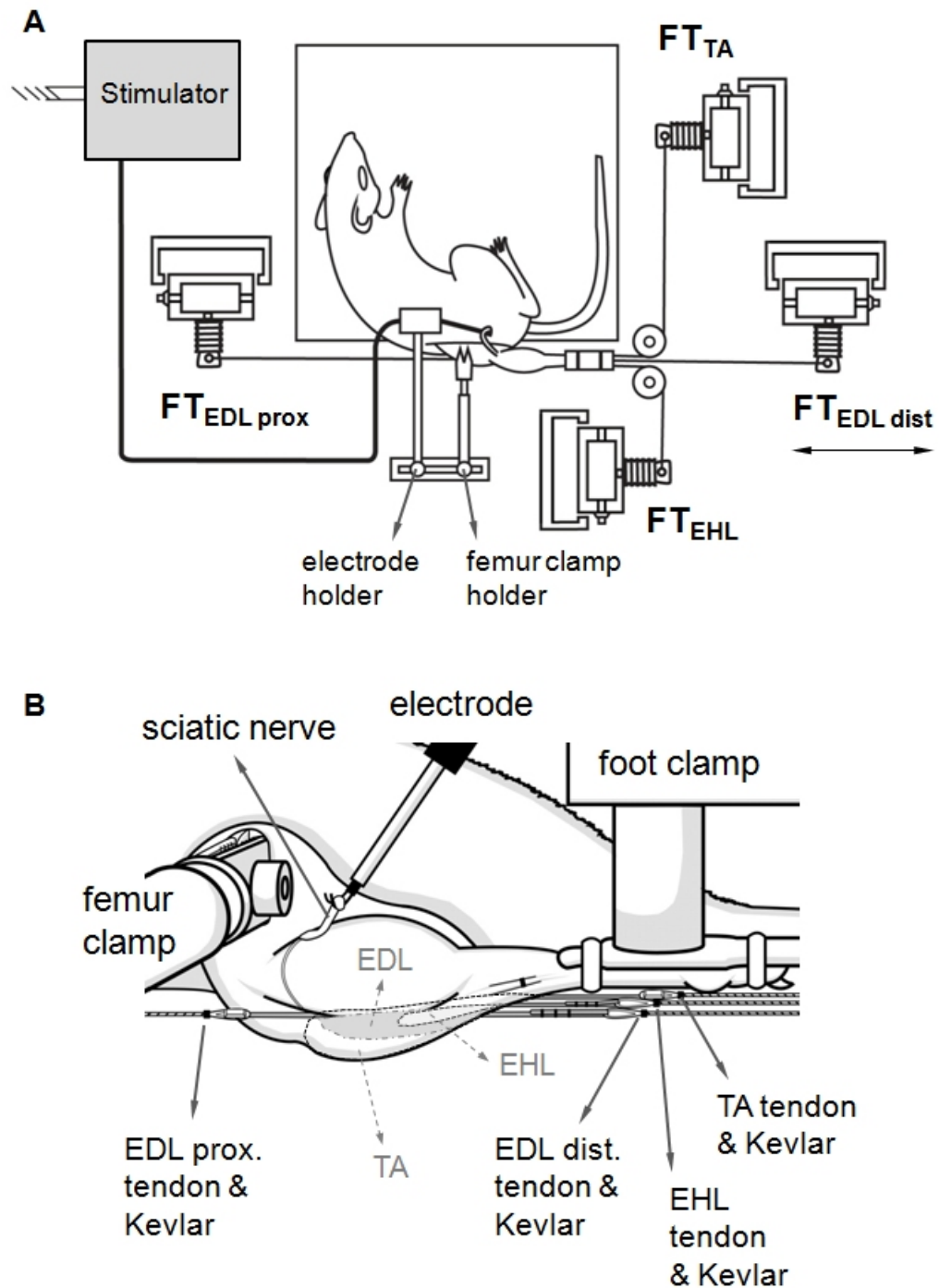


Figure 5.1 Schematic view of the experimental setup. (A) The following tendon (-groups) were connected to a separate force transducer (FT): (1) proximal EDL tendon, (2) the tied distal tendons of the EDL, (3) the distal tendon of TA (4) the distal tendon of EHL. Throughout the experiment, TA and EHL muscles were kept at constant muscle-tendon complex lengths. Exclusively, the distal force transducer of EDL was repositioned to progressively increase EDL length, at each of which isometric contractions were performed. (B) The femur and foot were fixed by metal clamps. The sciatic nerve was placed on a bipolar silver electrode. Kevlar threads (hatched lines) were sutured to tendons (solid lines) to provide connection to their respective FT.

Mathematical functions were least square fitted to the experimental data for further treatment and averaging [e.g. 169]. Passive length-force data were fitted using an exponential function and active muscle force was calculated by subtracting the measured passive force from total force during muscle activity. Active length-force data were fitted (polynomial function). The degree of the polynomial function that most adequately described a particular set of length-force data was selected using an analysis of variance (ANOVA) [125]. Optimal EDL force is defined as the maximum of the polynomial, and its corresponding length as optimum length. One-way ANOVA was also used to test for cumulative effects of muscle lengthening surgery on EDL's length range of active force exertion i.e., the range between muscle active slack length and optimum length. Two-way ANOVA's for repeated measures (factors: EDL length and surgical condition) were used to analyze effects of the interventions on EDL length-force characteristics and on forces of non-targeted TA and EHL. If significant effects were found, post hoc tests were performed using the Bonferroni procedure for multiple pair wise comparisons to locate differences. p values < 0.05 were considered significant.

5.3 Results

Target muscle-distal force ANOVA (factors: EDL length and condition) showed significant main effects on EDL distal active forces, and significant interaction. Compared to control condition (Fig. 2A), post hoc tests showed significant cumulative effects of AT causing EDL distal active forces to decrease (e.g., by 26.3% at optimum length), in contrast to increases at the lowest muscle lengths. Note that no significant effects of PD are found for distal EDL active force. Cumulative effects of muscle lengthening surgery cause EDL distal length range of active force exertion to increase significantly (from mean 9.1 mm (SE 1.1 mm) to mean 10.7 (SE 0.9 mm)). For EDL distal passive force, ANOVA (factors: EDL length and condition) showed significant main effects, and significant interaction. Compared to the control condition, post hoc tests showed (i) significant cumulative effects of muscle lengthening surgery causing EDL distal passive forces to increase (e.g., by 40.7% at optimum length). This increase is explained by higher stretch of EDL epimuscular connections in proximal direction.

(ii) No significant effects of PD were found for EDL distal passive force.

Target muscle-proximal force ANOVA (factors: EDL length and condition) showed significant main effects on EDL proximal active force and significant interaction. Compared to control condition (Fig. 2B), post hoc tests showed significant cumulative effects of muscle lengthening surgery causing EDL proximal active forces to decrease (e.g., by 44.5% at optimum length, note that this is more than the decrease of its distal counterpart Fig. 2A). However, no significant effects of PD were found for EDL proximal active force (post hoc test). In contrast to effects found distally, cumulative effects of muscle lengthening surgery caused no significant change in length range of active force exertion at the EDL proximal tendon. ANOVA (factors: EDL length and condition) showed significant effects of length on EDL proximal passive forces; but neither significant effects of condition nor of interaction.

Non-operated TA ANOVA (factors: EDL length and condition) showed significant main effects on TA active forces, but no significant interaction. Compared to control condition (Fig. 3A), post hoc tests showed significant cumulative effects of muscle lengthening surgery (mean decrease for EDL lengths studied equaled 11.9%). Note that post hoc tests also indicate that PD causes TA active forces to decrease (mean decrease for EDL lengths studied equaled 4.9%). ANOVA (factors: EDL length and condition) showed significant effects of condition on TA passive forces; but no significant effects of length or a significant interaction. Compared to control condition, post hoc tests showed significant cumulative effects of muscle lengthening surgery causing TA passive forces to decrease (the mean force decrease for the EDL lengths studied equaled 11.6%). However, no significant effects of PD were shown (post hoc test).

Non-operated EHL ANOVA (factors: EDL length and condition) showed significant main effects on EHL active forces, but no significant interaction. Compared to control condition (Fig. 3B), post hoc tests showed significant cumulative effects of muscle lengthening surgery causing EHL distal active forces to decrease, despite its constant muscle tendon complex length (for EDL lengths studied, mean force decrease equals 8.4%). However, no significant effects of PD on EHL active force were found

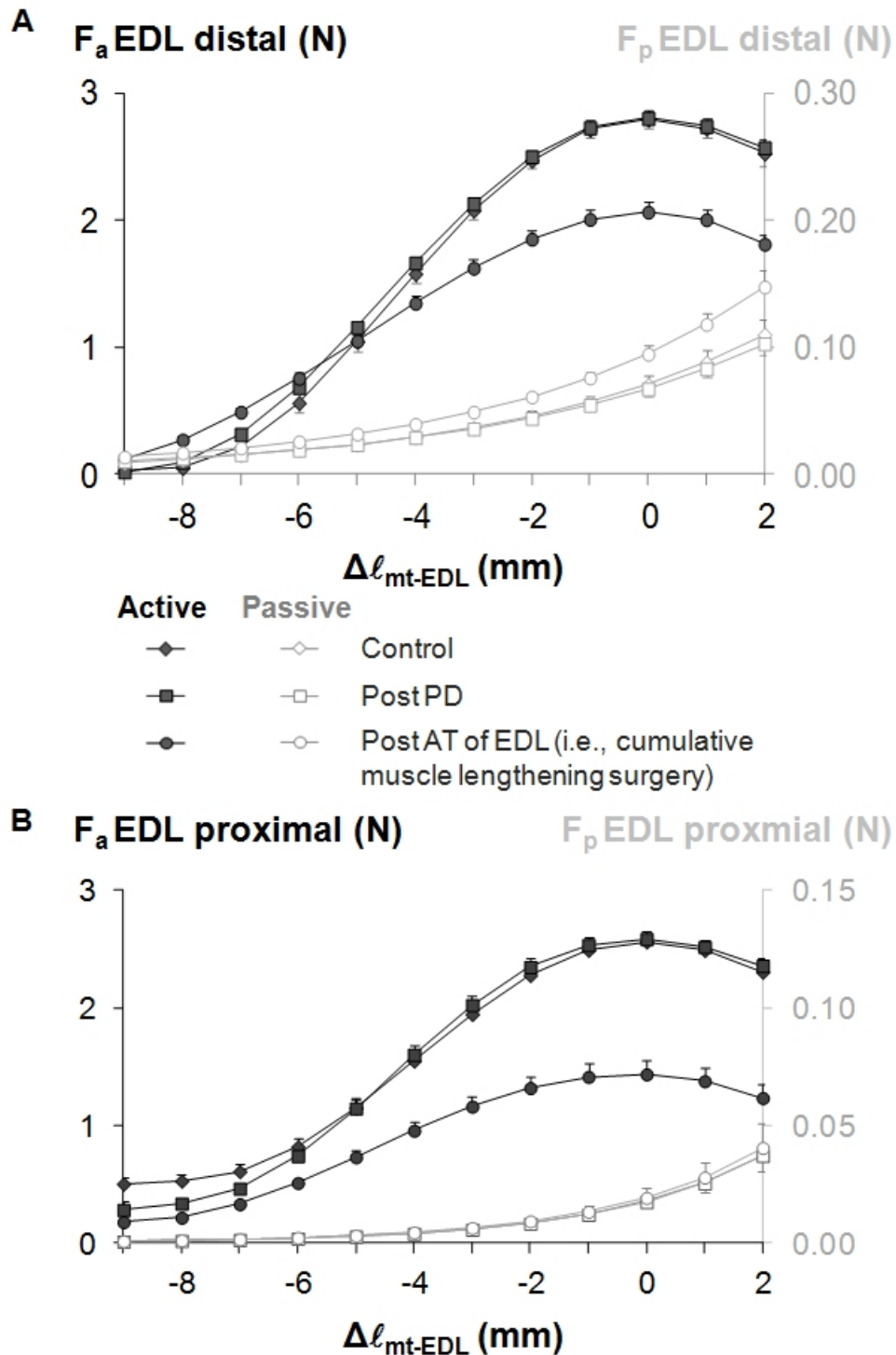


Figure 5.2 The isometric muscle force-length curves of target EDL muscle. (A) Distally EDL force. (B) Proximally EDL force. Active and passive isometric EDL forces were plotted for the following conditions: (1) control, (2) after preparatory dissection (post PD) and (3) after aponeurotomy (post AT). Note that the post AT condition represents the cumulative effects of muscle lengthening surgery. EDL muscle-tendon complex length is expressed as a deviation (Δl_{mt-EDL}) from its optimum length. All force values are shown as mean (SE). EDL active force reductions and EDL passive distal force increase were significant as cumulative effects of muscle lengthening surgery, but not after PD.

(post hoc test). ANOVA (factors: EDL length and condition) showed only significant effects of EDL length on EHL passive force, despite its constant muscle tendon complex length; but neither significant effects of condition nor of interaction.

It is concluded that the cumulative effects of muscle lengthening surgery on the target muscle operating with most of its normal connective tissue environment intact are different distally and proximally. In contrast to the increase in target muscle distal length range of active force exertion, no such effect was found proximally, but force reduction effects were much more pronounced proximally. An important finding is that cumulative effects of muscle lengthening surgery cause considerable force reductions also for non-operated muscles of the compartment. Only TA is affected to a limited extent by PD.

5.4 Discussion

One characteristic effect of EMFT is exertion of unequal forces at proximal and distal tendons [63, 140]. The presence of proximo-distal force differences indicate net epimuscular myofascial loads acting on the muscle and the source of such loads is stretching of muscle's epimuscular connections upon changes in muscle relative position [164]. Forces of isometric synergistic and also antagonistic muscles were shown to change with altered muscle relative positions [23, 107, 170]. However, recently, actuator independence of cat muscle was studied [171]. At constant ankle and hip joint angles, a robot manipulated knee and hip joint angle, and changes of muscular relative positions of passive gastrocnemius and plantaris muscles were imposed with respect to partially activated m. soleus. Based on lack of significant changes in m. soleus ankle moment, a generalizing conclusion was drawn that mechanical interaction between muscles does not occur under physiological circumstances in vivo. However, MRI analyses in human lower leg muscles in vivo [142, 172] show that at constant ankle angle, knee angle changes cause major heterogeneous deformations not only within m. gastrocnemius, but also within all other lower leg muscles despite their globally isometric condition. This indicates that mechanical interaction between muscles is characterized by local

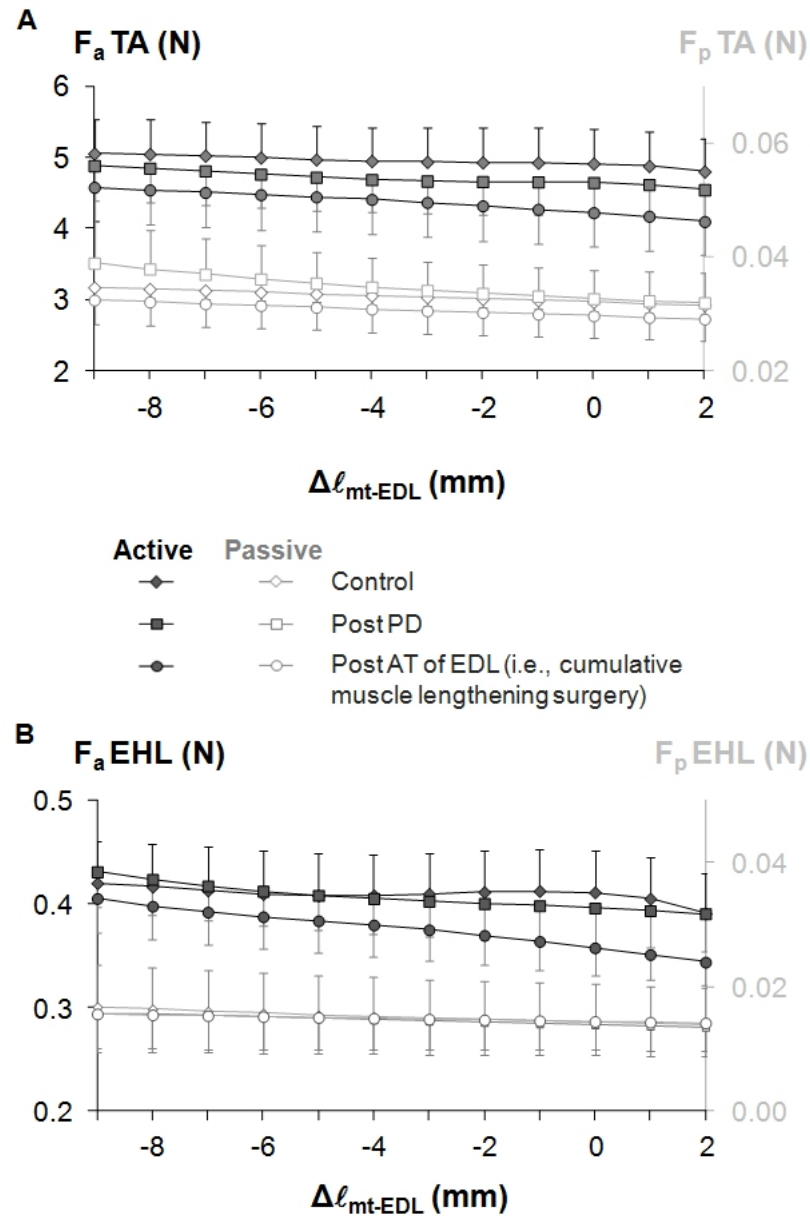


Figure 5.3 Forces exerted by non-operated TA and EHL muscles. (A) Distal TA force. (B) Distal EHL force. Active and passive isometric TA and EHL forces were plotted for the following conditions: (1) control, (2) after preparatory dissection (post PD) and (3) after aponeurotomy (post AT). Note that the post AT condition represents the cumulative effects of muscle lengthening surgery. EDL muscle-tendon complex length is expressed as a deviation ($\Delta\ell_{mt-EDL}$) from its optimum length. All force values are shown as Non-operated TA ANOVA (factors: EDL length and condition) showed significant main effects on TA active forces, but no significant interaction. Compared to control condition (Fig. 3A), post hoc tests showed significant cumulative effects of muscle lengthening surgery (mean decrease for EDL lengths studied equaled 11.9%). Note that post hoc tests also indicate that PD causes TA active forces to decrease (mean decrease for EDL lengths studied equaled 4.9%). ANOVA (factors: EDL length and condition) showed significant effects of condition on TA passive forces; but no significant effects of length or a significant interaction. Compared to control condition, post hoc tests showed significant cumulative effects of muscle lengthening surgery causing TA passive forces to decrease (the mean force decrease for the EDL lengths studied equaled 11.6%). However, no significant effects of PD were shown (post hoc test).

epimuscular myofascial loads on those muscles with variable magnitude and direction. If the net effect of EMFT on forces exerted at the tendon would be small, a mechanical balance of counteracting epimuscular myofascial loads rather than their absence can explain this. Therefore, in contrast to the conclusion of Maas and Sandercock [171], a mechanical interaction of muscles is tenable in most conditions. We expect that this plays a role in surgery as well.

In the control condition, the anterior crural compartment was not interfered with, hence epimuscular connections were intact. PD performed in our experiment to gain access to the AT site, as in clinical practice [156], was minimized to limit interference with the compartment. We showed that even for a deeper target muscle and its synergistic muscle, it does not contribute to cumulative effects of muscle lengthening surgery. Present dissection was performed exclusively within the proximal compartment half, leaving intact distal parts of fasciae. Meijer et al. [144] concluded that these tissues are particularly stiff if TA and EHL are shortened which imposes a stretch on them causing increased distally directed net epimuscular myofascial loads acting on EDL. High stiffness of connections is likely in our conditions as TA and EHL are kept at lower lengths. Therefore, effects of PD on epimuscular myofascial loads acting on deeper located muscles are likely to remain small. However, for TA, PD alone, independent from EDL length, reduced its contribution to the moment exerted at the distal joint. Therefore, effects of PD are confined to superficial muscles, conceivably due to a reduced stiffness of its epimuscular connections (e.g., the TA branch of the neurovascular tract) creating conditions unfavorable for force exertion. In general, more compartmental disruption is expected to cause reduction in muscle force [173], additional to that caused by AT. If PD remains limited, remaining integrity of EMFT pathways is likely to cause effects similar to those shown presently.

Previous studies on isolated muscle [82-83] allowed improvement of our understanding of mechanisms of AT affecting intramuscular mechanics. Although a discontinuity within the aponeurosis directly prevents myotendinous force transmission for a part of the muscle fibers, this intervention per se was shown to have only minor effects, but subsequent rupturing of intramuscular connective tissues below the AT location

yields major effects on muscle length-force characteristics [82]. Therefore, a central issue is interference with MFT, which effectively causes manipulation of myofascial loads (i.e., forces exerted onto muscle fibers by the ECM and via that by sarcomeres located in the neighboring muscle fibers). This causes characteristic sarcomere length distributions within the aponeurotomed muscle yielding changes in muscle length-force characteristics. Enhanced sarcomere length heterogeneity within the target muscle causes an acute increase in muscle length range of force exertion. Therefore, in addition to causing acutely a lengthening of muscle, AT facilitates exertion of active force for an enhanced range of joint angles also. In addition to contributing to that effect, major shortening of sarcomeres occurs within muscle fibers without myotendinous connections to bone. This is responsible for most of the force reductions due to AT.

An important present finding is that effects on forces exerted at proximal and distal tendons of the target muscle are not equal. This in accordance with the presence of proximo-distal force differences indicating net epimuscular myofascial loads acting on the muscle. Such loads were shown to change in vivo muscular mechanics substantially [142] and affect local sarcomere lengths, forces exerted, as well as length range of active force exertion [25]. Epimuscular myofascial loads plausibly cause sarcomeres in the proximal ends of fibers of the target muscle located proximally to the AT site to attain lengths less favorable for force exertion which explains the effect of higher force reductions proximally. Lack of an increased proximal length range of active force exertion indicates that such loads also diminish sarcomere length heterogeneity within the target muscle. This may not only explain the asymmetry in effects of muscle lengthening surgery for joints spanned by the target muscle, but also suggest that integrity of the EMFT network limits acute effects of AT, also in clinical practice. Previous modeling study [84] confirmed that epimuscular myofascial loads present in conditions representing removal of muscles, other than the target muscle from the compartment, will cause diminished sarcomere shortening within the population of muscle fibers distal to the location of AT, and less pronounced sarcomere length heterogeneity within the muscle. We conclude that acute cumulative effects of muscle lengthening surgery on mechanics of the target muscle are affected to a large extent by EMFT.

For clinicians it is important to realize that surgically correcting functional problems at a distal joint may alter muscle mechanics at the proximal joint as well. This suggests that care is indicated when considering the overall surgical outcome, particularly if the target muscle is bi- or poly-articular. For example, in combined equinus and crouch gait [157], AT of m. gastrocnemius may improve gait because contributions to both plantar flexion and knee flexion moments may decrease. However, for combined crouch and hip flexor tightness, AT of the semimembranosus [168] may deteriorate conditions at the proximal joint due to reduced contributions to hip extension moment. The asymmetry shown for decreased contribution of the target muscle to moments exerted at the joints it spans is due to EMFT, since for truly isolated muscle this would not occur. Note that, AT on the distal aponeurosis would prevent myotendinous force transmission for a different population of muscle fibers and may change acute effects of the intervention. However, these muscle fibers are exposed also to EMFT. This will also affect asymmetry effects shown presently only for a proximal AT. Also note that imposed distal muscle length changes of the present study mimic movements exclusively of the distal joint. Therefore, our results are not direct indicators of how proximal length range of force exertion is affected. However, identical lengthening imposed distally or proximally of intact EDL yielded asymmetric proximal and distal length ranges of active force exertion [174]. This implies that, lengthening surgery of a target muscle with most of its connective tissues intact should not be expected to yield symmetrical lengthening effects for joints spanned.

A key finding is that cumulative effects of muscle lengthening surgery involve considerable reductions also of distal force exerted by non-operated synergistic muscles. These results indicate that the surgeon should be aware of possible other and unintended acute effects, in addition to those for the target muscle.

It should be noted that synergistic muscles will change lengths simultaneously during joint movement and in similar direction as the agonist muscle. This may limit changes of relative position of synergistic muscles. However, even after lengthening of the whole anterior crural group, increased effects of EMFT were reported compared to single EDL lengthening [144]. Note that such equal and simultaneously imposed

muscle length changes may differ from in vivo conditions, as differences in moment arms of synergistic muscles are present [175] contributing to relative movement of muscles. Moreover, differences in number of joints spanned by synergistic muscles will contribute also to relative movement of muscles and movement of muscle with respect to bones. Joint angle changes in vivo have been shown to indicate effects of EMFT such as interactions between finger forces [176-177], as well as local displacements [166] or deformations [142] within muscles remaining globally isometric. Therefore, acute effects of muscle lengthening surgery on non-operated synergistic muscles, similar to those shown presently, are plausible also for in vivo function.

Although motor control plays no role in our experiments, one should be aware that surgical interventions may have important effects on the afferent sensory machinery. Firstly, PD alone may cause some of fascial afferents [e.g. 178] to be disrupted or may also affect sensory machinery via modified stiffness of compartmental connective tissues. Therefore, PD, even though we find it to have relatively small effects on muscle length-force characteristics, in vivo may still cause neuromotor changes. In addition, within the aponeurotomed muscle, populations of muscle fibers, which lose their myotendinous connections, shorten considerably subsequent to rupturing of intramuscular connective tissues [82, 179]. Mechanical unloading of the intrafusal fibers and reduced afferent response was reported in conditions causing shortened extrafusal fibers [180-181]. Therefore, for this shortened part of the aponeurotomed muscle, the tonic stretch reflex threshold may shift to higher values. Skeletal muscle spasticity is characterized by exaggerated stretch reflexes [e.g. 34]. Therefore, this is regarded as a positive effect of treatment. However, muscle fibers between the location of intervention and the tendon attain in general higher lengths, which may cause opposite effects. Modeling studies showed that an aponeurotomy closest to the tendon dominates the effect and enhances intended mechanical effects [83]. This effect is so important that additional aponeurotomies performed on the same model muscle do not further improve the outcome considerably [182]. These arguments suggest that modification of the proprioceptive input may also be optimized by a choice of intervention location. On the other hand, effects at a higher level of organization than the target muscle are quite conceivable. Force reductions shown presently for synergistic muscles suggest

that their muscle fibers attain lower lengths as an effect of the surgical interventions. Therefore, PD and AT may cause threshold of the tonic stretch reflex of also these muscles to shift to higher values. Similar effects of mechanical unloading of spindles of co-contracting intact muscles were reported previously [183]. However, after tenotomy of gastrocnemius and plantaris muscles, opposite findings were reported for afferents of soleus muscle [184]. This implies that, similar as for AT, tenotomy is not interfering solely with myotendinous force transmission and that manipulation of mechanical interactions between muscles may change afferent sensory machinery in a complex way, even if no damage were done to the sensory system.

Note that threshold of the tonic stretch reflex (represented by λ) is regarded as a key control variable in motor control studies based on Equilibrium-Point Hypothesis [185-186]. According to this viewpoint, for a single muscle, surgical modification of muscle length may shift the equilibrium point of the system leading to a change in λ . This theory was elaborated and extended to be linked to the idea that motor synergies and bodily movement is controlled at much higher levels of organization than the level of individual muscles [187-188]. Our results suggest that the whole synergistic interaction is affected by modifying mechanics of one muscle component within the synergy. The issues argued in the preceding paragraph may be relevant for agreement of the present findings with motor control theories. In our view, intra- and epimuscular MFT provides coupling between neuromuscular mechanisms suggesting that it is an important determinant for the changes to occur in λ . Muscle stiffness is a component of this and is important also for intended remedial effects of muscle lengthening surgery. As AT causes a part of the muscle to shorten and PD disrupts integrity of the connective tissues, an expected effect for most of the compartment is reduced stiffness of muscular and non-muscular tissues. Compared to its untreated properties, after healing, the aponeurosis was shown to be more compliant and longer [189]. Therefore, effects of muscle lengthening surgery on mechanical, as well as afferent sensory machinery of the target muscle are likely also for the long-term. Long-term adaptations in neuromotor properties due to potential changes in epimuscular connections need to be considered as well. Only partial or no neural adjustments were found to occur after tendon transfer surgery [190-191]. Rectus femoris muscle,

transferred to a flexor insertion was reported not to move as a knee flexor [192]. This is in agreement with its epimuscular mechanical interaction with the knee extensors and may explain absence of such adjustments. However, after AT, substantial neuromotor adaptations were reported [193-194]. Those studies focused either on the target muscle or a selected antagonist muscle, but not on synergistic muscles. As multilevel surgical treatment is common [78, 195], systematic testing of neural control of relevant muscles including non-targeted synergistic muscles is indicated.

In summary, effects of muscle lengthening surgery performed to improve impeded joint mechanical function are dominated by effects of EMFT causing (i) differential effects at the proximal and distal tendons of a poly-articular target muscle, and (ii) sizable effects also at unintended sites via non-operated muscles. These differential and unintended effects on muscle forces may yield additional favorable effects for the target joint, but also contrasting effects particularly for the non-targeted joint. It is therefore important to consider the role of EMFT in order to enhance control of the surgical outcome of the operation. New specific studies are indicated to assess neuromotor changes acutely as well as in the long-term.

6. BTX-A ADMINISTRATION TO THE TARGET MUSCLE AFFECTS FORCES OF ALL MUSCLES WITHIN AN INTACT COMPARTMENT

6.1 Introduction

Botulinum toxin type A (BTX-A) is a chemical denervant that acts at motor nerve endings to block acetylcholine release [65], which causes paralysis of muscle fibers [64], hence, muscle weakness (i.e., decreased ability for force production). Due to its effectiveness in avoiding the development of contractures [196], BTX-A is used widely in patients with cerebral palsy as an alternative treatment to surgery [197-199].

The effects of BTX-A have been widely studied by quantifying the area of paralysis [66], compound muscle action potential [67] and electromyography [68]. However, reports on mechanical parameters, e.g., twitch and tetanic force have been limited to selected muscle lengths or joint positions [e.g. 67, 69]. Herzog et al. made a major contribution to filling this gap in the literature by measuring joint torques in a range of joint angles [200-202]. Experiments on the rabbit quadriceps musculature showed that BTX-A causes more pronounced reductions in knee extension torque at more flexed knee positions [202]. This suggests that the effects of BTX-A on muscle forces and increasing muscle length may be negatively correlated.

Recently, Yaraskavitch et al. showed that the force-length characteristics of both injected soleus and non-injected plantaris muscles of the cat are affected by the poison [71]. BTX-A has been shown to spread through muscle fascia [70], and its effects beyond the injection site are plausible [72]. As these effects may not be confined only to a neighboring muscle, an experimental model that involves measurement of forces of mono- and biarticular muscles of an entire muscle compartment can allow for a comprehensive assessment of the effects of BTX-A both at and beyond the injection site.

Collagenous connections between adjacent muscles and extramuscular connective tissues such as collagen-reinforced neurovascular tracts and compartmental boundaries provide connections between the muscular and non-muscular structures of an intact compartment [20, 63, 86]. These epimuscular connections feature complex mechanical properties. Similar to other connective tissue structures, these connections have nonlinear force-deformation characteristics [203-205]. In addition, they have been shown to be pre-strained [23] and to have inhomogeneous mechanical properties (e.g., the proximal parts of the neurovascular tracts of the anterior crural compartment of the rat are stiffer than the distal parts [22]). Previous studies have shown the occurrence of epimuscular myofascial force transmission (EMFT) via these structures [23, 140-141]. Such EMFT is characterized by the interplay of stiffness of muscular tissues and epimuscular connections and it is determined by changes in the position of muscle relative to its neighboring structures [e.g. 27, 109]. Recently it has been shown that due to such force transmission, the global length changes of human gastrocnemius muscle and local strains within the muscle can be very different and despite its global isometric condition, local and heterogeneous deformations were found also within the soleus muscle [142].

BTX-A exposure changes the stiffness of muscular tissues because it causes paralysis of muscle fibers within parts of the muscle belly [66]. Therefore, compared to the no BTX-A injected condition, identical changes in relative position globally of the muscle-tendon complex is expected to lead locally to different interactions between the muscular tissues and their epimuscular connections. Consequently, the epimuscular connections can operate at different segments of their complex mechanical properties and cause the EMFT mechanism to change. Note that previously, the effects of BTX-A on the non-injected adjacent muscle were explored after the intactness of the compartment and the connections of the muscles with surrounding structures had been disrupted and the two muscles' forces were not measured simultaneously [71]. Therefore, the effects of BTX-A on the forces of muscles operating in an intact compartment as well as on EMFT mechanism remain unknown. We hypothesized that BTX-A affects (1) the forces of not only the injected but also the noninjected muscles of an entire intact compartment, and (2) EMFT. The goal of this study was to test these hy-

potheses. Additionally, it was to assess the existence of a correlation between injected muscle's length and the effects of BTX-A. These goals were addressed by measuring the force-length properties of the injected muscle as well as the isometric forces of the restrained non-injected muscles of the intact anterior crural compartment of the rat simultaneously, and in conditions close to those in vivo.

6.2 Methods

Surgical and experimental procedures were approved by the Committee on the Ethics of Animal Experimentation at Bogaziçi University. Male Wistar rats were divided into two groups: (1) Control ($n = 8$, mean \pm SD body mass = 318.5 ± 12.5 g). (2) BTX ($n = 8$, mean \pm SD body mass = 312.5 ± 14.6 g).

After imposing a mild sedation with an intraperitoneal dose of 1mg/kg ketamine, a circular region of approximately 15 mm radius from the center of the knee cap was shaved. The tibialis anterior (TA) muscle was located by palpation when the ankle was in maximal plantar flexion and the knee angle approximated 90° . After marking the center of the knee cap, a second marker was placed at a point 10 mm distal to that, along the tibia. The injection location was 5 mm lateral (along the direction normal to the line segment drawn between the two markers) to the second marker and over the TA muscle. All injections were made exclusively into this muscle, to a depth of 3 mm. Note that at the site of injection, the diameter of the TA approximates 5 to 5.5 mm, whereas the thickness of the skin approximates 0.7 to 1mm. Therefore, the injections were made into the superficial half of the TA muscle.

For the BTX group, each 100 unit vial of vacuum dried, botulinum type A neurotoxin complex (BOTOX, Allergan Pharmaceuticals, Ireland) was reconstituted with 0.9% sodium chloride. The animals received a one-time intramuscular BTX-A injection at a total dose of 0.1 units. The injected volume equaled 20 μ l. The control group was injected with the same volume of 0.9% saline solution exclusively. All injections were performed five days prior to testing. The animals were kept separately

until the day of the experiment in standard cages and in a thermally regulated animal care room with a 12h dark-light cycle.

6.2.1 Surgical procedures

The animals were anesthetized using an intraperitoneally injected urethane solution (1.2 ml of 12.5% urethane solution/100 g body mass). Additional doses were given if necessary (maximally 0.5 ml). Immediately following the experiments, the animals were sacrificed by the administration of an overdose of urethane solution.

During the surgery and data collection, the animals were kept on a heated pad (Harvard Apparatus, Homoeothermic Blanket Control Unit) to prevent hypothermia. A feedback system utilizing an integrated rectal thermometer allowed for the control of body temperature at 37 °C by adjusting the temperature of the heated pad.

The skin and the biceps femoris muscle of the left hind limb were removed and the anterior crural compartment including the extensor digitorum longus (EDL), the TA, and the extensor hallucis longus (EHL) muscles were exposed. Only a limited distal fasciotomy was performed to remove the retinaculae (i.e., the transverse crural ligament and the crural cruciate ligament). The connective tissues at the muscle bellies within the anterior crural compartment were left intact.

The specific combination of knee joint and ankle angles (120° and 100° , respectively) was selected as the reference position. In the reference position, the four distal tendons of the EDL muscle were tied together using silk thread. Matching markers were placed on the distal tendons of the EDL, the TA and the EHL muscles, as well as on a fixed location on the lower leg. Subsequently, the distal EDL tendon complex as well as the TA and the EHL tendons were cut as distally as possible. The proximal EDL tendon was cut from the femur, with a small piece of the lateral femoral condyle still attached. In order to provide connection to force transducers, Kevlar threads were sutured to: (1) the proximal tendon of the EDL muscle (2) the tied distal tendons of

the EDL muscle, (3) the distal tendon of the TA muscle, and (4) the distal tendon of the EHL muscle.

Within the femoral compartment, the sciatic nerve was dissected free of other tissues, during which process all nerve branches to the muscles of that compartment were cut. Subsequently, the sciatic nerve was cut as proximally as possible.

6.2.2 Experimental set-up

The animal was mounted in the experimental set-up (Figure 6.1). The femur and foot were fixed with metal clamps such that the ankle was in maximal plantar flexion (180°) to allow for the free passage of the Kevlar threads to the distal force transducers. The knee angle was set at 120° . Each Kevlar thread was connected to a separate force transducer (BLH Electronics Inc., Canton MA). Care was taken to ensure the alignment of the Kevlar threads were in the muscle line of pull. The distal end of the sciatic nerve was placed on a bipolar silver electrode.

6.2.3 Experimental conditions and procedures

Room temperature was kept at 26°C . For the duration of the experiment, muscle and tendon tissues were irrigated regularly by isotonic saline to prevent dehydration.

The distal and proximal tendons of the EDL and the distal tendon of the EHL muscles were kept in their reference positions at all times during the experiment. The isometric TA force was measured at various muscle–tendon complex lengths. Starting at muscle active slack length, the TA length was increased by moving its force transducer (in increments of 1 mm), until it was 2 mm over the length at which the highest TA force was measured. TA muscle tendon complex length is expressed as deviation ($\Delta\text{lmt TA}$) from its active slack length. Simultaneously, the proximal and distal EDL forces and the distal EHL force were measured.

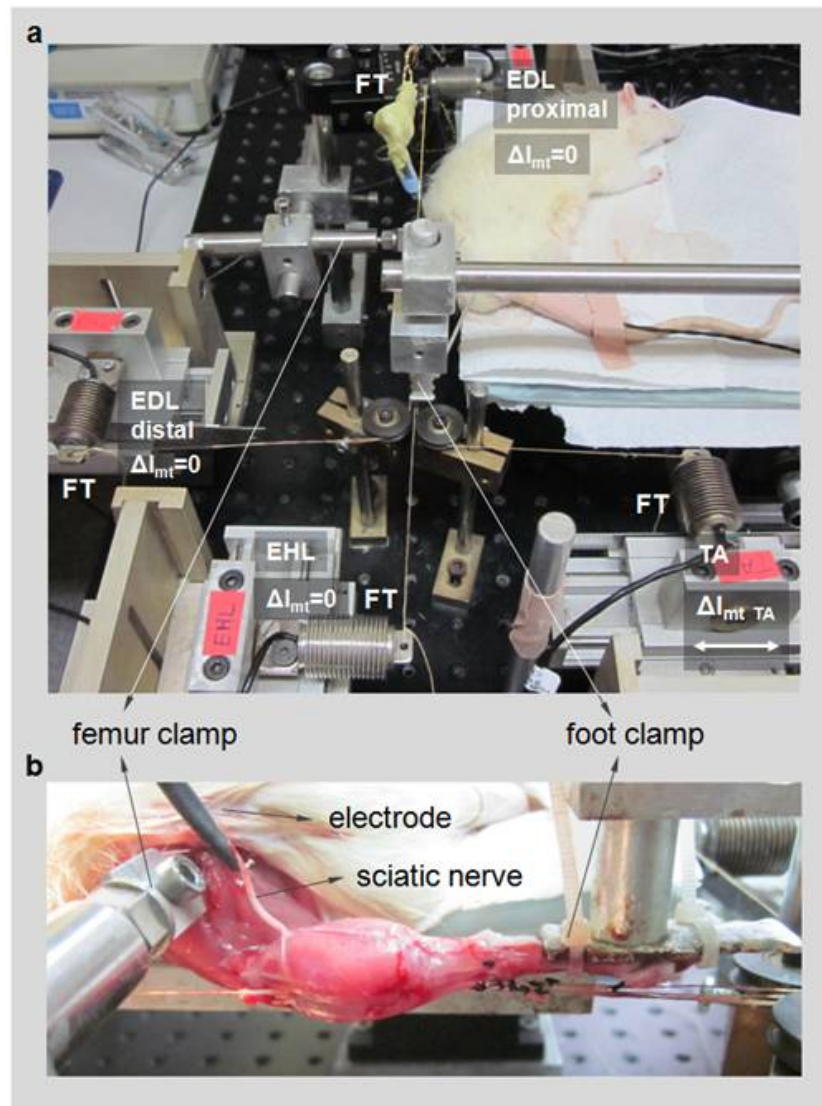


Figure 6.1 The experimental set-up. (a) Distal tendons of the tibialis anterior muscle (TA) and the extensor hallucis longus muscle (EHL) as well as the proximal and the tied distal tendons of the EDL muscle (EDL proximal and EDL distal respectively) were each connected to a separate force transducer (FT). Throughout the experiment, the EDL and EHL muscles were kept at constant muscle-tendon complex lengths ($\Delta l_{mt} = 0$). Exclusively, the TA muscle was lengthened ($\Delta l_{mt TA}$) to progressively increasing lengths, at which isometric contractions were performed. Lengthening (indicated by double arrow) started from muscle active slack length at 1 mm increments by changing the position of the TA force transducer. (b) Experimental condition for joint angles: knee angle = 120° and the ankle is at maximal plantar flexion. The femur and the foot were fixed by metal clamps and the distal end of the sciatic nerve was placed on a bipolar silver electrode.

All muscles studied were activated maximally by supramaximal stimulation of the sciatic nerve (Biopac Systems stimulator, STMISOC) using a constant current of 2mA (square pulse width 0.1ms). After setting the TA muscle to a target length, two twitches were evoked and 300 ms after the second twitch, the muscles were tetanized (pulse train 400 ms, frequency 100 Hz). At 200 ms after the tetanic contraction, another twitch was evoked. After each application of this stimulation protocol, the muscles were allowed to recover for 2 minutes. For the TA muscle, recovery was allowed to occur near the active slack length, whereas the lengths of the other muscles were not altered.

6.2.4 Processing of experimental data and statistics

Muscle passive isometric forces were determined 100 ms after the second twitch, and muscle total isometric forces were determined during the tetanic plateau (the mean force for a 200 ms interval, 150 ms after evoking tetanic stimulation). Data for total muscle force (F_t) in relation to muscle-tendon complex length were fitted with a polynomial function using a least squares criterion

$$y = b_0 + b_1x + b_2x^2 + \dots + b_nx^n \quad (1)$$

where x represents muscle-tendon complex length. $b_0, b_1 \dots b_n$ are coefficients determined in the fitting process. Data for passive muscle force (F_p) in relation to muscle-tendon complex length were fitted with an exponential function using a least squares criterion

$$y = e^{a_1 + a_2x} \quad (2)$$

where x represents passive muscle-tendon complex length and a_1 and a_2 are coefficients determined in the fitting process.

Polynomials that best described the experimental data were selected by using one-way analysis of variance (ANOVA) [30]: the lowest order of the polynomials that

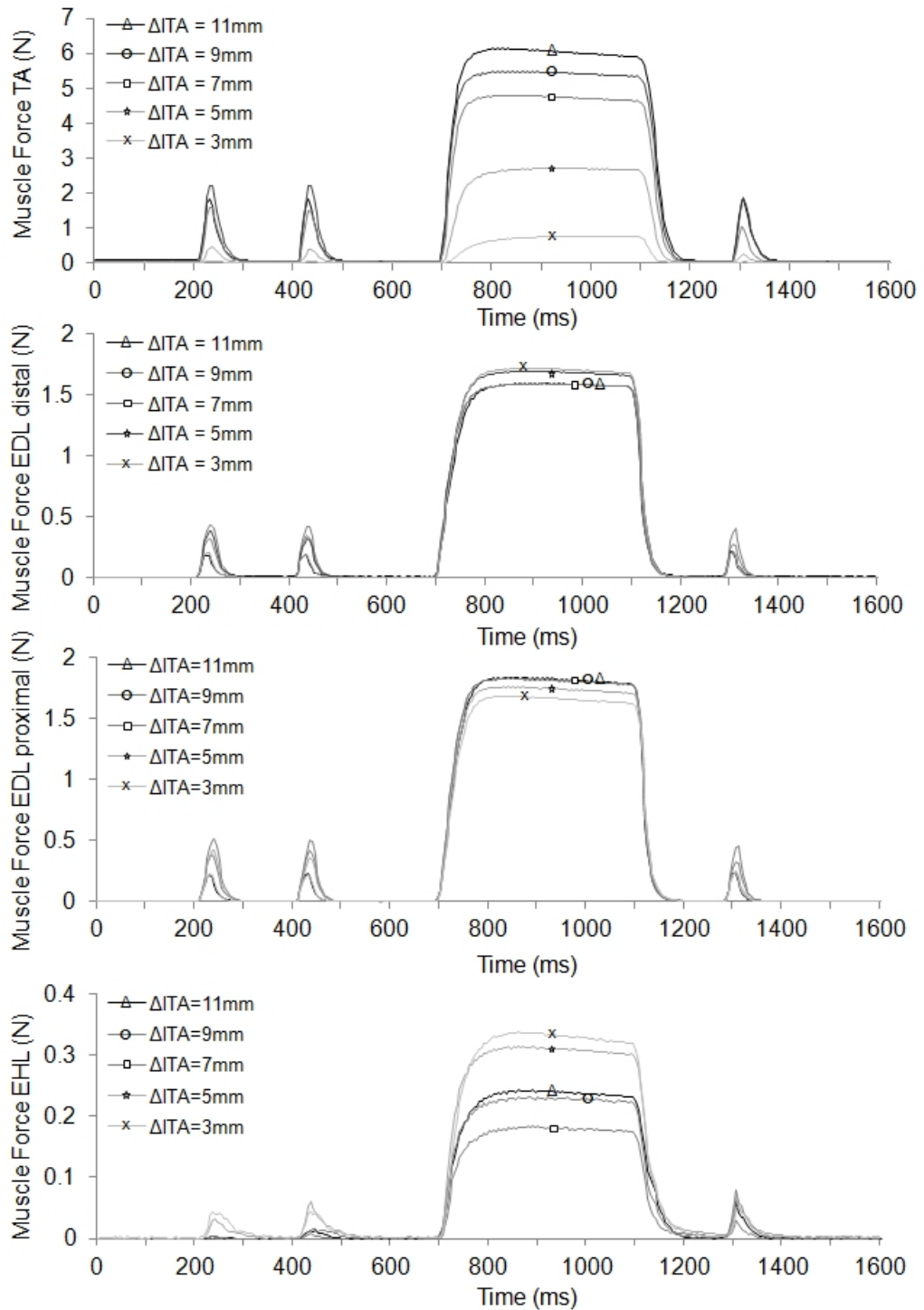


Figure 6.2 Typical examples of force time traces measured at tendons of muscles of the anterior crural compartment. Superimposed traces recorded at 5 TA muscle lengths (a) the TA force, (b) the distal EDL force, (c) the proximal EDL force and (d) the EHL force.

still added a significant improvement to the description of changes of muscle-tendon complex length and muscle force data were selected. These polynomials were used for two purposes: (1) Averaging of data and calculation of standard deviations. Per each muscle studied, muscle forces at different TA muscle-tendon complex lengths were obtained by using these functions. Per each TA muscle-tendon complex length, forces were averaged and standard deviations (SD) were calculated to determine the muscle's force (mean \pm SD). (2) Determining the maximal TA force and the corresponding muscle length. For each individual TA muscle, the maximal TA force is defined as the maximum value of the fitted polynomial for total muscle force and the corresponding TA length is determined. One-way ANOVA was also used to test for the effects of BTX-A injection on the TA muscle's length range of force production, i.e., the range between muscle active slack length and the length at which maximal force is measured. Two-way ANOVA for repeated measures (factors: TA muscle-tendon complex length and animal group) was performed separately for the forces of each muscle. Differences were considered significant at $p < 0.05$. If significant main effects were found, Bonferroni post-hoc tests were performed to further locate significant force differences within the factors [30]. Spearman's Rank correlation coefficient was calculated to test if reductions in TA total forces due to BTX-A injection are correlated with TA muscle-tendon complex length. Reduction in force is calculated as the difference in mean force between the control and the BTX animal groups at each TA muscle-tendon complex length and expressed as a percentage of the mean force of the control group. Correlations were considered significant at $p < 0.05$.

6.3 Results

Figure 6.2 shows superimposed examples of force–time traces for muscles of the anterior crural compartment at 5 sample TA lengths selected from the range of 13 TA lengths tested between muscle active slack length and the length 2 mm over the length at which the highest TA force was measured.

TA force-length characteristics ANOVA (factors: TA length and animal group)

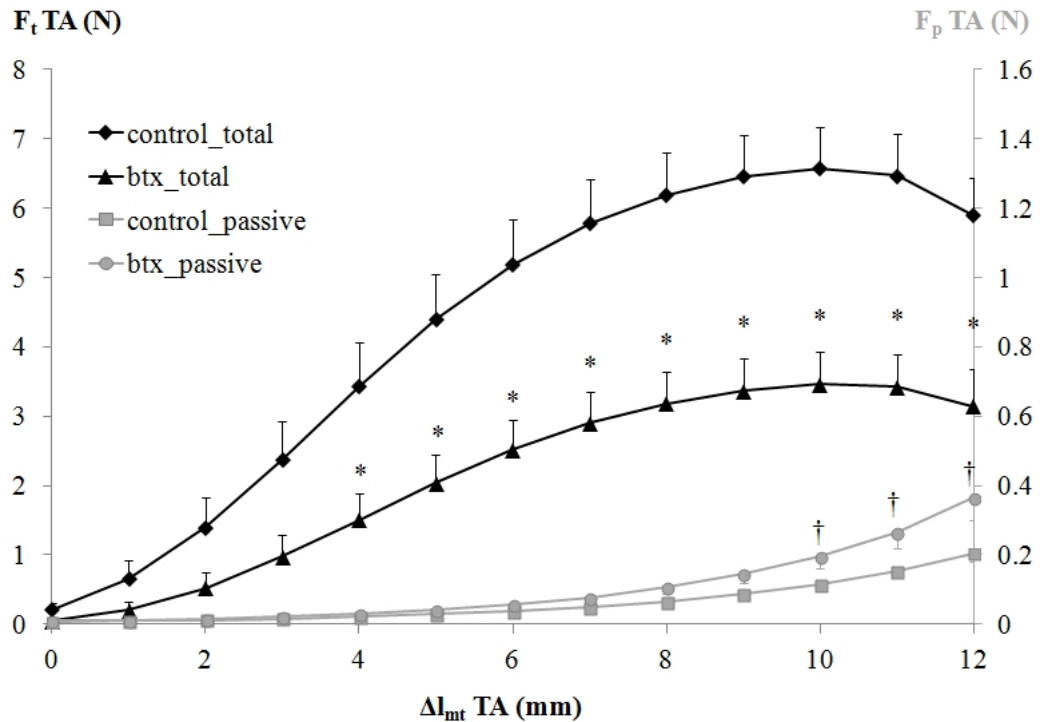


Figure 6.3 The effects BTX-A injection to TA muscle on its isometric muscle force-length characteristics. Absolute total and passive isometric forces are shown as mean values \pm SD for the control group and the BTX injected group of animals. The TA muscle-tendon complex length is expressed as a deviation ($\Delta l_{mt} \text{ TA}$) from the active slack length of BTX group. The reference position corresponds to $\Delta l_{mt} \text{ TA} = 4 \text{ mm}$. Significant differences between the TA force of the BTX group and the control group (Bonferoni post hoc test) are indicated by * (total force) and by † (passive force).

showed significant main effects on TA total forces, as well as a significant interaction. Post hoc test located significant major effects of BTX-A injection at most muscle lengths ($\Delta l_{mt} \text{ TA} > 4 \text{ mm}$). A significant negative correlation was found between reductions in TA total force with increasing TA length. Spearman's rank correlation coefficient was -0.94 ($p=0.0049$). BTX-A caused TA total force to decrease by, e.g., 55.9% at $\Delta l_{mt} \text{ TA} = 4 \text{ mm}$, by 47.3% at $\Delta l_{mt} \text{ TA} = 10 \text{ mm}$ (i.e., the length at which the maximum TA force was measured) and by 46.6% at the highest muscle length studied (i.e. $\Delta l_{mt} \text{ TA} = 12 \text{ mm}$). The length range of force production for the BTX group ($9.46 \pm 1.45 \text{ mm}$, mean \pm SD) was not significantly different from that of the control group ($10.35 \pm 1.42 \text{ mm}$, mean \pm SD). ANOVA showed significant main effects also on TA passive forces, as well as a significant interaction. Post hoc test showed significant effects of BTX-A injection at higher lengths ($\Delta l_{mt} \text{ TA} > 10 \text{ mm}$): passive forces were higher for the BTX group (maximally by 43.9%) (Figure 6.3).

EDL forces Both distally and proximally, ANOVA showed only a significant effect of BTX-A injection on EDL total forces; but no significant effects of TA length or a significant interaction. The mean force decreases BTX-A caused for the TA lengths studied were 67.8% distally and 62.9% proximally (Figure 6.4a, b). In contrast, ANOVA showed only a significant effect of TA length on EDL passive forces, thus neither significant effects of BTX-A injection nor a significant interaction. ANOVA also showed significant main effects on the EDL proximo-distal total force differences (Figure 6.4c) and a significant interaction. For the control group, the EDL distal forces were higher than proximal forces for $\Delta\text{mt TA} < 5$ mm and vice versa at higher TA lengths. Increasing the TA length was shown to change the force difference measured at $\Delta\text{mt TA} = 0$ mm significantly for $\Delta\text{mt TA} > 6$ mm. For the BTX group, the EDL proximal forces were higher than the distal forces for all TA lengths; however, no significant effect of increasing TA length was shown. Post hoc test located significant effects of the BTX-A injection on the EDL proximo-distal total force differences for $\Delta\text{mt TA} < 5$ mm.

EHL forces ANOVA showed significant main effects on EHL total forces, but no significant interaction. The mean force decrease BTX-A caused for the TA lengths studied was 9.2% (Figure 6.5). For both animal groups, the increased TA length caused the EHL forces to decrease significantly (by 34%) within almost the entire length range ($\Delta\text{mt TA} > 2$ mm) compared to EHL force measured at $\Delta\text{mt TA} = 0$ mm (post hoc). Regarding EHL passive forces, ANOVA showed neither significant main effects nor a significant interaction.

In summary, the present results make it evident that BTX-A administration causes the forces of not only the injected but also the non-injected muscles of an entire intact compartment to decrease. This confirms our first hypothesis. The results did show the existence of a significant correlation between injected muscle's length and the effects of BTX-A such that the force reductions decrease as the length of the muscle increases. The results also support the second hypothesis and show that BTX-A exposure has effects on the EMFT mechanism.

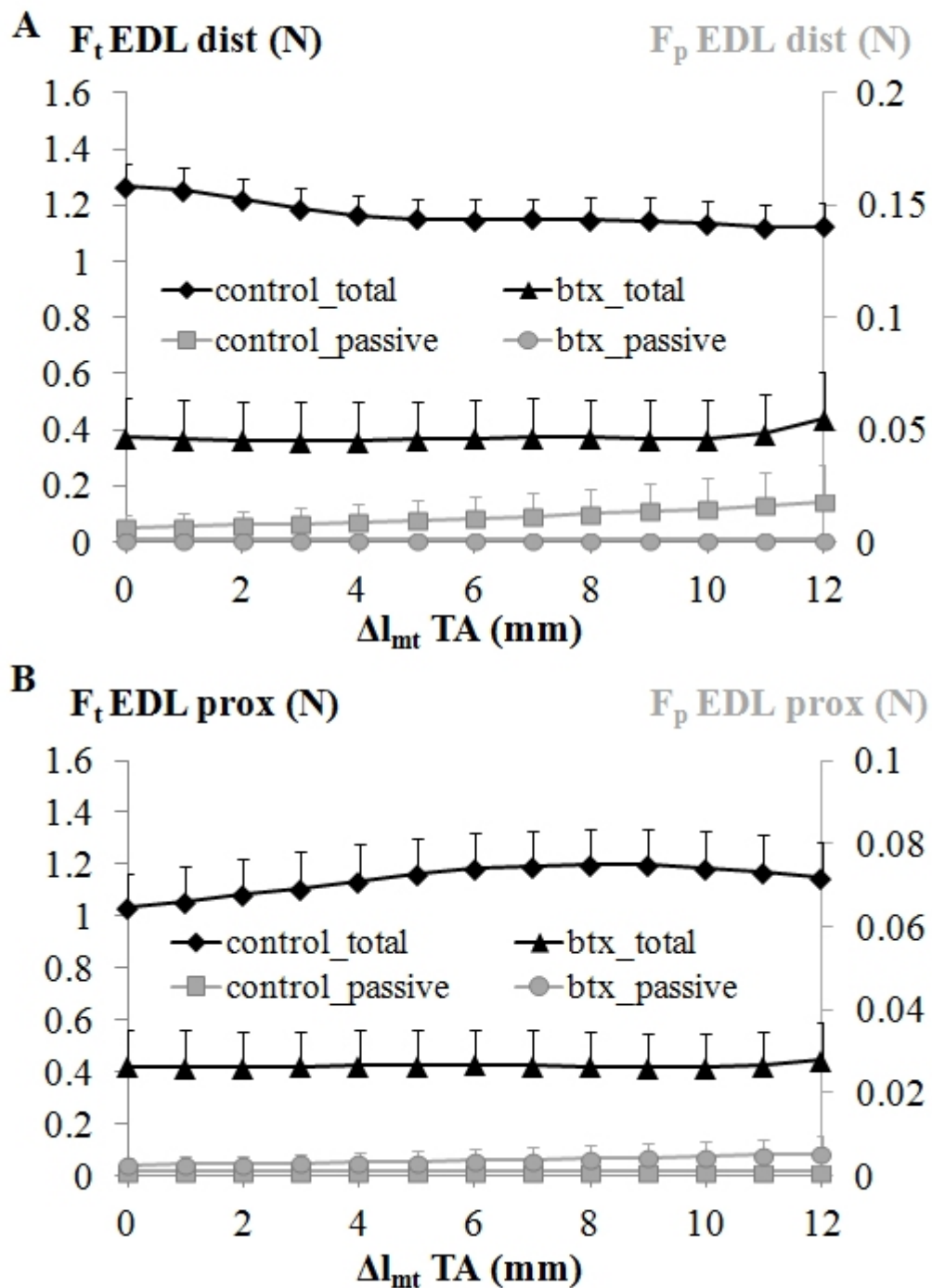


Figure 6.4 The effects of BTX-A injection to TA muscle on the EDL forces as a function of increasing TA muscle length. (a) Absolute total and passive forces exerted at the distal EDL tendon. (b) Absolute total and passive forces exerted at the proximal EDL tendon. (c) Normalized proximo-distal EDL total force differences. The EDL forces measured from the control group and the BTX group of animals, plotted as a function of TA length, are shown as mean values \pm SD. The TA muscle-tendon complex length is expressed as a deviation (Δl_{mt} TA) from the active slack length of BTX injected group. The reference position corresponds to Δl_{mt} TA = 4 mm. Forces in (c) are normalized with respect to the EDL peak total distal force of the corresponding animal group (i.e., 1.27 ± 0.22 N and 0.44 ± 0.48 N, respectively for the control and the BTX group). Note that a positive force difference indicates that a net epimuscular myofascial load is exerted on the EDL in the proximal direction and a negative force difference indicates a distally directed net epimuscular myofascial load.

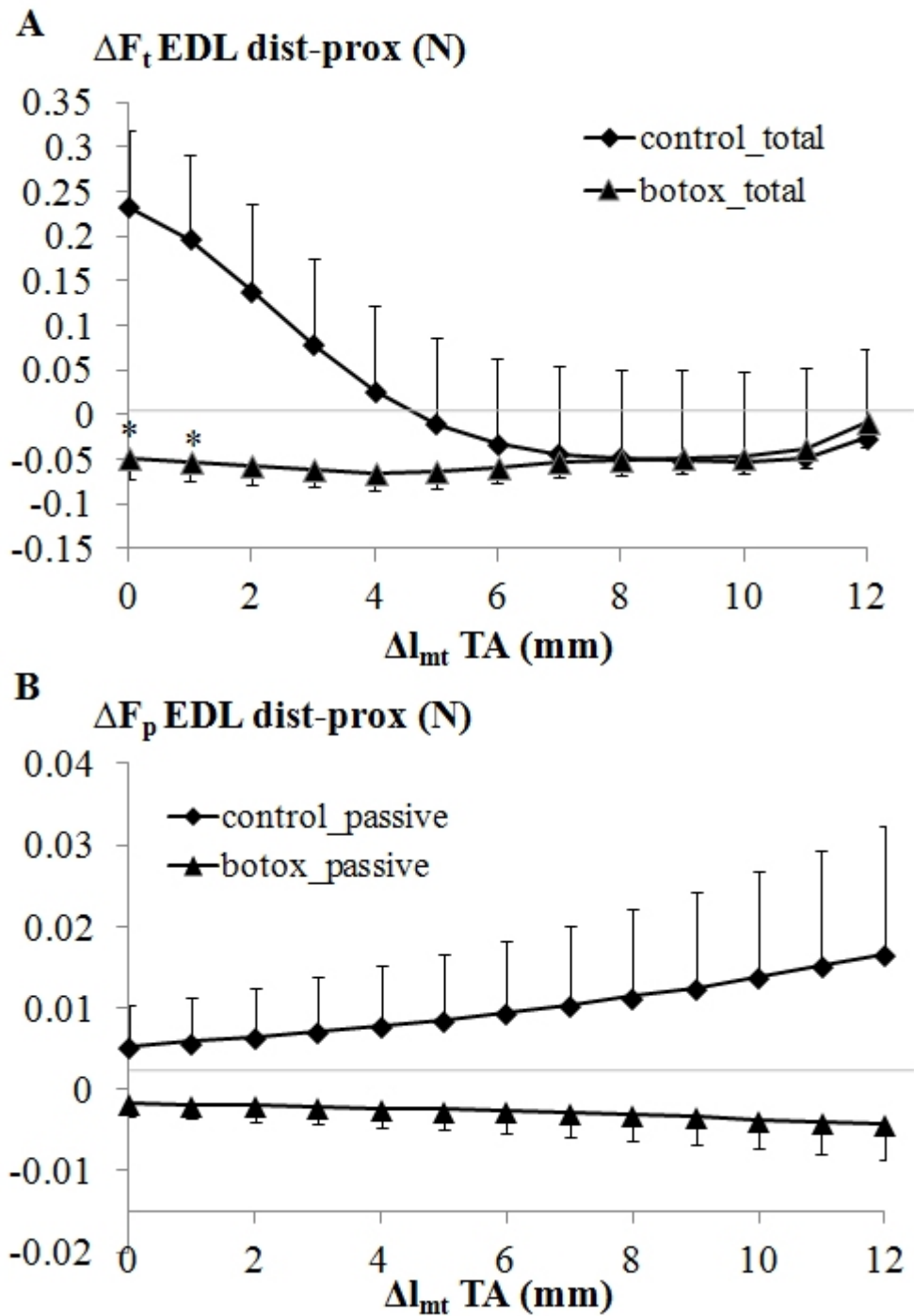


Figure 6.5 The effects of BTX injection to TA muscle on the EHL forces as a function of increasing TA muscle length. Absolute total as well as passive forces exerted at the distal tendon of the EHL muscle measured from the control group and the BTX group of animals are shown as mean values \pm SD. The TA muscle-tendon complex length is expressed as a deviation (Δl_{mt} TA) from the active slack length of BTX group. The reference position corresponds to Δl_{mt} TA = 4 mm.

6.4 Discussion

Effects of BTX-A on the forces of the injected and the non-injected muscles of the compartment An important finding is that force decreases caused by BTX-A are muscle length dependent such that the increased length of the injected muscle and the reduction in force are negatively correlated. Similar results were shown in the study of Yaraskavitch et al. [71] for the cat soleus muscle and were inferred from their torque-joint angle data by Longino et al. [13] after testing the quadriceps musculature of the rabbit. These findings obtained from different muscles suggest that muscle length dependency of the effects of BTX-A are important to consider. This may have clinical implications some of which are discussed in a successive paragraph.

Yaraskavitch et al. [71] based their explanation for the observed change in the force-length curve, i.e., a less steep ascending limb, on adaptation in the number of in-series sarcomeres, which could occur 4 weeks post-injection. However, in the present study, only 5 days postinjection, the occurrence of such adaptation is less likely. Denervation of adult mice muscle was shown to have no effect on the sarcomere number [206]. Therefore, the present results suggest that length dependent effects of BTX-A may not be due exclusively to changes in the number of in-series sarcomeres within the muscle. Instead, a mechanism that involves changes in lengths of in series sarcomeres may be responsible. For such mechanism, the fact that BTX-A causes paralysis of muscle fibers within parts of the muscle belly [66] is central. Due to that, BTX-A injection may lead to differences in two types of mechanical interactions occurring among the structures comprising the muscle-tendon complex: (1) Muscle-tendon interactions Tendon tissue has nonlinear force-deformation characteristics [205], and under lower magnitudes of forces, it has been shown to be more compliant [207-208]. For the BTX-A injected muscle, a general expected effect of the resulting reduction of muscle force is less extension of the tendon for the same muscle-tendon complex length. Therefore, a muscle tendon complex length dependent shifting of the sarcomere lengths to higher lengths is plausible. (2) Muscle fiber-extracellular matrix interactions Muscle fibers and the extracellular matrix (ECM) are mechanically connected not only at the ends of the muscle fibers, but also along their full peripheral length [161, 209-210]. Consequently,

muscle fibers can interact with the ECM and hence with each other mechanically [111, 162-163, 211]. In tetanized muscle, this mechanism has been shown to limit shortening of muscle fibers after tenotomy [111] and aponeurotomy [82, 179]: although some muscle fibers lost their myotendinous connection to the insertion of the muscle, the ECM connected to the muscle fibers via transsarcolemmal molecules [161] prevents the sarcomeres within these muscle fibers from shortening to their active slack length. In BTX-A injected muscle due to a lack of stimulation, the paralyzed muscle fibers do not shorten as activated muscle fibers of a non-paralyzed muscle would do. Therefore, the interaction mechanism described is expected to cause a resistance to the shortening of the sarcomeres within the activated muscle fibers. A common indicated effect therefore appears to be the shifted lengths of the sarcomeres within the activated muscle fibers. Recently, Turkoglu et al. [212] studied the principles of effects of BTX-A on muscular mechanics by extending a finite element model of rat muscle [28, 213]. They activated only selected parts of the muscle, and the remainder parts were considered to represent paralyzed muscle fibers. The model results show in agreement with [71] the arguments posed above that sarcomeres do attain higher lengths. Consequently, if the active sarcomeres of the partially paralyzed muscle are at the ascending limb of their force length curve, they can produce more force compared to their counterparts in the nonparalyzed muscle. This suggest that a net muscle force reduction effect of BTX-A originates exclusively from the presence of paralyzed muscle fibers, as the active ones may have even an enhanced potential of active force production. Note that the model results [212] indicate that compared to lower muscle lengths, this potential compromising the effectiveness of BTX-A is greater at intermediate muscle lengths because there is relatively more resistance to sarcomere shortening. On the other hand, if the active sarcomeres are at the descending limb of their force-length curve, the opposite is valid, i.e., as they attain higher lengths, they produce less force. Note that in conditions similar to the present ones i.e., for muscle with epimuscular connections to its surrounding structures, previous model studies suggest heterogeneity of sarcomere lengths within muscle fibers [23, 84, 109]. Particularly at higher muscle lengths, sarcomere length heterogeneity may include sarcomeres at both ascending and descending limbs of their force-length curves within the same muscle fibers [22, 25]. Therefore, for such lengths, a more complex mechanism may determine the effectiveness of BTX-A

in force reduction. Recall that the present results show a decrease in the force reduction effect of BTX-A at higher muscle lengths. According to the mechanism proposed, this suggests that most active sarcomeres may have been shifted to lengths favorable for force production. It is important to note that the mechanisms considered here to explain the length dependency of the effects of BTX-A are theoretical ones and they should be elaborated and verified in new studies. Medical imaging may be a feasible method to test these effects. Recently in no BTX-A injected condition has magnetic resonance imaging analyses shown the occurrence of local and heterogeneous muscle tissue deformations as caused by joint angle changes in human muscles in vivo [142]. Such deformations involve variable magnitudes of local lengthening occurring simultaneously with local shortening at other locations and indicate that distribution locally of lengths of muscle tissue is possible. Coupled with diffusion tensor imaging, such analyses may allow for quantification of length changes specifically along the muscle fiber direction [214].

BTX-A is used in treating patients with cerebral palsy, e.g., in the management of spastic equines gait [198-199] as well as in upper limb spasticity [215]. In these patients, spasticity is responsible for movement disorders and functional disability that can be characterized by a limited joint range of movement [38]. An improved understanding of how BTX-A affects the force production of muscle for different muscle lengths may be clinically relevant. However, the moment arm lengths of muscles vary with varying joint angles [126-127], which make it difficult to relate such understanding directly to joint movement. Therefore, based on the present results, it cannot be concluded that the effects of the treatment are variable for different joint angles. Muscle hypertonicity in spasticity [29-31] causes the joint to be forcefully kept in typically a flexed position in which the muscle is expected to be short. It may be important that a more pronounced muscle weakening effect is found for shorter muscle lengths. However, due to the indicated difficulty in relating muscle force-length properties to joint movement, it cannot be concluded that more pronounced effects are available for the joint positions that may correspond to short muscle lengths. Nevertheless, the findings of Longino et al. [201] may support this expectation because these authors showed that muscle weakness effects of BTX-A cumulatively on the rabbit knee extensors are knee

joint angle dependent, and are more pronounced for more extended knee positions. More importantly, the results of the present study show that potentially all muscles within a compartment can determine how BTX-A administration affects the mechanics at the joint, even though only one of them is injected. A noteworthy implication of this finding is that the non-targeted muscles may have unintended effects also at the other joints that they span. These findings are expected to have clinical relevance and the experimental approaches developed are suitable for addressing them in new studies. These studies should also impose muscle length changes for the non-targeted muscles.

Injection protocol employed in relation to the effects on muscle forces

[67] showed that the compound muscle action potential amplitude and the force exerted by lower hind limb flexors of the rat decreased predominantly in the first four days, with the decreases leveling off by the fifth day. Presently, the aim was to assess the short-term effects of BTX-A after stabilization. Therefore, all injections were performed five days prior to testing. Note that the present BTX-A injection protocol differs from common clinical practice: (1) the injected dose (0.1 U i.e., approximately 0.32 U/kg) was less than that used in patients for lower limb muscles (3-6 U/kg), including children with cerebral palsy [216-218]. (2) A single injection was made to the mid-belly of the target muscle instead of using multiple injection points [65, 70, 216, 219]. However, although they are not capable of showing whether an effective distribution of toxin is achieved, the present results strongly suggest that a considerable paralysis did occur within the target muscle. Shaari and Sanders showed that for the rat TA muscle, even a dose of 0.02U (a fifth of the dose used presently) injected to the mid-belly causes approximately a fifth of the total cross-sectional area to be paralyzed only 24 hours following the injection [66]. Shaari and Sanders also reported that an effective distribution of toxin is possible. Therefore, the quantity of BTX-A injected does not represent a low dose for the rat TA muscle as the difference with respect to the clinically used quantities would suggest and the present injection protocol was a suitable one for studying the effects of BTX-A on this muscle. On the other hand, BTX-A is reported to be highly diffusive [70]. Although it binds with high affinity to local targets within the muscle, a larger volume, single injection may cause that site to be

saturated and thus allow the spread of toxin to neighboring structures [216]. Therefore, the present injection protocol may have promoted toxin leakage to the adjacent EDL and EHL muscles. Yaraskavitch et al. explained their results with leakage of BTX-A into the noninjected muscle [71]; additionally, it is possible that partial paralysis of these muscles is responsible for the presently measured force decreases. Note that the spread of BTX-A beyond the injection site is considered to be a side effect [16, 56] and has been argued to occur not only after localized injections [14-15], but may be determined by the dose and concentration of injection [216]. New studies are indicated to test for the role of different injection protocols beyond the injection site within an intact compartment.

BTX-A has effects on EMFT

After imposing length changes to a muscle, EMFT previously has been shown to cause changes in forces of restrained muscles [e.g. 23, 141]. The present results showed similar effects for the control group: (1) The increased TA length caused significant changes in EDL proximo-distal force differences. Note that such force differences [15, 22, 25] are characteristic effects of EMFT [26] and represent the resultant of epimuscular myofascial loads acting on the EDL muscle. These forces originate from stretching epimuscular connections, which include direct collageneous connections between adjacent muscles as well as structures such as collagen-reinforced neurovascular tracts and compartmental boundaries.

They also include forces generated within the sarcomeres of neighboring muscles that are transmitted onto the EDL muscle via these structures [for a detailed discussion see 107]. Initially, the present EDL proximo-distal force differences were in favor of the distal force indicating that a resultant epimuscular myofascial load was acting on the muscle in the proximal direction. At the initial TA length, the length of the EDL muscle restrained at the reference position was conceivably higher causing interconnecting epimuscular connections between these muscles to be stretched as a source of such proximally directed loads.

However, the effect was reversed at higher TA lengths. (2) The increased TA length also caused EHL force to change significantly. No such EMFT effect on EHL muscle has been reported since in the previous studies, forces of this muscle were measured together with the forces of TA muscle via their tied tendons [25, 170]. However, EMFT between EHL and EDL muscles was shown previously to occur after imposing EHL length changes [23]. In those experiments, prior to testing, anterior crural compartment was opened and the TA muscle was removed. Therefore, only certain epimuscular connections of EHL muscle were left intact. In contrast, presently significant EMFT effects of TA length changes in a fully intact compartment were shown, which caused EHL forces to decrease approximately by a third. The results showed that similarly to the control group, increased TA length caused significant changes in the EHL force such that the EMFT effects remained as profound in the BTX group. This finding can be interpreted as BTX-A did not affect EMFT between EHL and TA muscles. However, like all muscles within the compartment, a muscle weakening effect was found for the EHL muscle, indicating that its stiffness in the active state decreased. Yet, the length changes of the TA muscle yielded the same relative decrease in EHL force for both groups. Therefore, the results indicate two findings: (1) the epimuscular connections between EHL and TA muscles remained sufficiently stiff to allow the occurrence of EMFT. (2) BTX-A causes manipulation locally of their stiffness, operationalized for the changes of muscle relative positions imposed. This is in agreement with our expectation that BTX-A administration changes the interplay of stiffness of muscular tissues and their epimuscular connections, and confirms that BTX-A affected EMFT between the EHL and the TA muscles.

On the other hand, BTX-A exposure did affect EDL proximo-distal force differences such that the effect of force differences initially in favor of the distal EDL force disappeared. This is an indicator that the epimuscular myofascial loads acting on the EDL muscle were manipulated by BTX-A. Also this result indicates that BTX-A administration changes the interplay of stiffness of muscular tissues and their epimuscular connections. Although it is not immediately apparent which component plays a dominant role, it is plausible that the epimuscular connections between the EDL and the TA muscles were less effective in EMFT after BTX-A administration.

A noteworthy effect presently shown is that at higher muscle lengths of the BTX-A injected TA muscle, the passive forces were significantly higher than those of the control group. A tenable explanation for this effect is an increased stiffness of the intramuscular connective tissues of the TA muscle and its epimuscular connections in combination. In agreement with this, the slope of the passive force-length curve of the BTX-A group was at least 86% higher than that of the control group for Δl_{mt} TA = 10 mm. Note that, in the passive state, any difference between the control and BTX groups in terms of existence of paralyzed muscle parts vanishes. Therefore, the increased passive TA forces cannot be ascribable to manipulated myofascial tissue stiffness, solely due to muscle relative position changes. Instead, it should also be considered that structural changes possibly occurred in these tissues. Within the first week following the denervation, atrophy of rat muscles was reported [220]. Also BTX-A was shown to cause atrophy [221-222]. Billante et al. showed that BTX-A causes decreased muscle fiber diameters as well as density [68]. Only for very high doses of BTX-A, even existence of fibrosis was observed by these authors within the muscle. However, no evidence is available whether passive muscle force increases accompanied such effects.

Moreover, these effects are limited to the intramuscular tissues exclusively. The lack of direct data to show if tissue structural changes occurred presently is a limitation of this study. However, increased passive force of BTX-A injected muscle with intact epimuscular connections is an interesting finding, implications of which on tissue adaptation should be addressed in new specific studies.

The results show that BTX-A has effects on EMFT. However, these effects are not uniform within the anterior crural compartment for the conditions studied and they imply that EMFT is affected not only by muscle weakening but also by manipulated mechanical properties of the connective tissues comprising the EMFT pathways. EMFT has been regarded to play an important role in the mechanics of spastic paretic muscle [62] and surgical treatment techniques of the related functional deficiencies [63]. Such concepts are likely to have clinical implications also for the treatment of these conditions using BTX-A. New studies are indicated to explore further the relationship

between the effects of BTX-A and those of EMFT.

6.5 Conclusions

The results show that exposure to BTX-A does affect the forces of all muscles operating in an intact compartment: (1) length dependent force decreases were found for the targeted TA muscle such that increased muscle length and the reduction in muscle force are negatively correlated. However, no change in the muscles' length range of active force production was found. (2) The simultaneously measured forces of the non-injected synergistic EDL and EHL muscles also decreased significantly, suggesting the presence of unintended additional effects both for the targeted distal joint and for the non-targeted proximal joint. The results also show that BTX-A exposure has effects on the EMFT mechanism. However, these effects are not uniform within the anterior crural compartment.

7. EFFECTS OF BTX-A ON NON-INJECTED BI-ARTICULAR MUSCLE INCLUDE A NARROWER LENGTH RANGE OF FORCE EXERTION AND INCREASED PASSIVE FORCE

7.1 Introduction

Botulinum toxin type A (BTX-A) causes muscle paralysis by inhibiting acetylcholine release into the presynaptic cleft in the neuromuscular junction [e.g., 65]. This chemodenervant is applied to spastic muscles of cerebral palsy (CP) patients to decrease muscle tonus [223-224]. A consequence of decreased hyperactivity is increased joint range of motion [225-227]. Therefore, it is aimed at improving joint function [228] and gait [218, 229-230]. BTX-A is also used to treat spasticity from several other origins such as stroke [231-232] and multiple sclerosis [233].

The effects of BTX-A have been widely studied by quantifying such parameters as the area of paralysis [66], electromyography [234] and compound muscle action potential [235]. Reports on twitch and tetanic force have been limited to selected muscle lengths or joint positions [e.g., 235, 236]. The difficulty of relating muscle force-length characteristics directly to joint movement due to moment arm lengths varying with joint angles [237-238] is apparent. Yet, such data have more potential for an improved understanding of effects of BTX-A on joint mechanics. For example, reduction of active force was shown to be variable as a function of muscle length instead of being constant [239].

BTX-A has been shown to spread through muscle fascia [70], and its effects beyond the injection site have been reported [240-242]. Therefore, it is also necessary to measure the effects not only on the target muscle but also on others that are affected. Recently, Yaraskavitch et al. [243] showed that the force-length characteristics

of both injected soleus and non-injected plantaris muscles of the cat are affected by the poison. Exposure exclusively of the tibialis anterior (TA) muscle of the anterior crural compartment of the rat affects the forces of also all other muscles i.e., m. extensor digitorum longus (EDL) and m. extensor hallucis longus (EHL) within the compartment [239]. On the other hand, it was reported to our knowledge for the first time that passive forces of muscle exposed to BTX-A increase [239]. As by using BTX-A in CP patients, an important goal is also to reduce passive resistance of the muscle at the joint [244-247], this finding is interesting.

For a bi-articular muscle, proximal and distal moment arms may differ, causing its contribution to mechanics of the joints it spans to be not symmetric. However, this may not be the exclusive source of such asymmetry. In BTX-A free conditions it was shown that the effects on muscle force-length characteristics of equal proximal and distal lengthening of bi-articular EDL muscle of the rat are not symmetric: e.g. distal lengthening yielded a lower distal optimal force than the proximal optimal force measured after proximal lengthening [174]. This effect is ascribable to mechanical interaction of muscle with its surrounding muscular and non-muscular tissues via its myofascial connections to those structures [63, 140-141]. Such mechanical interaction is feasible in an intact muscle compartment, as it is in vivo [142, 165]. Based on this, BTX-A may be expected to affect mechanics of a bi-articular muscle differently proximally and distally. However, this has not been tested.

We aimed at testing the hypothesis that BTX-A administration to the TA muscle of the rat affects the synergistic EDL muscle and causes changes to this muscle's active as well as passive contribution to mechanics of the joints it spans. This goal was addressed by measuring the force-length characteristics of the EDL muscle after proximal as well as distal lengthening. Key parameters studied were active force reduction, length range of active force exertion and passive muscle forces. For completeness, isometric forces of the TA and EHL muscles of the intact compartment were measured simultaneously.

7.2 Methods

7.2.1 Assessment of the effects of BTX on muscular mechanics

Surgical and experimental procedures were approved by the Committee on the Ethics of Animal Experimentation at Boğaziçi University. Male Wistar rats were divided into two groups: Control ($n = 8$, mean \pm SD body mass = 300.0 ± 6.9 g) and BTX ($n = 8$, mean \pm SD body mass = 315.0 ± 6.3 g).

After imposing a mild sedation with an intraperitoneal dose of 1mg/kg ketamine, a circular region of approximately 15 mm radius from the center of the knee cap was shaved. The tibialis anterior (TA) muscle was located by palpation when the ankle was in maximal plantar flexion and the knee angle approximated 90° . After marking the center of the knee cap, a second marker was placed at a point 10 mm distal to that, along the tibia. The injection location was 5 mm lateral (along the direction normal to the line segment drawn between the two markers) to the second marker and over the TA muscle. All injections were made exclusively into this muscle, to a depth of 3 mm.

For the BTX group, each 100 unit vial of vacuum dried, botulinum type A neurotoxin complex (BTX-A) (BOTOX, Allergan Pharmaceuticals, Ireland) was reconstituted with 0.9% sodium chloride. The animals received a one-time intramuscular BTX-A injection at a total dose of 0.1 units. The injected volume equaled 20 μ l. The control group was injected with the same volume of 0.9% saline solution exclusively. All injections were performed five days prior to testing. The animals were kept separately until the day of the experiment in standard cages and in a thermally regulated animal care room with a 12h dark-light cycle.

7.2.2 Surgical Procedures

The animals were anesthetized using an intraperitoneally injected urethane solution (1.2ml of 12.5% urethane solution/100g body mass). Additional doses were given

if necessary (maximally 0.5ml). Immediately following the experiments, the animals were euthanized by the administration of an overdose of urethane solution.

During the surgery and data collection, the animals were kept on a heated pad (Harvard Apparatus, Homoeothermic Blanket Control Unit) to prevent hypothermia. A feedback system utilizing an integrated rectal thermometer allowed for the control of body temperature at 37 °C by adjusting the temperature of the heated pad. The skin and the biceps femoris muscle of the left hind limb were removed and the anterior crural compartment including the EDL, the TA, and the EHL muscles were exposed. Only a limited distal fasciotomy was performed to remove the retinaculae (i.e., the transverse crural ligament and the crural cruciate ligament). The connective tissues at the muscle bellies within the anterior crural compartment were left intact.

The combination of knee joint and ankle angles (120° and 100°, respectively) was selected as the reference position. In the reference position, the four distal tendons of the EDL muscle were tied together using silk thread. Matching markers were placed on the distal tendons of the EDL, the TA and the EHL muscles, as well as on a fixed location on the lower leg. Subsequently, the distal EDL tendon complex as well as the TA and the EHL tendons were cut as distally as possible.

The femoral compartment was opened for two purposes: (1) to reach the proximal tendon of the EDL. After reaching it, this tendon was cut from the femur, with a small piece of the lateral femoral condyle still attached. (2) To expose the sciatic nerve. After this was done, the sciatic nerve was dissected free of other tissues, during which process all nerve branches to the muscles of the femoral compartment were cut. Subsequently, the sciatic nerve was cut as proximally as possible.

In order to provide connection to force transducers, Kevlar threads were sutured to: (1) the proximal tendon of the EDL muscle (2) the tied distal tendons of the EDL muscle, (3) the distal tendon of the TA muscle, and (4) the distal tendon of the EHL muscle.

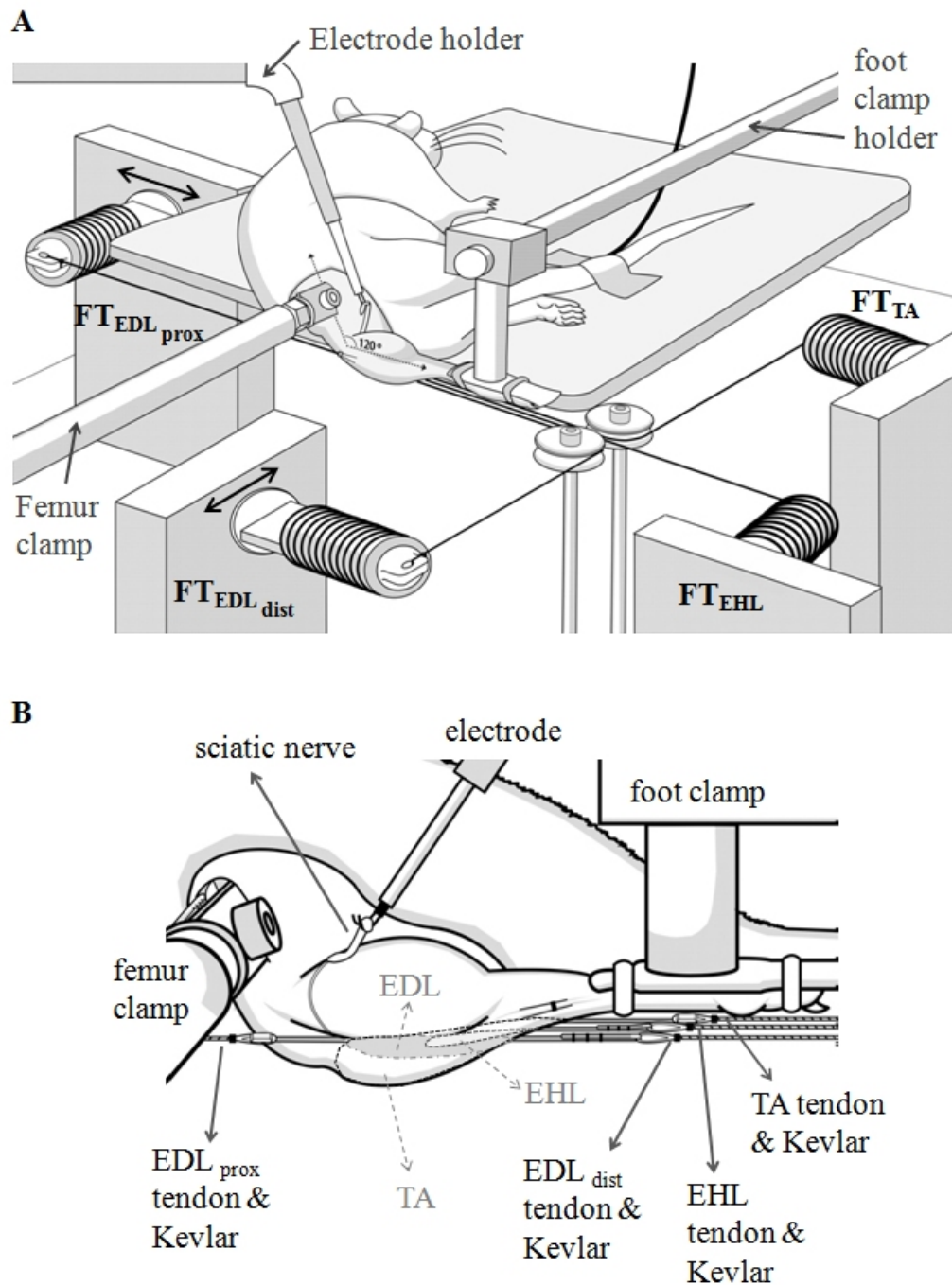


Figure 7.1 Schematic view of the experimental setup. (a) The proximal and the tied distal tendons of the EDL muscle (EDL prox and EDL dist, respectively) as well as the distal tendons of the tibialis anterior muscle (TA) and the extensor hallucis longus muscle (EHL) were each connected to a separate force transducer (FT). Throughout the experiment, the TA and the EHL muscles were kept at constant muscle-tendon complex lengths. Exclusively, the EDL muscle was lengthened either proximally or distally to progressively increasing lengths, at which isometric contractions were performed. Lengthening (indicated by double arrow) started from muscle active slack length at 1mm increments by changing the position of the target EDL force transducer. During the proximal lengthening condition, $FT_{EDL\ dist}$, and during the distal lengthening condition, $FT_{EDL\ prox}$ was kept in its reference position. (b) Experimental condition for joint angles: knee angle=120° and the ankle is at maximal plantar flexion. The femur and the foot were fixed by metal clamps and the distal end of the sciatic nerve was placed on a bipolar silver electrode. Kevlar threads (hatched lines) were sutured to tendons (solid lines) to provide connection to their respective FT.

7.2.3 Experimental set-up

The animal was mounted in the experimental set-up (Fig. 1A). The femur and foot were fixed with metal clamps such that the ankle was in maximal plantar flexion (180°) to allow for the free passage of the Kevlar threads to the distal force transducers. The knee angle was set at 120° . Each Kevlar thread was connected to a separate force transducer (BLH Electronics Inc., Canton MA). Care was taken to ensure the alignment of the Kevlar threads were in the muscle line of pull. The distal end of the sciatic nerve was placed on a bipolar silver electrode (Fig. 1B).

7.2.4 Experimental conditions and procedures

Room temperature was kept at 26°C . For the duration of the experiment, muscle and tendon tissues were irrigated regularly by isotonic saline to prevent dehydration. The distal tendons of TA and EHL muscles were kept in their reference positions at all times during the experiment. The isometric forces of all muscles were measured simultaneously at various muscle-tendon complex lengths of the EDL either by moving its proximal force transducer in the proximal direction (i.e., proximal lengthening condition) or by moving its distal force transducer in the distal direction (i.e., distal lengthening condition): starting from its active slack length, the EDL length was increased in increments of 1 mm, until it was 2 mm over the optimum length. EDL distal tendon was kept in its reference position.

EDL muscle-tendon complex lengths are expressed as deviation from the related optimum length (i.e., Δl_{ma} EDL proximal or Δl_{ma} EDL distal).

All muscles studied were activated maximally by supramaximal stimulation of the sciatic nerve (Biopac Systems stimulator, STMISOC) using a constant current of 2mA (square pulse width 0.1ms). After setting the EDL muscle to a target length, two twitches were evoked and 300ms after the second twitch, the muscles were tetanized (pulse train 400ms, frequency 100Hz). At 200ms after the tetanic contraction, another

twitch was evoked. After each application of this stimulation protocol, the muscles were allowed to recover for 2 minutes. For the EDL muscle, recovery was allowed to occur near the active slack length, whereas the lengths of the other muscles were not altered.

Subsequent to isometric force measurements, a glycogen depletion process was carried out in the BTX group: the peroneal branch of sciatic nerve was stimulated (20 Hz) continuously for 15 min [66, 70]. The anterior crural muscles were removed immediately after the animal was euthanized and their mid portions were prepared for histological assessment: fixation was followed by processing (Leica TP1020) and paraffin embedding (Leica EG1150H). 8 μ m sections were cut (Leica RM2255) for every 100 μ m. Glycogen staining was performed using periodic acid-Schiff (PAS) (Sigma-Aldrich, USA). Photographs of stained sections were taken under microscope (Leica DM2500, 10X magnifications). Effectiveness of PAS staining technique was assessed (Fig. 2A) in the control group (n=1, with glycogen depletion and n=1, with no glycogen depletion).

7.2.5 Assessments of the effects of BTX-A on intramuscular connective tissue content

Changes in intramuscular connective tissue content were assessed histologically in a separate set of male Wistar rats, again divided into two groups: Control (n = 6, mean \pm SD body mass = 321.7 \pm 29.3 g) and BTX (n = 6, mean \pm SD body mass = 319.3 \pm 8.1 g). After the injection protocol described above was employed, the animals were kept for five days in identical conditions with the previous set. TA, EDL, and EHL muscles were removed. Total wet muscle mass was measured using a scale (Precisa XB 320M) with high resolution (0.001 g). Subsequently, the muscles were prepared for histological assessment, cut into sections and photographed using the equipment described above. However, for this set, a detailed and quantitative analysis was carried out: 5 μ m cross-sections were cut for every 20 μ m. The sections were stained using Gomori's Trichrome (Bio-Optica-30-30110, Italy), which stain has been used in

distinguishing intramuscular collagen e.g., in neuromuscular diseases [248-249].

7.2.6 Data processing and statistics

Muscle isometric forces were determined 100ms after the second twitch. Force in such inactivated state represents the mechanical resistance potential of the muscular tissues at a particular muscle length tested and is referred to as passive muscle force (F_p). Muscle total isometric forces were determined during the tetanic plateau (the mean force for a 200ms interval, 150 ms after evoking tetanic stimulation). Data for active muscle force (F_a) calculated by subtracting the measured passive force from total force in relation to muscle-tendon complex length were fitted with a polynomial function using a least squares criterion

$$y = b_0 + b_1x + b_2x^2 + \dots + b_nx^n \quad (1)$$

where y represents F_a , x represents muscle-tendon complex length. $b_0, b_1 \dots b_n$ are coefficients determined in the fitting process. Data for passive muscle force in relation to muscle-tendon complex length were fitted with an exponential function using a least squares criterion

$$y = e^{a_1 + a_2x} \quad (2)$$

where y represents F_p and x represents passive muscle-tendon complex length and a_1 and a_2 are coefficients determined in the fitting process.

Polynomials that best described the experimental data were selected by using one-way analysis of variance (ANOVA) [125]: the lowest order of the polynomials that still added a significant improvement to the description of changes of muscle-tendon complex length and muscle force data were selected. These polynomials were used for averaging of data and calculation of standard deviations. Per each muscle studied, muscle forces at different EDL muscle-tendon complex lengths were obtained by using

these functions. Per each EDL muscle-tendon complex length, forces were averaged and standard deviations (SD) were calculated to determine the muscle's force (mean \pm SD).

The major determinants of muscle length-force characteristics are muscle optimal force (the maximum isometric force exerted by an active muscle), the corresponding muscle length, and muscle active slack length (the shortest length at which the muscle can still exert nonzero force). Muscle optimal force often is taken as an indication of a muscle's capacity for force production, and the range from active slack length to length at which optimal force is exerted is taken as an indicator of movement capability with active force exertion within the potential range of motion of a certain joint.

In order to account for these issues, the polynomials obtained were used also for the following purposes: determining (i) the optimal EDL force (i.e., for each individual EDL muscle, the maximum value of the fitted polynomial for active muscle force) as well as the corresponding muscle length and (ii) EDL active slack length. EDL muscle's length range of active force exertion (lrange) was determined as the range between the muscle's active slack length and the length at which optimal force is measured. Assessed were the proximal lrange in proximal lengthening condition and distal lrange in distal lengthening condition.

One-way ANOVA was also used to test for the effects of BTX administration on EDL muscle's lrange and to compare changes to lrange in proximal lengthening vs. distal lengthening conditions. Two-way ANOVA for repeated measures (factors: EDL muscle-tendon complex length and animal group) was performed separately for the forces of each muscle. Differences were considered significant at $p < 0.05$. If significant main effects were found, Bonferroni post-hoc tests were performed to further locate significant force differences within the factors [125].

Forces of both groups were aligned for their optimum length. Reduction in active force is calculated as the difference in mean force between the control and the BTX animal groups at each EDL muscle-tendon complex length and expressed as

a percentage of the mean force of the control group. Spearman's Rank correlation coefficient (ρ) was calculated to test if reductions due to BTX-A administration in (i) EDL proximal active forces are correlated with EDL proximal muscle-tendon complex length and (ii) EDL distal active forces are correlated with EDL distal muscle-tendon complex length. Correlations were considered significant at $p < 0.05$. Glycogen staining was assessed qualitatively to show that BTX-A causes partial paralysis for the muscles of the anterior crural compartment.

Intramuscular connective tissue staining on the other hand was assessed quantitatively to test whether BTX-A causes changes in the collagen content for these muscles. Using a self programmed code (MATLAB, R2012a) section images were analyzed to distinguish pixels stained in light green color (showing intramuscular connective tissue) from pixels stained in dark blue (showing contractile material). For both control and BTX groups (i) percentage of intramuscular connective tissue content in the sections studied was quantified and (ii) summed anterior crural muscle mass was normalized for the body mass. One-way ANOVA was performed to test for the effects of BTX administration. Differences were considered significant at $p < 0.05$.

7.3 Results

Glycogen staining shows that BTX-A administration causes partial paralysis for all muscles of the anterior crural compartment (Fig. 2).

7.3.1 Effects of BTX-A on the TA and EHL muscles

Significant main effects of only BTX-A injection on forces of restrained TA and EHL muscles were found. The mean active force decreases BTX-A caused for the EDL lengths studied were 82.8% for proximal lengthening and 74.8% for distal lengthening conditions, for the TA muscle (Fig. 3A, C) and 43.7% for proximal lengthening and 53.5% for distal lengthening conditions, for the EHL muscle (Fig. 3B, D). Passive EHL

force increased for both conditions (4 folds for distal lengthening condition); whereas, TA passive force increased significantly only for distal lengthening condition (by a sixth).

7.3.2 Effects of BTX-A after proximal lengthening of the EDL

Proximal forces ANOVA (factors: EDL length and animal group) showed significant main effects on EDL proximal active forces, as well as a significant interaction. Post hoc test showed significant major effects of BTX-A at all muscle lengths (Fig. 4A). EDL active force reductions (e.g., 90.1%, 84.3% and 83.3%, respectively at Δl_{ma} EDL = -6 mm, Δl_{ma} EDL = 0 mm and Δl_{ma} EDL = 2 mm) were shown to be inversely correlated with increasing EDL muscle length ($\rho = -0.98$, $p < 0.0001$). The proximal range of the control group (8.47 ± 0.98 mm) decreased significantly after BTX-A injection (6.57 ± 1.40 mm) (Fig. 4A). ANOVA showed significant main effects also on EDL proximal passive forces, as well as a significant interaction. Post hoc test showed significant effects of BTX-A (Δl_{ma} EDL ≥ 1 mm): e.g., at Δl_{ma} EDL = 2mm the passive force increased about 8 folds (Fig. 4A).

Distal forces ANOVA (factors: EDL length and animal group) showed significant main effects on EDL distal active forces, as well as a significant interaction. Post hoc test showed significant major effects of BTX-A for most muscle lengths (Δl_{ma} EDL > -5 mm) (Fig. 4B). Minimal active force reduction was 85.0% (Δl_{ma} EDL = 0 mm). ANOVA showed significant main effects also on EDL distal passive forces, as well as a significant interaction. Post hoc test showed significant effects of BTX-A injection (Δl_{ma} EDL ≥ 1 mm): e.g., at Δl_{ma} EDL = 2mm, the passive force increased about 9 folds (Fig. 4B).

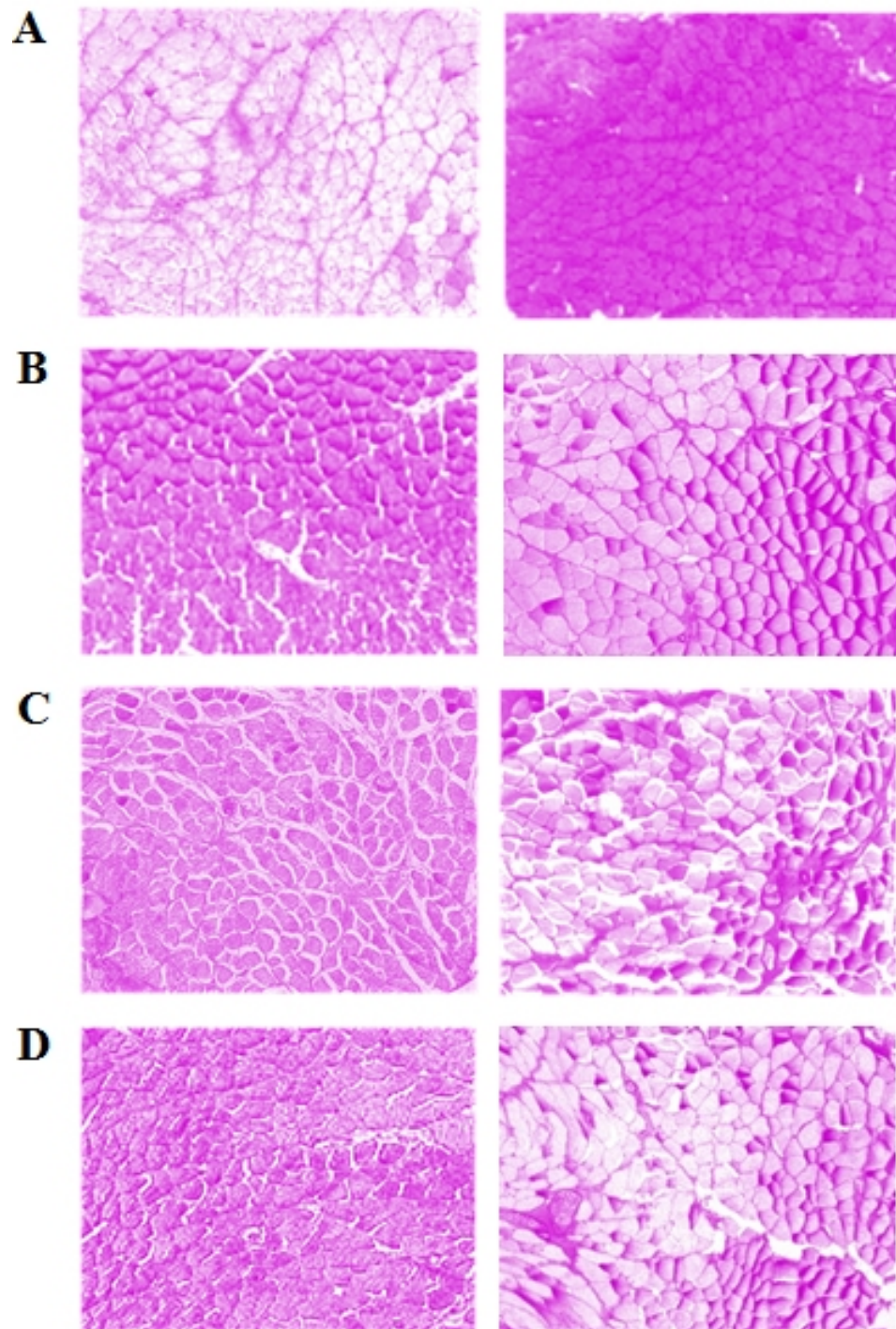


Figure 7.2 Sample histological sections of anterior crural muscles stained using PAS for glycogen. Retained glycogen in paralyzed muscle fibers appears dark after PAS stain. Control group: (A) Sections from the TA muscle subjected to glycogen depletion (left panel) and with no glycogen depletion employed (right panel). Glycogen in the contractile material is consumed after glycogen depletion. BTX group: Sections showing parts of (B) the TA muscle, (C) the EHL muscle and (D) the EDL muscle include retained glycogen entirely (left panels) or partially (right panels) indicating that muscles of the anterior crural compartment are all affected from BTX-A injection to the TA muscle.

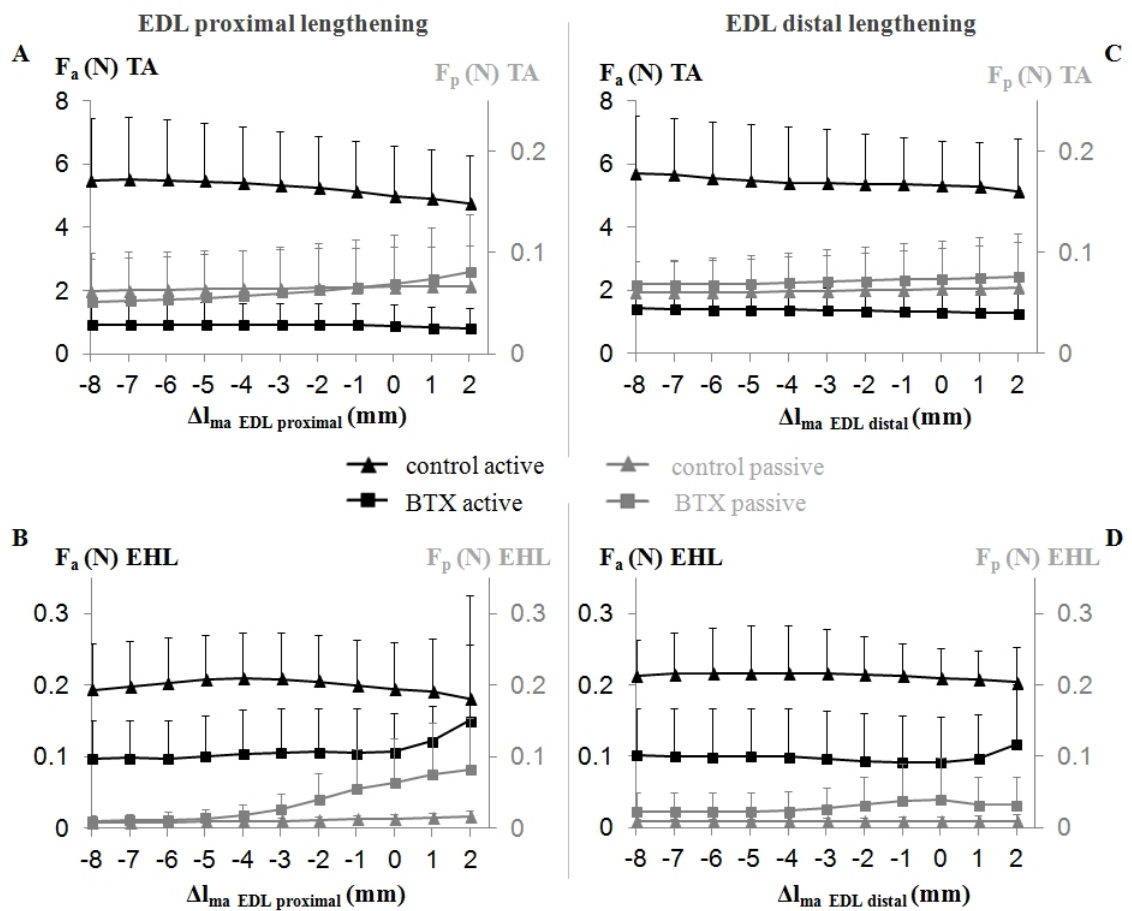


Figure 7.3 Forces of the TA and EHL muscles as a function of increasing EDL muscle length. Active as well as passive isometric muscle forces are shown as mean values \pm SD for the control and BTX groups. (A) TA and (B) EHL forces obtained after EDL proximal lengthening. (C) TA and (D) EHL forces obtained after EDL distal lengthening. EDL muscle-tendon complex length is expressed as a deviation from its optimum length.

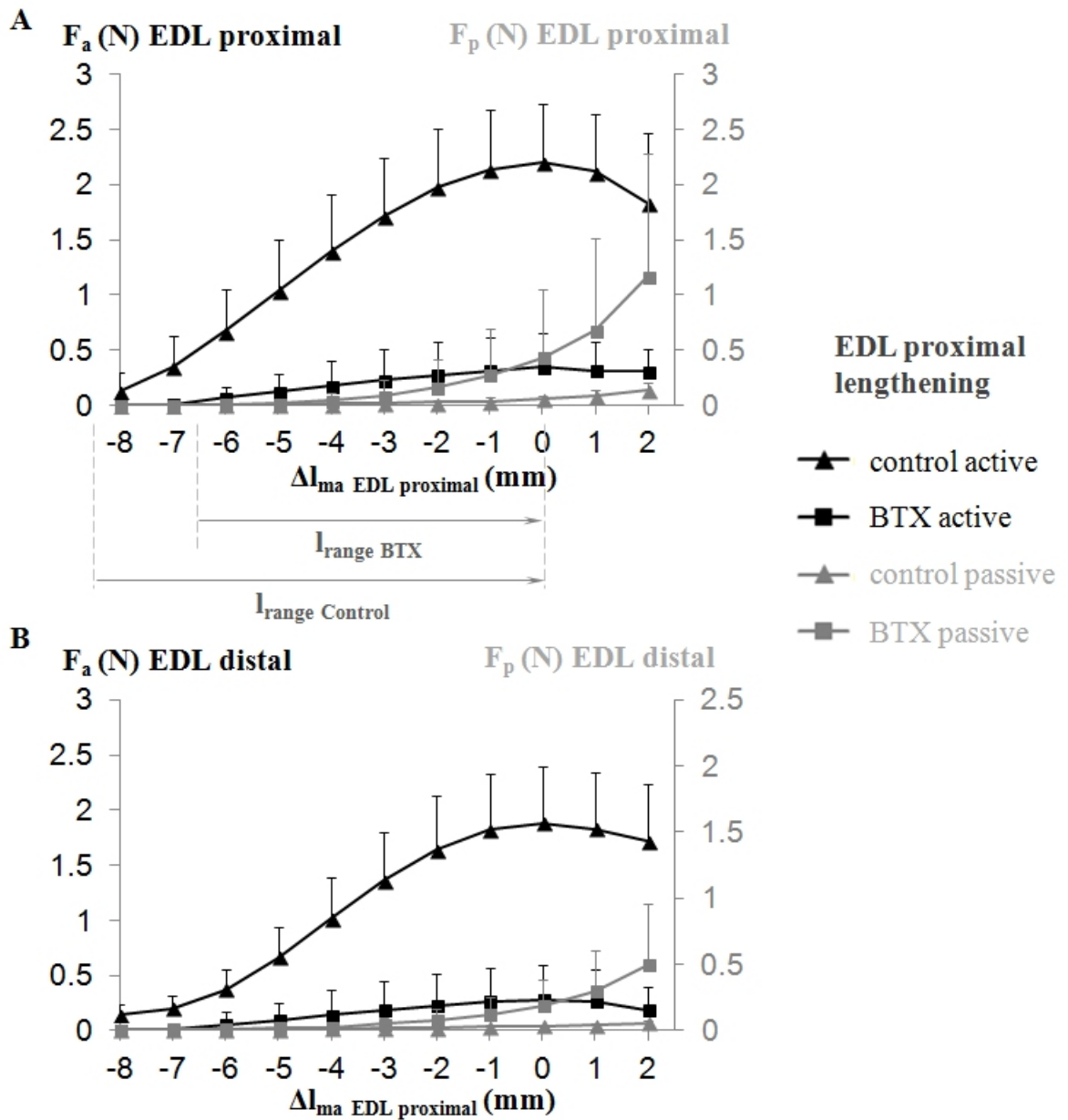


Figure 7.4 EDL force-length characteristics obtained after proximal lengthening. (A) Proximally and (B) distally exerted active as well as passive isometric EDL forces are shown as mean values \pm SD for the control and BTX groups. EDL muscle-tendon complex length is expressed as a deviation from its optimum length. Part (A) shows a representation of the significant decrease found for proximal length range of active force exertion after BTX-A injection: for the control group l_{range} control = 8.48 ± 0.98 mm, whereas for the BTX group l_{range} BTX = 6.57 ± 1.40 mm.

7.3.3 Effects of BTX-A after distal lengthening of the EDL

Distal forces ANOVA (factors: EDL length and animal group) showed significant main effects on EDL distal active forces, as well as a significant interaction. Post hoc test showed significant major effects of BTX-A injection for most muscle lengths (Δl_{ma} EDL > -5 mm) (Fig. 5A). However, EDL active force reduction (e.g., 82.8%, 85.6% and 83.7%, respectively at Δl_{ma} EDL = -5 mm, Δl_{ma} EDL = 0 mm and Δl_{ma} EDL = 2 mm) was not significantly correlated with increasing EDL muscle length ($\rho = 0.19$, $p = 0.65$). The distal range for the control group (8.24 ± 0.55 mm) decreased significantly after BTX-A injection (6.09 ± 1.36 mm) (Fig. 7.5A).

ANOVA showed significant main effects on EDL distal passive forces, but no significant interaction. The mean passive force increase was about 3 folds (Fig. 7.5A).

Proximal forces ANOVA (factors: EDL length and animal group) showed significant main effects on EDL proximal active forces, as well as a significant interaction. Post hoc test showed significant major effects of BTX-A injection at all muscle lengths (Fig. 7.5B). Minimal active force reduction was 83.7% (Δl_{ma} EDL = -6 mm).

ANOVA showed significant main effects also on EDL proximal passive forces, as well as a significant interaction. Post hoc test showed significant effects of BTX-A injection (Δl_{ma} EDL ≥ 1 mm): e.g., at Δl_{ma} EDL = 2mm the passive force increased about 12 folds (Fig. 7.5B).

7.3.4 Distal vs. proximal lengthening condition

An indicator of asymmetry of effects of BTX-A was that EDL active force reduction was inversely correlated with increasing EDL muscle length in the proximal lengthening condition, whereas no such correlation was found in the distal lengthening condition. However, decrease in distal l_{range} due to BTX-A injection was not significantly different than that in proximal l_{range} .

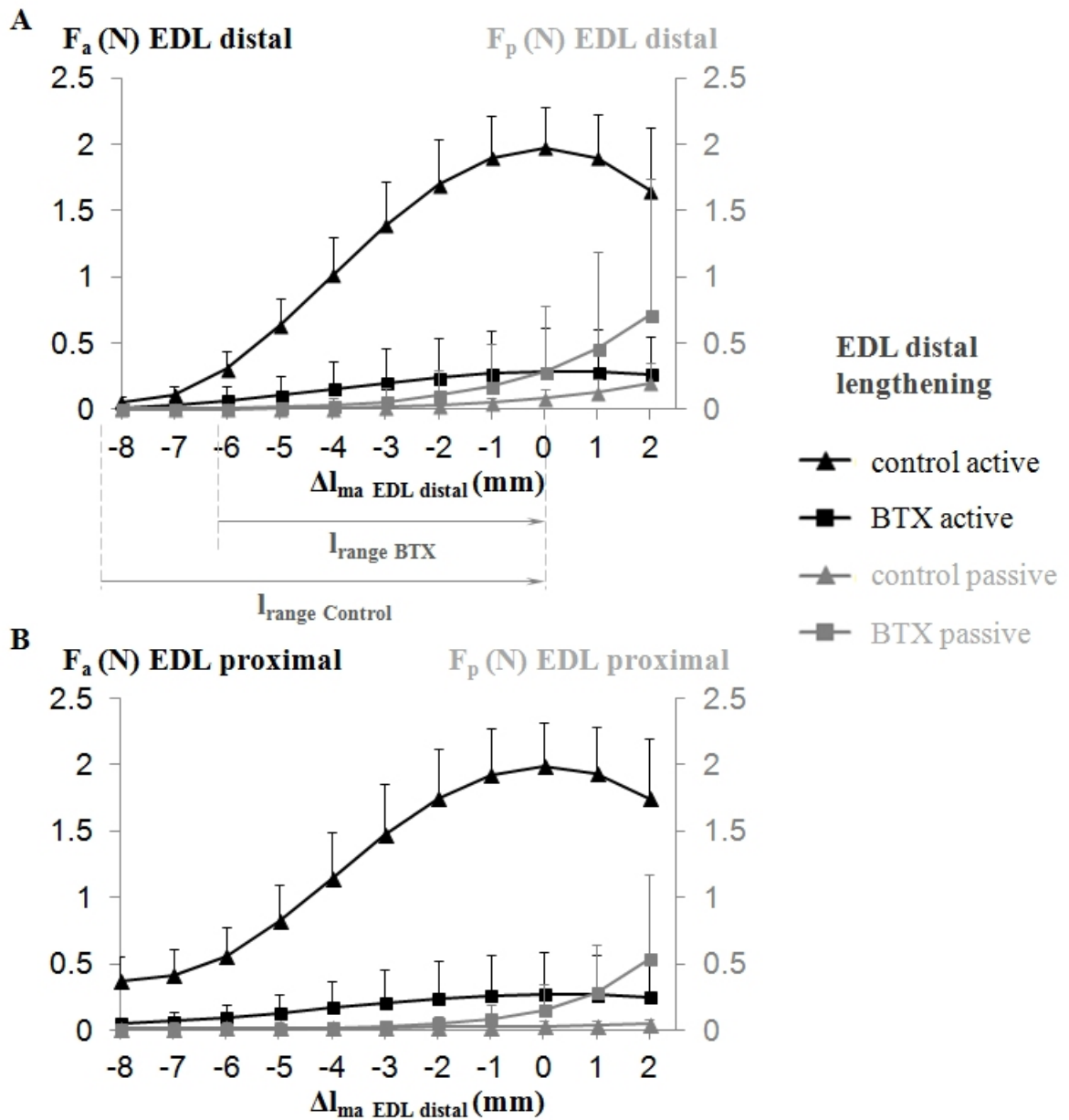


Figure 7.5 EDL force-length characteristics obtained after distal lengthening. (A) Distally and (B) proximally exerted active as well as passive isometric EDL forces are shown as mean values \pm SD for the control and BTX groups. EDL muscle-tendon complex length is expressed as a deviation from its optimum length. Part (A) shows a representation of the significant decrease found for distal length range of active force exertion after BTX-A injection: for the control group l_{range} control = 8.24 ± 0.55 mm, whereas for the BTX group l_{range} BTX = 6.09 ± 1.36 mm.

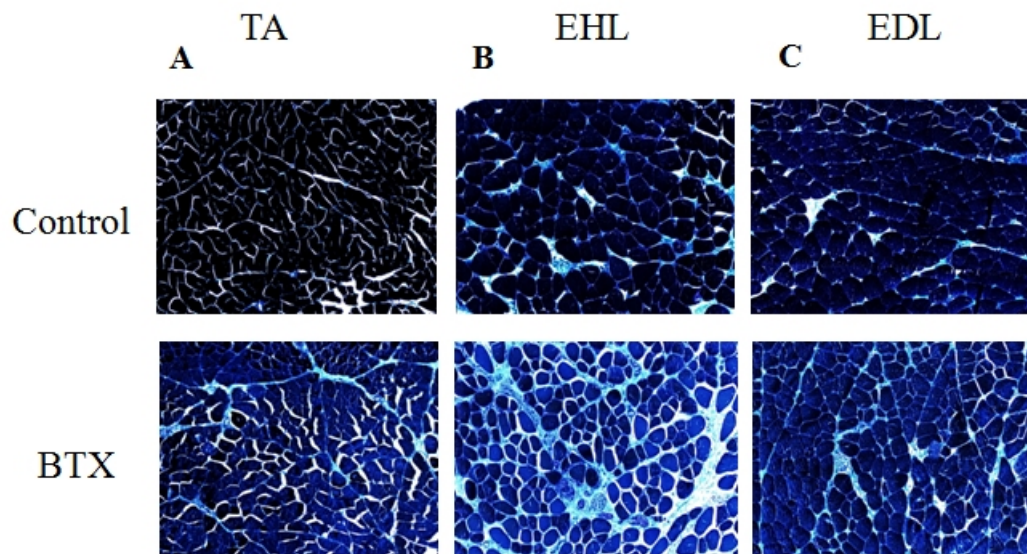


Figure 7.6 Sample histological sections of anterior crural muscles stained using Trichrome Gomori for collagen. The sections presented show parts of (A) the TA, (B) the EHL, and (C) the EDL muscles of Control group (upper panels) and BTX group (lower panels). Trichrome Gomori staining allows distinguishing intramuscular connective tissue (appear light green in the sample sections) from contractile material (appear dark blue in the sample sections). For a quantitative analysis indicating increased intramuscular connective tissue content after exposure to BTX-A, see text.

7.3.5 Effects of BTX-A on intramuscular connective tissue content

Fig. 7.6 shows sample histological sections for intramuscular connective tissue staining. Percentage of intramuscular connective tissue content values for muscles of the BTX group (mean \pm SD = 1.5% \pm 0.6%, 6.3% \pm 1.3% and 4.6% \pm 1.2% for the TA, EHL and EDL, respectively) were significantly higher than those for muscles of the control group (mean \pm SD = 0.5% \pm 0.2%, 3.2% \pm 1.0% and 1.3% \pm 0.5% for the TA, EHL and EDL, respectively). BTX-A caused a significant decrease in muscle mass (9.9% \pm 4.7%).

7.4 Discussion

Among a wide range of doses of BTX-A from 0.02U to 20.0U injected into the TA muscle of the rat, even the smallest dose was shown to cause approximately a fifth of the total cross-sectional area to be paralyzed only 24 hours following the injection [66]. This dose is a fifth of the dose used presently and the injection was performed to

the mid-belly of the TA as it was done in the present study. Misiaszek and Pearson [250] demonstrated that the peak effectiveness of the BTX usually occurred around day five and Cichon et al. [67] reported occurrence of most force decreases of the lower hind limb flexors of the rat in the first four days after the injection and level off by the fifth day. On the other hand, remodeling of the neuromuscular junctions may occur [250]. Nerve sprouting was observed after the first week [251]. Based on these studies we determined the present injection protocol and aimed at assessing the short-term effects of BTX-A. Our choice of conducting the experiments five days after the injection conceivably allowed for testing after force decreases reach a steady state and before remodeling of the neuromuscular junctions may become profound.

However, differences between the present protocol and common clinical practice should be discussed for which, the following three issues appear to be important: (1) Doses used in lower limb muscles of children with cerebral palsy range between 3 to 6U/kg [218, 240], whereas, the quantity of BTX-A injected presently equal approximately 0.32U/kg. (2) A single injection was made to the mid-belly of the target muscle instead of using multiple injection points [216, 252]. (3) Electrical stimulation guidance is often used in injection of BTX-A in the clinical practices [253-254], whereas such guidance was not used presently.

Although the first issue suggests that in a direct comparison, the present dose is much smaller than typical clinically used doses, substantial muscle force reductions were shown indicating that it was quite effective in the rat muscles studied. We used histological assessment to show existence of paralyzed muscle parts, which sustains the above judgment. Shaari and Sanders [66] showed with more detailed histological assessments that for the rat TA muscle, an increase of 10-25 fold of the dose (0.2U to 2.0U for 10 μ l and 0.2U to 5.0U for 25 μ l) was needed to double the area of paralysis. However, at constant dose, they showed that it takes much more (100 fold) increase in volume to achieve similar increase in the area of paralysis. These findings suggest that the volume injected is also a key determinant however it is relatively less important in determining the effects of BTX-A compared to the dose. On the other hand, although it is in the same order of magnitude with what was used by Shaari and Sanders [66],

also the present volume injected (approximately 64 μ l/kg) appears very low in a direct comparison with volumes used in lower limb muscles (2.5-8ml/kg) of children with cerebral palsy [227, 240]. Other examples of dose and dilution volume values per kg of the different animals tested include 8.3U-0.83ml in the mouse [255], 3.5U-0.23ml in the cat [71], 1 to 10U-0.04ml in the rabbit [219]. Therefore, there is considerable variability among the injection protocols used in different species as well. The points discussed here imply that an explicit relationship between animal studies and clinical practice cannot be easily built. This is a general limitation and hence a limitation of the present study as well. We suggest that new specific studies are necessary to bridge the doses used in clinical and fundamental studies and a consideration of muscle size and body mass is necessary in order to achieve a useful scaling of BTX-A doses and volumes injected.

With regard to the second issue, a single injection as done presently has a higher potential of saturating the local binding sites within the injected muscle and facilitating spread of BTX-A to neighboring structures [216]. Therefore, the present injection protocol may have promoted toxin leakage to the adjacent EDL and EHL muscles. Note however that the spread of BTX-A beyond the injection site was shown to occur also after multiple injections [70]. Such spread is considered as a side effect [216, 256-257] and hence it presents a challenge to control of the effects of the treatment. On the other hand, studies with conclusions not in concert with these points were also reported. Frasson et al. [240] showed recently that in children with hemiplegic CP, BTX-A spreads from foot flexors to even antagonistic extensors. These authors argue that such spread may be responsible in part for improving gait of the patients. Although in animal studies effects of possible BTX-A spread were shown among synergistic muscles [71, 239], Misiaszek and Pearson [250] showed in the cat that injection of BTX to lateral gastrocnemius, soleus and plantaris muscles causes their EMG activity to decrease whereas, that of the non-injected medial gastrocnemius increases. These authors suggested that the non-injected muscle remains quite active and functional and it compensates for the paralysis in the other muscles. Remarkably, the dose of BTX-A injected was as high as 20 to 80U per muscle. This challenges the common clinical expectation that BTX-A may diffuse to adjacent muscles. Despite the fact that asso-

ciation of increased EMG signals with increased activity in the medial gastrocnemius is a tenable one, no data directly showing absence of reduced force of this muscle is available. These points indicate that spread of BTX-A to neighboring structures is a complex and important issue. Therefore, its effects deserve to be understood well. Our study helps improving such understanding in terms of muscular mechanics. However, the mechanism of how such spread occurs remains unknown. Evidence was shown for local diffusion [70] to cause such spread. Effects of BTX-A injection were detected even in the contralateral limb [258] suggesting that vascular diffusion is also likely. Presently, both mechanisms may have played a role. In order to distinguish those, new specific studies should be performed. Another limitation is that effects of possible spread to antagonistic muscles are not assessed. This could be studied by extending our experimental procedures.

Regarding the third issue, electrical stimulation guidance for BTX-A injection was shown to improve the localization for deep-seated muscles [254]. Also, if the target muscles are very small or adjacent to muscle groups that have similar functions [253, 259], it is suggested for enhancing accuracy and specificity. On the other hand, such guidance was shown not to be superior to the manual placement method using anatomical landmarks and palpation for a superficial muscle such as gastrocnemius muscle [260]. We studied presently effects of an injection to the TA muscle on force-length characteristics of its bi-articular synergistic EDL muscle. It was not difficult to locate the superficial TA using palpation and care was taken to standardize the injection location and depth. However, if a deeper lying muscle is to be tested after being injected, electrical stimulation guidance may improve specificity considerably.

In the light of the discussion above, new studies are indicated to test for the role of different injection protocols at and beyond the injection site. Animal models are good approaches to improve our understanding of fundamental phenomena regarding the effects of BTX-A on muscular mechanics because of their controlled nature of testing. Studying the effects directly on muscle forces and for a wide range of muscle lengths may facilitate an improved understanding. The present findings obtained employing such an approach confirm our hypothesis and show that data measured from the bi-articular

EDL's tendon relocated to impose muscle length changes include decreased active forces (muscle length dependent for the proximal lengthening condition) accompanied by a narrower range both proximally and distally. Moreover, EDL passive forces were higher in the BTX group. These findings include new viewpoints for a muscle affected by BTX-A, with potentially important implications addressed in the subsequent paragraphs. However, as discussed above the animal experiments do not directly represent a typical scenario for human treatment.

An important finding, which to our knowledge has not been reported before is that BTX-A administration causes a decrease in the range of a muscle affected. Recent experimental [239] and model data [212] imply that BTX-A causes sarcomeres of the affected muscle to shift to longer lengths. The muscle is paralyzed partially and on excitation, the paralyzed muscle fibers do not shorten as they would do in a BTX-A free muscle. Due to that, the less stiff muscle can take up a greater portion the muscle-tendon complex length. Moreover, interaction of muscle fibers with the extracellular matrix (ECM) [28, 111, 162] can limit sarcomere shortening in the activated muscle fibers. Modeling shows that this effect becomes more pronounced with increasing stiffness of the ECM and hence it becomes increasingly important with increasing muscle length [212]. In contrast, at very low muscle lengths it is not effectual. Occurrence of such "longer sarcomere effect" can cause the muscle's optimum length to shift to a lower length, which can be responsible for narrowing of range shown presently. Another tenable explanation is shifting of the muscle's active slack length to a higher length. Note that since the BTX and control data were obtained from separate groups of animals, a comparison of only the l_{range} can be done and it is not possible to distinguish if the shifting of one of the characteristic muscle lengths dominates the other. Therefore, we will consider the potential effects of both shifts in addressing the clinical implications of narrowing of the l_{range} in the successive paragraph. On the other hand, the data also show that length dependency of the force reductions is a possibility. This finding sustains the previous results that more pronounced active force reductions are likely at lower muscle lengths [71, 239] or at joint angles that may correspond to short muscle lengths [202].

Muscle hypertonicity in spasticity [29-30, 40] causes the joint to be forcefully kept in typically a flexed position in which the muscle is expected to be short. Shifting of the muscle's active slack length to a higher length and the possible occurrence of more pronounced active force reductions at lower muscle lengths may mean that a more pronounced muscle weakening is available for shorter muscle lengths. This implies that after exposure to BTX-A, contribution of an affected muscle to the joint moment in flexed joint positions is compromised more, which may be a preferable effect. On the other hand, spasticity typically causes the joint range of motion to be compromised [39-40, 261-262]. lrange is considered as an indicator of movement capability with active force exertion of a muscle within the potential range of motion of a certain joint. Compromised lrange indicates that the muscle may exert active force for a smaller portion of such joint range i.e., the joint movement may be limited before being limited by ligaments or bony constraints. Our present results show that after exposure to BTX-A, occurrence of such compromised contribution of an affected muscle to joint movement is also likely. It should be noted that we don't know whether the lrange determined experimentally is fully functional in vivo. Although this may be unlikely, narrowing of the lrange does not seem to agree well with an intention of improving joint range of motion. Therefore, it may be regarded as an inferior effect.

It has been argued that in spasticity, muscle weakness itself is a primary source of the functional problem [32, 52, 154, 244, 263] and that BTX-A treatment involves a paradox of weakening the muscle to achieve better functionality [244]. Excessive muscle weakening has been reported as an adverse effect [216, 231, 257, 264-266]. Awareness of potential effects of BTX-A on muscle lrange in addition to a variable force reduction for different muscle lengths may be important for a good clinical judgment which was indicated as necessary [e.g., 244] to control the produced weakness. A situation occurring frequently is that spasticity affects both distal and proximal joints [224]. The present findings indicate that that the effects shown are conceivable for both joints a bi-articular affected muscle spans. This may have clinically relevant implications, which need to be tested in new studies. For example, in combined equinus and crouch gait, contributions of m. gastrocnemius to both plantar flexion and knee flexion moments may decrease. This appears to agree with the intended improvement

in gait. However, for combined crouch and hip flexor tightness, reduced contributions of e.g., semimembranosus to hip extension moment may deteriorate conditions at the proximal joint. A decreased l_{range} on the other hand, does not appear to be a favorable effect for neither of such conditions. It should be noted that whether direct injection of BTX-A into a bi-articular muscle or its diffusion from an injected muscle to such muscle leads to the same effects remains unknown. Therefore, our results may be representative of conditions in which such a muscle may be affected through leakage of BTX-A only. It should also be noted that in the present conditions, asymmetry of effects of proximal or distal length changes on muscle force-length characteristics remain limited. Additionally, effects of BTX-A on the TA and EHL muscles were not affected from changing EDL length. This shows in contrast to our previous animal experiments performed in BTX-A free conditions [e.g., 25, 107] that mechanical interaction of muscle with its surrounding muscular and non-muscular tissues plays a smaller role. Certain effects of such epimuscular myofascial force transmission mechanism were reported in our previous experimental study also after exposure to BTX-A but they were less pronounced compared to those shown for the control group of animals [239]. This may be due to the presence of paralyzed parts within the muscles of the compartment i.e., due to reduced active force production as our results show that passive forces can increase. The exact mechanical mechanism is not immediately apparent and needs to be studied e.g., using muscle modeling [e.g., 25]. However, if partial muscle paralysis is responsible for this effect, epimuscular myofascial force transmission is plausible to affect muscular mechanics in long term after the discontinuation of BTX-A treatment.

The present results show that BTX-A changes the passive properties of the muscular tissues as well. The slope of EDL passive force-length curves of the BTX-A group was higher than that of the control group (e.g., for Δl_{ma} EDL proximal ≥ 1 mm by approximately 9 folds). This is a positive indicator of increased stiffness of muscular connective tissues after exposure to BTX-A. Increased passive forces suggest more specifically that stiffness of the ECM may have increased. Such elevated ECM stiffness was reported recently for isolated rat muscle fiber bundles after BTX-A injection [267]. Increased intramuscular connective tissue content shown for the BTX group may explain this. Note that our histological assessment confirms an increased

proportion of the ECM rather than a net increase of the ECM. Denervation leads to atrophy of rat muscles within the first week [220]. Also BTX-A was reported to cause atrophy [221-222]. Similarly our results indicate occurrence of atrophy as muscle mass normalized to body mass was shown to decrease. Biliante et al. [68] showed that such atrophy involves decreased muscle fiber diameters as well as density. Therefore, a net increase of the ECM is tenable.

However, ruling out the possibility that the muscle's epimuscular connections may have also become stiffer is not possible. One reason for this is that increased passive forces were shown not only at higher muscle lengths at which the ECM is stretched, but also at lower. Passive distal EDL forces measured after distal lengthening were higher after BTX-A administration for all muscle lengths including short ones. Moreover, the increased passive forces of the TA and EHL muscles were measured at lower lengths at which they were restrained. These results indicate occurrence of an increased stiffness of also the epimuscular connections, which should be tested specifically.

The possibility that BTX-A causes an increase in the stiffness of muscular connective tissues does not seem to be in concert with the intended reduction of passive resistance of spastic muscle at the joint [232, 246, 256, 268-269]. It should be noted that the clinical finding that BTX-A causing decreased passive resistance to stretch [232, 270-271] is mainly ascribable to decreased hypertonicity of the spastic muscle i.e., a reduced spasticity [272]. Even in non-spastic mouse muscle, large doses of BTX-A were shown to cause reduced tone and disrupted stretch reflex, leading to decreased passive resistance during stretching [273]. The present experiments were conducted also on normal muscles however, the measurements do not include a passive stretching with movement as used in the evaluation of spasticity, and no reflex loop was active. Therefore, a modulation of muscle tone is not a part of our findings, and the present increase in muscle passive force reflects enhanced muscular tissue stiffness. The term "stiffness" is used interchangeably with "passive resistance to stretch" [272, 274]. We consider that the latter involves the former, which characterizes mechanical resistance of non-contractile muscular structures to increased length. Based on the present and previous findings, we suggest the following. Decreased passive resistance to stretch af-

ter BTX-A injection is a net effect of decreased hypertonicity and may be compromised by increased tissue stiffness. On the other hand, the present findings were obtained only five days after BTX-A injection. However, similar effects on passive mechanical properties shown by Thacker et al. [267] were obtained 1 month after, suggesting their continuation in time. These authors argued that the effects of BTX-A on normal muscle and on spastic muscle may be different. Recently, we have shown that human spastic Gracilis muscle tested intra-operatively shows no abnormal mechanics [143]. However, passive muscle force was not available together with data from healthy subjects. Given the lack of data allowing for a direct comparison, also Thacker et al.'s suggestion may explain the difference between findings obtained from conditions in health and spasticity. Nevertheless, we believe whether BTX-A causes increased muscular connective tissue stiffness also in spasticity may be an important question that needs to be addressed in new specific studies. BTX-A injections are usually combined with additional techniques such as strengthening exercises [275-276], exercises performed to improve joint range of motion [277] as well as stretching and splinting [278-279]. The functional benefit expected by using BTX-A may depend largely on these techniques and our findings may be relevant for them.

In conclusion, our results indicate that the effects of BTX-A on muscular mechanics are more complex than just weakening of the affected muscle characterized by a reduction in its active force. They also include a potential length dependency of reduction of the active force and narrowing of the muscle's length range of active force exertion. Moreover, not only the active properties but also the passive properties may change featuring increased passive muscle forces. Therefore, BTX-A may lead to compromised joint movement due to both a narrower active movement range and an increased passive resistance. Spread of BTX-A to a bi-articular muscle may cause both joints the muscle spans to be affected. Such effects may be clinically relevant because, as some are additional to the intended ones, others may even be unintended.

8. GENERAL DISCUSSION AND CONCLUSIONS

In this thesis, the effects of spastic cerebral palsy on muscle mechanics were investigated with human experiments and the effects of botulinum toxin administration as a conservative therapy applied to spastic muscles, and aponeurotomy (AT) as a surgical method to correct impaired joint function were investigated with animal experiments. Myofascial force transmission was addressed as a key concept both to understand the etiology of the disease and treatment methods widely used.

8.1 Mechanics of Human Spastic Muscles, Limitations, and Future Directions

The knowledge on the mechanics of human muscles is very important for understanding locomotion in health and also in disease. Most of the information gained from the studies on muscle architecture by investigating cadavers [87] or by using modeling [89] or imaging methods such as ultrasound [49-50] and magnetic resonance imaging [51-53] did not give direct data on force production capacity of muscles. Other indirect approaches used dynamometry [90] or torque measurements [88-89] were targeted the joints. However, there has been a lack of information on relating the force production capacity of specific muscles and the joint angle which is associated with functional joint problems. One of our studies presented in chapter 2 [120] showed a capability to close such gap for human GRA muscle with a novel intra-operative force measurement method developed.

Healthy GRA muscle isometric forces with respect to knee angle measured showed substantial inter-subject variability: the values of muscle forces, stress over tendons, and the knee angle where the maximum force generated were differential for the subjects. This study suggested that typical subject anthropometrics cannot be used as predictors due to these experimentally obtained data not being correlated with subject anthropometrics. It was also shown for the first time that GRA muscle in

health has very large operational length range at least it spans 120° of knee flexion to full knee extension. This is consistent with its architectural features with long fibers [134] and large excursion [98].

Additionally, this study [120] showed the occurrence of history effects at first time for healthy human muscles. History effects defined as force changes at lower muscle lengths due to muscle activity at high lengths should be taken into consideration if consecutive measurements are performed since they interfere with the results. In the Appendix-A, to ensure such measurements, a certain preconditioning method was suggested. In chapter 5, this method was used in the animal experiments since consecutive measurements were performed: We tested the effects of aponeurotomy (AT) following force-length data collections in the intact condition and after preparatory dissections (PD)). On the other hand, for the human experiments presented at chapter 2-4, and also for the animal experiments using different groups of animals to compare the applied conditions such as BTX-A (presented at chapter 6 and 7) no isometric force measurements were performed subsequent to activity at high length. Therefore, preconditioning was not needed. It should be noted that if similar experiments including consecutive data collection are planned in human, muscles should also be preconditioned by activating at high and low lengths until the same amount of isometric force was measured at low lengths.

In spastic cerebral palsy, treatments are mostly applied to particular muscles or muscle groups such as administration of BTX-A or lengthening surgery performed on knee flexors to correct crouch gait or on gastrocnemius or Achilles tendon to correct equines deformity. However, the contributions of the specific muscles on the joints they span are not well known. One of our present intra-operative studies on CP patients [143] revealed the contribution of spastic GRA muscle on knee joint. The main outcome of this study was that the spastic GRA muscle did show no abnormal characteristics. Even muscles were diagnosed with spasticity, (i) GRA did not have a narrow joint range of force exertion and (ii) at low length, higher forces presumably causing knee joint to stay in flexed position were not available. In the experiments, although most of the neighboring structures were intact, the synergistic or antagonistic mus-

cles were not activated. Considering the experimental conditions including exclusive stimulation of GRA, the possibility of Dr. Huijing's hypothesis [62] to be valid was suggested: The source of high forces observed in the flexed joint positions should be due to activation of antagonistic muscles at high lengths. Such approach should include epimuscular myofascial force transmission mechanism to be held between antagonists [107, 170]. We improved that approach and test if spastic GRA characteristics change with simultaneous stimulation of its antagonist vastus medialis (VM) in the context of (i) narrowed joint range and (ii) availability of high force at knee flexion. In this study presented at Chapter 4, operational range of spastic GRA muscle was found to be narrowed and peak GRA forces shifted to more flexed position due to simultaneous activity of VM. Also, comparably higher forces were measured at flexion. This indicates the determinant role of inter-antagonistic force transmission due to stiffened epimuscular pathways.

Our results on human spastic muscles indicated that impeded joint motion is not due to abnormal function of each muscle but simultaneous activation of agonist-antagonists. It should be noted that our data are limited with a single muscle and the effects of activating its antagonist. To understand the knee joint function in spastic CP other muscles crossing the knee should be investigated. It may be critical to discriminate the characteristics of long fibered GRA from that of the short fibered biceps femoris since they are known to differentiate in function, they may also differentially adapt to spasticity. Functional map for all knee flexors and extensors seems to be crucial for also understanding the myofascial pathways which are presently shown to have a major and determinant role. Another important limitation of our intra-operative method is the lack of capability of measuring passive forces since the force transducers work on a principle of torque measurement [94]. Therefore, our results do not reflect passive tissue stiffness presumably high for spastic muscles [57-59].

In conclusion, our results suggesting the key role of inter-antagonistic force transmission should be further investigated with spastic muscle model to reveal such mechanism in detail and also by adding histological examinations to our experimental method improved to measure passive forces.

8.2 Treating Spastic Cerebral Palsy, Limitations, and Future Directions

Animal experimentation facilitates collecting specific information in a more controlled manner even the limitations such as difficulty to reflect the results to the clinics should be considered. Experimental protocols have been highly standardized for numerous animals to study muscle force-length characteristics. However, many protocols included measuring forces at one muscle length or from only one tendon of a bi-articular muscle and assumed that such measurements represent the isometric muscle function. Moreover, treatment methods for neuromuscular disorders are determined according to such approaches neglecting length effects and also not considering myofascial force transmission. Our experimental protocols considering the intactness of most of the epimuscular connections did show that the effects of some treatment methods are not limited with the target muscle. Present studies on animals revealed that EMFT determines not only the etiology but also the treatment methods of spasticity.

8.2.1 Muscle lengthening surgery

Aponeurotomy (AT) i.e. cutting of the aponeurosis transversely aimed at lengthening the contracted muscles. In surgery, it is applied after preparatory dissection (PD) to reach the targeted area. Our experimental procedure mimicking PD and subsequent AT on anterior crural muscles of rat (presented at chapter 5) showed (i) differential effects at proximal and distal tendons of target muscle and (ii) substantial force decrease for the non-operated neighboring muscle. Therefore, EMFT mechanism was suggested to dominate the effects of muscle lengthening surgery. Since these differential and unintended effects on muscle forces may yield additional favorable effects for the targeted joint, but also contrasting effects particularly for the non-targeted joint, we conclude that EMFT should be taken into account to improve the functional outcome of the surgery planned to correct the impeded joint.

The importance of such effects was also shown for other treatment methods

such as tenotomy and tendon transfer surgery. For instance, Kreulen et al. [60] showed for flexor carpi ulnaris muscle that distal tenotomy caused only a minor effect however, subsequent dissection of epimuscular connections of the muscle caused substantial changes in both muscle shortening and activation. Also, previous studies [192, 280-281] showed that e.g. flexor muscle whose tendon was transferred to support extension still produces flexor moment. It was suggested that muscle connected to its origin with epimuscular connections caused such unexpected outcomes. To further investigate the implications of this approach, e.g. tendon splitting surgery or other conservative treatments for musicians arm or repetitive strain injury should be tested with controlled experimental methods like the ones presented in this thesis.

8.2.2 BTX-A Application

It is aimed at reducing muscle spasticity with the injection of BTX-A that inhibits acetylcholine release into the presynaptic cleft in the neuromuscular junction [e.g., 65]. Such treatment on the other hand creates a dilemma with its weakening effect contrary to the need of CP patients to improve joint function. To prevent joint from excessive weakening while reducing spasticity concurrently, it is essential to understand the effects of BTX-A on the whole compartment. BTX-A injection has known to affect the muscles beyond the injection site [70, 72]. However, such effects on the neighboring muscles have not been studied systematically. A novel animal experimental model [239] presented at chapter 6 was developed to investigate acutely the effects of BTX-A on force-length characteristics not only of the injected but also of the non-injected muscles of an entire intact compartment in conditions close to those in vivo. Additional to the major active force reductions due to BTX-A, length dependency of the effects (i.e. correlation between injected muscle's length and the effects of BTX-A) and in contrast, passive force increases were shown. The following study focusing on bi-articular muscle characteristics presented here at Chapter 7 showed (i) the narrowed length range of force exertion that BTX-A caused even acutely and (ii) pronounced passive force increase for all the muscles in the compartment which is in contrast to the general aim of the treatment. Furthermore, the length dependency of the effects

was shown to be not valid for every experimental condition.

These studies focused on the acute effects of BTX-A suggested that to improve the overall function unintended force reductions shown (i) for non-targeted joint due to the differential effects on bi-articular target muscle and also (ii) for neighboring muscle should be taken into account. One of the most important outcomes of this study was to find a passive force increase due to BTX-A injection. Such passive force enhancement was explained with increased and possibly stiffened collagen content in contrast to the atrophy occurs even at fifth day of BTX-A administration. In any condition, passive force increase due to BTX-A shown in our present studies at first time should be considered when determining additional treatments such as physical therapy or strengthening exercises.

On the other hand, our studies showed that BTX-A caused a prominent reduction in proximo-distal force differences which are direct measures of myofascial loads. Such disappearing of EMFT may be an important part of the BTX-A treatment mechanism. If the therapy with this toxin is effective since it diminishes the effects of connections even the amount of ECM increases. Then, such mechanism should further be revealed with new studies investigating how (i) the toxin cause collagen content increase and (ii) epimuscular loads changes in the presence of other muscles than the targeted. Experimental and modeling methods should both be used for that. Moreover, the changes in passive force, interaction of muscles, and accordingly the amount of collagen are needed to be examined in long term.

Appendix A. PRECONDITIONING REMOVES LENGTH HISTORY EFFECTS AND ENSURES SUCCESSIVE FORCE-LENGTH MEASUREMENTS

A.1 Introduction

Previous activity at high (over optimum) muscle lengths affects muscular mechanics at lower lengths [15] causing typically a reduction in the force measured at the same low length again. Such length history effects were shown to occur for tibialis anterior [170], deep flexors [107], and extensor digitorum longus (EDL) [15, 282] muscles of the rat, a commonly used species for an animal muscle mechanics model. However, sizable length history effects were also reported for human gracilis muscle [120] suggesting that they are not restricted to the rat.

Testing the effects of different conditions with successive measurements of muscle force-length (FL) characteristics is an important and common practice [24, 27, 92, 283-284] for muscle mechanics experimentation. In order to isolate the role of the condition tested, length history effects need to be removed. A method proposed for that purpose was preconditioning of the muscle to be lengthened [20]: subsequent isometric contractions at high and low lengths to be performed prior to the experiment until the force reduction at low length vanishes. These alternating contractions were reported to eliminate length history effects for a set of FL data [20, 62, 174, 285-286]. However; the outcome of such preconditioning for successive FL measurements is not known. The goal of this study was to test if such preconditioning is a safe method for three consecutive FL measurements for both lengthened and restrained muscles.

A.2 Methods

A.2.1 Surgical procedures

Surgical and experimental procedures were approved by the Committee on Ethics of Animal Experimentation at the Boğaziçi University.

Male Wistar rats ($n=8$, mean body mass 325.5 ± 13.7 g) were anaesthetized using intraperitoneally injected urethane solution (1.2 ml of 12.5% urethane solution/100 g body mass). Additional doses were given if necessary (maximally 0.5 ml). Immediately following experiments, animals were sacrificed by using an overdose of urethane solution. After surgery needed to expose EDL, tibialis anterior (TA) and extensor hallicus longus (EHL) muscles (Figure A1 a) the rat was mounted in the experimental setup (Figure A1 b).

A.2.2 Experimental conditions and procedure

All muscles studied were activated maximally by stimulation of the sciatic nerve (Biopac Systems stimulator, STMISOC) with a constant current of 2mA (0.1ms pulse width, 100 Hz). After setting EDL to a target length, two twitches were evoked, 500 ms after the second twitch, the muscles were tetanized and 400 ms subsequently, another twitch was evoked. During the tetanic plateau, muscle total forces were measured and averaged at an interval of 150 ms subsequent to 25 ms after evoking tetanic stimulation. After each application of this stimulation protocol, the muscles were allowed to recover at low muscle length, for 2 minutes.

Isometric forces were measured simultaneously from EDL proximal and TA+EHL distal tendons (kept at their reference position at all times during the experiment) and from the distal tendon of EDL which was repositioned (in 1 mm steps until 2 mm over distal optimum length, starting at active slack length) to quantify FL characteristics.

Subsequent to a full measurement of each FL data, control contractions (CC) were performed at EDL reference low length (l_{ref} , i.e., 3 mm over distal active slack length) in order to determine the effects of previous activity at high length (over optimum length) on forces exerted by the experimental muscles at lower lengths.

Preconditioning Isometric forces at low (l_{ref}) and high ($l_{opt}+2$) lengths of EDL muscle distally were measured sequentially until the force difference between successively measured forces at identical lengths were less than 3%. Each experiment involved collection of a complete set of FL data and subsequent control measurements. The first experiment (FL-1 and CC-1) was performed without any preconditioning. Therefore, the data was prone to length history effects. Prior to the subsequent three experiments (FL -2 to 4 and CC-2 to 4) however, a preconditioning was performed. Therefore, it was tested (i) if such preconditioning does remove length history effects acutely and (ii) if its effects are reliable for subsequent two experiments.

A.2.3 Processing of data and statistics

Data for muscle total forces (F) in relation to muscle-tendon complex length (l_{mt}) were fitted with a polynomial function using a least squares criterion

$$y = b_0 + b_1x + b_2x^2 + \dots + b_nx^n \quad (1)$$

where y represents F and x represents l_{mt} . $b_0, b_1 \dots b_n$ are coefficients determined in the fitting process. Polynomials that best described the experimental data were selected by using one-way analysis of variance (ANOVA) [125]: the lowest order of the polynomials that still added a significant improvement to the description of changes of muscle-tendon complex length and muscle force data were selected. These functions were used for determining mean forces, standard errors (SE), and EDL optimum length distally. One-way ANOVA was used to test for the history effects within each experiment: differences between EDL forces exerted at l_{ref} (i) during collection of FL data and (ii) after CC were considered significant at $p < 0.05$.

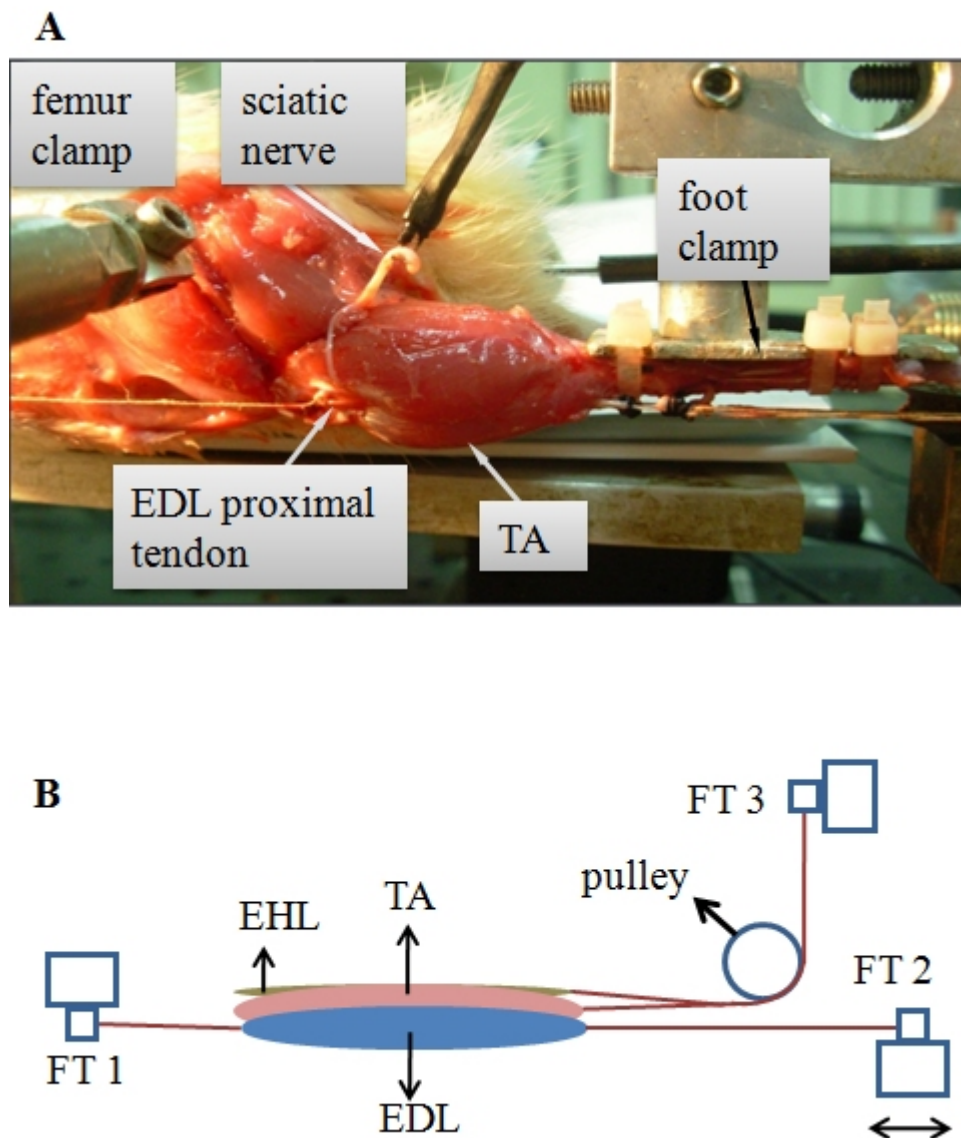


Figure A.1 The experimental set-up. (a) Distal tendon of the tibialis anterior muscle (TA) with the distal tendon of extensor hallucis longus muscle (EHL) was tied to a force transducer (FT). Proximal and the tied distal tendons of the EDL were each connected to a separate FT. Experimental condition for joint angles: knee angle = 120° and the ankle is at maximal plantar flexion. The femur and the foot were fixed by metal clamps and the distal end of the sciatic nerve was placed on a bipolar silver electrode. (b) Schematic representation of distal lengthening condition. Throughout the experiment, the TA+ EHL (tied to FT3) and EDL proximal (tied to FT1) tendons were kept at constant lengths. FT2 tied to EDL distal tendon was exclusively lengthened to progressively increasing lengths, at which isometric contractions were performed. Lengthening (indicated by double arrow) started from muscle active slack length at 1 mm increments by changing the position of the FT2.

Two-way ANOVA for repeated measures (factors: EDL muscle-tendon complex length (lmt) and experiment) was performed to test for the effects of preconditioning across experiments on EDL muscle distal and proximal FL characteristics and TA+EHL distal forces. Bonferroni post-hoc tests were performed to further locate significant differences.

A.3 Results

A.3.1 EDL

For experiment 1 and for both proximal and distal EDL forces, ANOVA showed significant differences (drops of 48.0% and 33.4%, respectively) between forces measured at l_{ref} during collection of FL data and after CC. In contrast, after preconditioning no such significant force differences were shown indicating that preconditioning can remove length history effects occurring at lower muscle lengths within three successive experiments.

Both distally and proximally, ANOVA (factors EDL lmt and experiment) showed significant main effects, but no significant interaction. Significant effects were located only between experiment 1 and 2 (post-hoc test) indicating that preconditioning removes length history effects also across experiments. Lack of a significant interaction indicates that effects are similar for FL data at four experiments for all length range spanned. On the other hand, if EDL forces collected during experiment 1 to 4 are tested for each EDL length (one-way ANOVA), significant effects of the experiment were shown only for a few lengths around l_{ref} distally (Figure A.2a) and proximally (Figure A.2b). The same test showed no significant effects of experiments at any length if FL -1 was excluded. Therefore, these analyses indicate that length history effects are limited to lower muscle lengths and disappear after preconditioning.

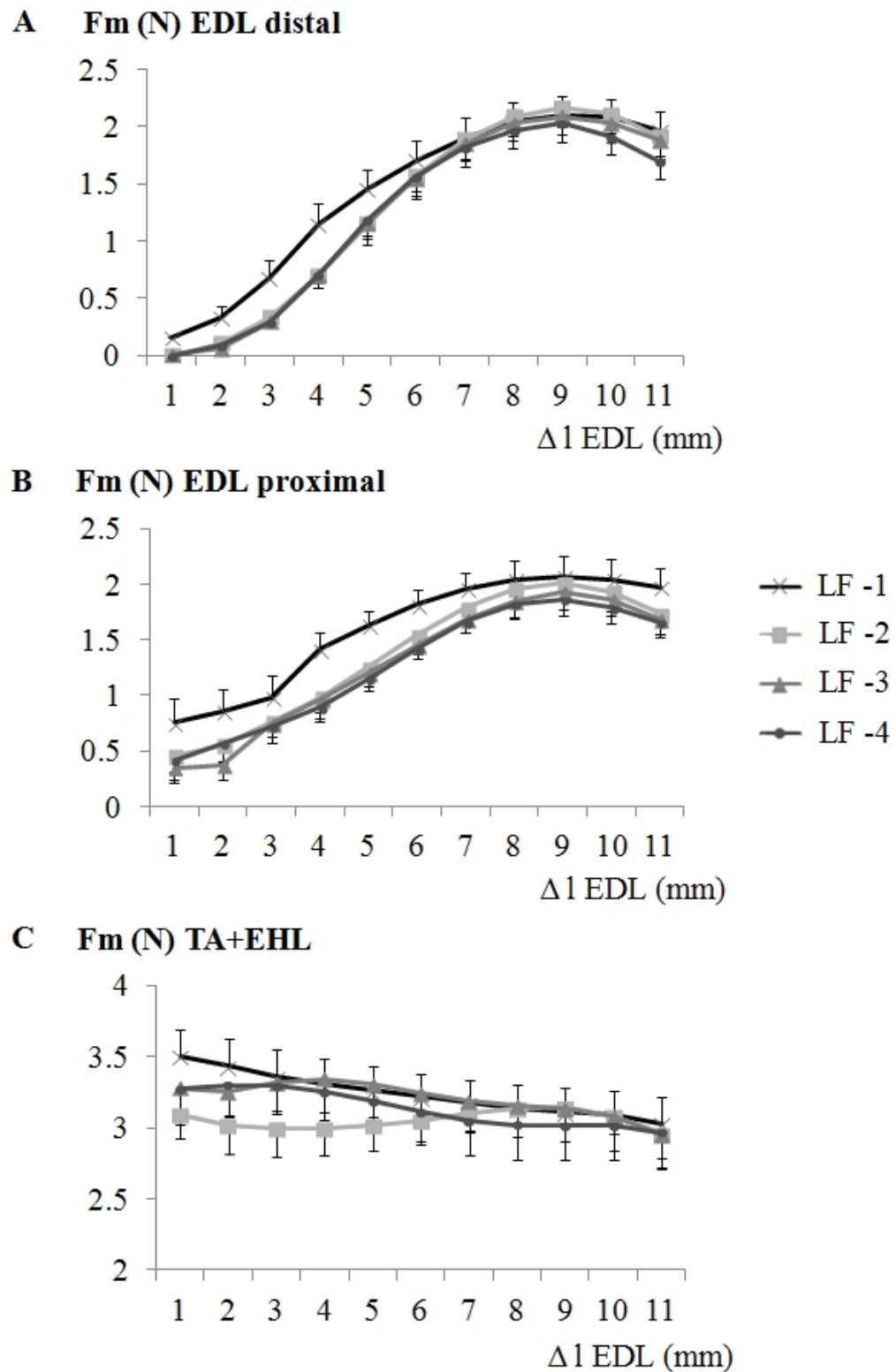


Figure A.2 Force-length characteristics of (a) EDL distal, (b) EDL proximal, and (c) TA+EHL muscles obtained after distal lengthening. Total isometric forces are shown as mean values \pm SD for FL1, FL2, FL3, and FL4 conditions. Muscle-tendon complex length is expressed as a deviation from EDL optimum length (Δl EDL=10mm) at FL1.

A.3.2 TA+EHL

ANOVA showed no significant differences between forces measured at l_{ref} during collection of FL data and after CC within each experiment. Therefore, TA+EHL forces are not affected by previous activity of its synergistic muscle at high length.

On the other hand, ANOVA (factors EDL lmt and experiment) showed only a significant effect of experiment thus neither significant effects of EDL length nor a significant interaction. Significant effects were located only between experiment 1 and 2 (post-hoc test). These findings of analyses performed across experiments indicate that preconditioning of EDL muscle does affect the forces of TA+EHL similarly for all EDL lengths and it also stabilizes forces of TA+EHL for three successive experiments performed subsequently.

A.4 Discussion

The size of length history effects characterized by force depression particularly at low muscle lengths following the activity at high lengths [15] was suggested to be determined by CC at low reference length [62]. In previous studies [107, 170, 282], differences between the force measured during FL data collection and CC at identical low length were used to quantify such effects. Our present results showing length history effects for EDL before preconditioning confirm previous findings. Also, significant effects across experiments shown for low lengths around l_{ref} indicate that control measurements (in our case 3 mm over active slack length) performed after collecting a set of FL data do reflect the effects of previous activity and confirm that quantifying method used.

Mechanism of length history effects is not exactly apparent; however, viscoelastic properties of muscle and fascial tissues presumably having major role suggest that considering the experimental protocols particularly include lengthening, there is potential for systematic changes that may interfere with the results. With the intention of

collecting reproducible data, preconditioning of viscoelastic materials known to minimize variability is performed [287-289]. Loading and unloading is a widely used method for various biological tissues such as tendon [290], ligament [291], spinal cord [292], or skin [293]. With same principle, by applying stretch and release on passive muscle fibers of rat soleus with constant velocity were shown to stabilize sarcomere lengths and forces after third cycle [294]. Basic warm-up and stretching exercises performed mostly to prevent damage [295-296] also aimed to precondition muscles isometrically. In our case, EDL was preconditioned by isometric contractions at high and low muscle lengths to principally mimic the following FL data collection. Such preconditioning tested systematically at our present study for the first time is shown to serve the purpose of generating the same amount of force with non-significant deviation at the same length for identical conditions.

Additionally, our present study showed history effects for the restrained muscles before preconditioning. Such effects may be ascribed to previously stretched inter- and extramuscular connections with muscle lengthening. Thus, it suggests the substantial role of connective tissue on history effects. Our previous results indicating the importance of both intermuscular connections and compartmental fascia are consistent with present results: compartmental fasciotomy and subsequently dissecting the intermuscular connections of anterior crural muscles of rat caused history effects to decrease [231]. Therefore, passive tissues having a partial role on history effects should be considered for preconditioning.

In conclusion, our present study showed that preconditioning removes history effects and ensures at least three consecutive force-length measurements for both lengthened and restrained muscles. History effects limited with lower muscle lengths are dependent on the activity of muscle at high lengths since major force reductions before preconditioning were shown for the lengthened muscle. On the other hand, minor but significant effects shown for the restrained muscles due to being adjacent to the lengthened muscle with stretched fascial connections during lengthening preconditioning was also shown to stabilize the neighboring restrained muscles.

REFERENCES

1. Lieber, R.L., "Skeletal muscle architecture: implications for muscle function and surgical tendon transfer," *J Hand Ther*, Vol. 6, p. 105-13, 1993.
2. Huijing, P.A., "Muscle, the motor of movement: properties in function, experiment and modelling," *J Electromyogr Kinesiol*, Vol. 8, p. 61-77, 1998.
3. Maganaris, C.N., V. Baltzopoulos, and A.J. Sargeant, "In vivo measurements of the triceps surae complex architecture in man: implications for muscle function," *J Physiol*, Vol. 512 (Pt 2), p. 603-14, 1998.
4. Narici, M.V., L. Landoni, and A.E. Minetti, "Assessment of human knee extensor muscles stress from in vivo physiological cross-sectional area and strength measurements," *Eur J Appl Physiol Occup Physiol*, Vol. 65, p. 438-44, 1992.
5. Willems, M.E. and P.A. Huijing, "Heterogeneity of mean sarcomere length in different fibres: effects on length range of active force production in rat muscle," *Eur J Appl Physiol Occup Physiol*, Vol. 68, p. 489-96, 1994.
6. Fukunaga, T., et al., "Muscle architecture and function in humans," *J Biomech*, Vol. 30, p. 457-63, 1997.
7. Gans, C. and A.S. Gaunt, "Muscle architecture in relation to function," *J Biomech*, Vol. 24 Suppl 1, p. 53-65, 1991.
8. Gans, C. and W.J. Bock, "The functional significance of muscle architecture--a theoretical analysis," *Ergeb Anat Entwicklungsgesch*, Vol. 38, p. 115-42, 1965.
9. Narici, M.V., et al., "In vivo human gastrocnemius architecture with changing joint angle at rest and during graded isometric contraction," *J Physiol*, Vol. 496 (Pt 1), p. 287-97, 1996.
10. Kawakami, Y., et al., "Specific tension of elbow flexor and extensor muscles based on magnetic resonance imaging," *Eur J Appl Physiol Occup Physiol*, Vol. 68, p. 139-47, 1994.
11. Rutherford, O.M. and D.A. Jones, "Measurement of fibre pennation using ultrasound in the human quadriceps in vivo," *Eur J Appl Physiol Occup Physiol*, Vol. 65, p. 433-7, 1992.
12. Tidball, J.G., "Force transmission across muscle cell membranes," *J Biomech*, Vol. 24 Suppl 1, p. 43-52, 1991.
13. Patel, T.J. and R.L. Lieber, "Force transmission in skeletal muscle: from actomyosin to external

- tendons," *Exerc Sport Sci Rev*, Vol. 25, p. 321-63, 1997.
14. Pardo, J.V., J.D. Siliciano, and S.W. Craig, "A vinculin-containing cortical lattice in skeletal muscle: transverse lattice elements ("costameres") mark sites of attachment between myofibrils and sarcolemma," *Proc Natl Acad Sci U S A*, Vol. 80, p. 1008-12, 1983.
 15. Huijing, P.A. and G.C. Baan, "Extramuscular myofascial force transmission within the rat anterior tibial compartment: proximo-distal differences in muscle force," *Acta Physiol Scand*, Vol. 173, p. 297-311, 2001.
 16. Huijing, P.A., "Muscular force transmission necessitates a multilevel integrative approach to the analysis of function of skeletal muscle," *Exerc Sport Sci Rev*, Vol. 31, p. 167-75, 2003.
 17. Huijing, P., "Muscular force transmission: a unified, dual or multiple system? A review and some explorative experimental results," *Arch Physiol Biochem*, Vol. 107, p. 292-311, 1999.
 18. Nishimura, T., A. Hattori, and K. Takahashi, "Ultrastructure of the intramuscular connective tissue in bovine skeletal muscle. A demonstration using the cell-maceration/scanning electron microscope method," *Acta Anat (Basel)*, Vol. 151, p. 250-7, 1994.
 19. Huijing, P.A. and G.C. Baan, "Myofascial force transmission causes interaction between adjacent muscles and connective tissue: effects of blunt dissection and compartmental fasciotomy on length force characteristics of rat extensor digitorum longus muscle," *Arch Physiol Biochem*, Vol. 109, p. 97-109, 2001.
 20. Huijing, P.A., H. Maas, and G.C. Baan, "Compartmental fasciotomy and isolating a muscle from neighboring muscles interfere with myofascial force transmission within the rat anterior crural compartment," *J Morphol*, Vol. 256, p. 306-21, 2003.
 21. Huijing, P.A., et al., "Extramuscular myofascial force transmission also occurs between synergistic muscles and antagonistic muscles," *J Electromyogr Kinesiol*, Vol. 17, p. 680-9, 2007.
 22. Yucesoy, C.A., et al., "Extramuscular myofascial force transmission: experiments and finite element modeling," *Arch Physiol Biochem*, Vol. 111, p. 377-88, 2003.
 23. Yucesoy, C.A., et al., "Pre-strained epimuscular connections cause muscular myofascial force transmission to affect properties of synergistic EHL and EDL muscles of the rat," *J Biomech Eng*, Vol. 127, p. 819-28, 2005.
 24. Maas, H., H.J. Meijer, and P.A. Huijing, "Intermuscular interaction between synergists in rat

- originates from both intermuscular and extramuscular myofascial force transmission," *Cells Tissues Organs*, Vol. 181, p. 38-50, 2005.
25. Yucesoy, C.A., et al., "Effects of inter- and extramuscular myofascial force transmission on adjacent synergistic muscles: assessment by experiments and finite-element modeling," *J Biomech*, Vol. 36, p. 1797-811, 2003.
 26. Maas, H., G.C. Baan, and P.A. Huijing, "Muscle force is determined also by muscle relative position: isolated effects," *J Biomech*, Vol. 37, p. 99-110, 2004.
 27. Maas, H., et al., "The relative position of EDL muscle affects the length of sarcomeres within muscle fibers: experimental results and finite-element modeling," *J Biomech Eng*, Vol. 125, p. 745-53, 2003.
 28. Yucesoy, C.A., et al., "Three-dimensional finite element modeling of skeletal muscle using a two-domain approach: linked fiber-matrix mesh model," *J Biomech*, Vol. 35, p. 1253-62, 2002.
 29. Brown, J.K., et al., "Neurophysiology of lower-limb function in hemiplegic children," *Dev Med Child Neurol*, Vol. 33, p. 1037-47, 1991.
 30. Mirbagheri, M.M., et al., "Intrinsic and reflex stiffness in normal and spastic, spinal cord injured subjects," *Exp Brain Res*, Vol. 141, p. 446-59, 2001.
 31. O'Dwyer, N.J. and L. Ada, "Reflex hyperexcitability and muscle contracture in relation to spastic hypertonia," *Curr Opin Neurol*, Vol. 9, p. 451-5, 1996.
 32. Gracies, J.M., "Pathophysiology of spastic paresis. I: Paresis and soft tissue changes," *Muscle Nerve*, Vol. 31, p. 535-51, 2005.
 33. Katz, R.T. and W.Z. Rymer, "Spastic hypertonia: mechanisms and measurement," *Arch Phys Med Rehabil*, Vol. 70, p. 144-55, 1989.
 34. Gracies, J.M., "Pathophysiology of spastic paresis. II: Emergence of muscle overactivity," *Muscle Nerve*, Vol. 31, p. 552-71, 2005.
 35. Huijing, P.A. and R.T. Jaspers, "Adaptation of muscle size and myofascial force transmission: a review and some new experimental results," *Scand J Med Sci Sports*, Vol. 15, p. 349-80, 2005.
 36. Williams, P.E. and G. Goldspink, "Changes in sarcomere length and physiological properties in immobilized muscle," *J Anat*, Vol. 127, p. 459-68, 1978.
 37. Williams, P.E. and G. Goldspink, "Connective tissue changes in immobilised muscle," *J Anat*, Vol. 138 (Pt 2), p. 343-50, 1984.

38. Tardieu, C., et al., "Muscle hypoextensibility in children with cerebral palsy: I. Clinical and experimental observations," *Arch Phys Med Rehabil*, Vol. 63, p. 97-102, 1982.
39. Botte, M.J., V.L. Nickel, and W.H. Akeson, "Spasticity and contracture. Physiologic aspects of formation," *Clin Orthop Relat Res*, p. 7-18, 1988.
40. O'Dwyer, N.J., L. Ada, and P.D. Neilson, "Spasticity and muscle contracture following stroke," *Brain*, Vol. 119 (Pt 5), p. 1737-49, 1996.
41. Sheean, G., "The pathophysiology of spasticity," *Eur J Neurol*, Vol. 9 Suppl 1, p. 3-9; discussion 53-61, 2002.
42. Farmer, S.E. and M. James, "Contractures in orthopaedic and neurological conditions: a review of causes and treatment," *Disabil Rehabil*, Vol. 23, p. 549-58, 2001.
43. Tedroff, K., et al., "Does loss of spasticity matter? A 10-year follow-up after selective dorsal rhizotomy in cerebral palsy," *Dev Med Child Neurol*, Vol. 53, p. 724-9, 2011.
44. Olsson, M.C., et al., "Fibre type-specific increase in passive muscle tension in spinal cord-injured subjects with spasticity," *J Physiol*, Vol. 577, p. 339-52, 2006.
45. McDowell, B.C., et al., "Passive Range of Motion in a Population-Based Sample of Children with Spastic Cerebral Palsy Who Walk," *Physical & Occupational Therapy in Pediatrics*, Vol. 32, p. 139-150, 2012.
46. Lin, F.M. and M. Sabbahi, "Correlation of spasticity with hyperactive stretch reflexes and motor dysfunction in hemiplegia," *Arch Phys Med Rehabil*, Vol. 80, p. 526-30, 1999.
46. Sheean, G. and J.R. McGuire, "Spastic hypertonia and movement disorders: pathophysiology, clinical presentation, and quantification," *PM R*, Vol. 1, p. 827-33, 2009.
48. Nordmark, E., et al., "Development of lower limb range of motion from early childhood to adolescence in cerebral palsy: a population-based study," *BMC Med*, Vol. 7, p. 65, 2009.
48. Fry, N.R., M. Gough, and A.P. Shortland, "Three-dimensional realisation of muscle morphology and architecture using ultrasound," *Gait Posture*, Vol. 20, p. 177-82, 2004.
50. Malaiya, R., et al., "The morphology of the medial gastrocnemius in typically developing children and children with spastic hemiplegic cerebral palsy," *J Electromyogr Kinesiol*, Vol. 17, p. 657-63, 2007.
51. Oberhofer, K., et al., "Subject-specific modelling of lower limb muscles in children with cerebral palsy," *Clin Biomech (Bristol, Avon)*, Vol. 25, p. 88-94, 2010.

52. Elder, G.C., et al., "Contributing factors to muscle weakness in children with cerebral palsy," *Dev Med Child Neurol*, Vol. 45, p. 542-50, 2003.
53. Lampe, R., et al., "MRT-measurements of muscle volumes of the lower extremities of youths with spastic hemiplegia caused by cerebral palsy," *Brain Dev*, Vol. 28, p. 500-6, 2006.
54. Barber, L., et al., "Medial gastrocnemius muscle volume and fascicle length in children aged 2 to 5 years with cerebral palsy," *Dev Med Child Neurol*, Vol. 53, p. 543-8, 2011.
55. Bandholm, T., et al., "Dorsiflexor muscle-group thickness in children with cerebral palsy: relation to cross-sectional area," *NeuroRehabilitation*, Vol. 24, p. 299-306, 2009.
56. Moreau, N.G., S.A. Teefey, and D.L. Damiano, "In vivo muscle architecture and size of the rectus femoris and vastus lateralis in children and adolescents with cerebral palsy," *Dev Med Child Neurol*, Vol. 51, p. 800-6, 2009.
57. Harlaar, J., et al., "Passive stiffness characteristics of ankle plantar flexors in hemiplegia," *Clin Biomech (Bristol, Avon)*, Vol. 15, p. 261-70, 2000.
58. Sinkjaer, T. and I. Magnussen, "Passive, intrinsic and reflex-mediated stiffness in the ankle extensors of hemiparetic patients," *Brain*, Vol. 117 (Pt 2), p. 355-63, 1994.
59. Smith, L.R., et al., "Hamstring contractures in children with spastic cerebral palsy result from a stiffer extracellular matrix and increased in vivo sarcomere length," *J Physiol*, Vol. 589, p. 2625-39, 2011.
60. Kreulen, M., et al., "Biomechanical effects of dissecting flexor carpi ulnaris," *J Bone Joint Surg Br*, Vol. 85, p. 856-9, 2003.
61. Smeulders, M.J., et al., "Spastic muscle properties are affected by length changes of adjacent structures," *Muscle Nerve*, Vol. 32, p. 208-15, 2005.
62. Huijing, P.A., "Epimuscular myofascial force transmission between antagonistic and synergistic muscles can explain movement limitation in spastic paresis," *J Electromyogr Kinesiol*, Vol. 17, p. 708-24, 2007.
63. Yucesoy, C.A. and P.A. Huijing, "Substantial effects of epimuscular myofascial force transmission on muscular mechanics have major implications on spastic muscle and remedial surgery," *J Electromyogr Kinesiol*, Vol. 17, p. 664-79, 2007.
64. Blasi, J., et al., "Botulinum neurotoxin A selectively cleaves the synaptic protein SNAP-25," *Nature*, Vol. 365, p. 160-3, 1993.

65. Brin, M.F., "Botulinum toxin: chemistry, pharmacology, toxicity, and immunology," *Muscle Nerve Suppl*, Vol. 6, p. S146-68, 1997.
66. Shaari, C.M. and I. Sanders, "Quantifying how location and dose of botulinum toxin injections affect muscle paralysis," *Muscle Nerve*, Vol. 16, p. 964-9, 1993.
67. Cichon, J.V., Jr., et al., "The effect of botulinum toxin type A injection on compound muscle action potential in an in vivo rat model," *Laryngoscope*, Vol. 105, p. 144-8, 1995.
68. Billante, C.R., et al., "Comparison of neuromuscular blockade and recovery with botulinum toxins A and F," *Muscle Nerve*, Vol. 26, p. 395-403, 2002.
69. Dimitrova, D.M., M.S. Shall, and S.J. Goldberg, "Short-term effects of botulinum toxin on the lateral rectus muscle of the cat," *Exp Brain Res*, Vol. 147, p. 449-55, 2002.
70. Shaari, C.M., et al., "Quantifying the spread of botulinum toxin through muscle fascia," *Laryngoscope*, Vol. 101, p. 960-4, 1991.
71. Yaraskavitch, M., T. Leonard, and W. Herzog, "Botox produces functional weakness in non-injected muscles adjacent to the target muscle," *J Biomech*, Vol. 41, p. 897-902, 2008.
72. Kuehn, B.M., "Studies, reports say botulinum toxins may have effects beyond injection site," *JAMA*, Vol. 299, p. 2261-3, 2008.
73. Rush, S.M., L.A. Ford, and G.A. Hamilton, "Morbidity associated with high gastrocnemius recession: retrospective review of 126 cases," *J Foot Ankle Surg*, Vol. 45, p. 156-60, 2006.
74. Strayer, L.M., "Recession of the gastrocnemius; an operation to relieve spastic contracture of the calf muscles.," *J Bone Joint Surg*, Vol. 32-A, p. 671-676, 1950.
75. Khot, A., et al., "Adductor release and chemodenervation in children with cerebral palsy: a pilot study in 16 children," *J Child Orthop*, Vol. 2, p. 293-9, 2008.
76. Ma, F.Y., et al., "Lengthening and transfer of hamstrings for a flexion deformity of the knee in children with bilateral cerebral palsy: technique and preliminary results," *J Bone Joint Surg Br*, Vol. 88, p. 248-54, 2006.
77. Borton, D.C., et al., "Isolated calf lengthening in cerebral palsy. Outcome analysis of risk factors.," *J Bone Joint Surg Br.*, Vol. 83, p. 364-370, 2001.
78. Nene, A.V., G.A. Evans, and J.H. Patrick, "Simultaneous multiple operations for spastic diplegia. Outcome and functional assessment of walking in 18 patients," *J Bone Joint Surg Br*, Vol. 75, p. 488-94, 1993.

79. Sutherland, D.H., et al., "Psoas release at the pelvic brim in ambulatory patients with cerebral palsy: operative technique and functional outcome," *J Pediatr Orthop*, Vol. 17, p. 563-70, 1997.
80. Park, M.S., et al., "Effects of distal hamstring lengthening on sagittal motion in patients with diplegia: hamstring length and its clinical use," *Gait Posture*, Vol. 30, p. 487-91, 2009.
81. Baumann, J.U. and H.G. Koch, "Lengthening of the anterior aponeurosis of the gastrocnemius muscle.," *Operat Orthop Traumatol*, Vol. 1, p. 254, 1989.
82. Yucesoy, C.A., et al., "Finite element modeling of aponeurotomy: altered intramuscular myofascial force transmission yields complex sarcomere length distributions determining acute effects," *Biomech Model Mechanobiol*, Vol. 6, p. 227-43, 2007.
83. Yucesoy, C.A. and P.A. Huijing, "Assessment by finite element modeling indicates that surgical intramuscular aponeurotomy performed closer to the tendon enhances intended acute effects in extramuscularly connected muscle," *J Biomech Eng*, Vol. 131, p. 021012, 2009.
84. Yucesoy, C.A., et al., "Extramuscular myofascial force transmission alters substantially the acute effects of surgical aponeurotomy: assessment by finite element modeling," *Biomech Model Mechanobiol*, Vol. 7, p. 175-89, 2008.
85. Gordon, A.M., A.F. Huxley, and F.J. Julian, "The variation in isometric tension with sarcomere length in vertebrate muscle fibres.," *J Physiol.*, Vol. 184, p. 170-192, 1966.
86. Maas, H., G.C. Baan, and P.A. Huijing, "Intermuscular interaction via myofascial force transmission: effects of tibialis anterior and extensor hallucis longus length on force transmission from rat extensor digitorum longus muscle," *J Biomech*, Vol. 34, p. 927-40, 2001.
87. Huijing, P.A., "Architecture of the human gastrocnemius muscle and some functional consequences," *Acta Anat (Basel)*, Vol. 123, p. 101-7, 1985.
88. Herzog, W. and H.E. ter Keurs, "Force-length relation of in-vivo human rectus femoris muscles," *Pflugers Arch*, Vol. 411, p. 642-7, 1988.
89. Winter, S.L. and J.H. Challis, "Reconstruction of the human gastrocnemius force-length curve in vivo: part 1-model-based validation of method," *J Appl Biomech*, Vol. 24, p. 197-206, 2008.
90. Maganaris, C.N., "Force-length characteristics of the in vivo human gastrocnemius muscle," *Clin Anat*, Vol. 16, p. 215-23, 2003.
91. Komi, P.V., S. Fukashiro, and M. Järvinen, "Biomechanical loading of Achilles tendon during normal locomotion.," *Clin Sports Med.*, Vol. 11, p. 521-531, 1992.

92. Freehafer, A.A., P.H. Peckham, and M.W. Keith, "Determination of muscle-tendon unit properties during tendon transfer," *J Hand Surg Am*, Vol. 4, p. 331-9, 1979.
93. Smeulders, M.J., et al., "Intraoperative measurement of force-length relationship of human forearm muscle," *Clin Orthop Relat Res*, p. 237-41, 2004.
94. An, K.N., et al., "Direct in vivo tendon force measurement system," *J Biomech*, Vol. 23, p. 1269-71, 1990.
95. Ralston, H.J., V.T. Inman, and A. Strait, "Mechanics of human isolated voluntary muscle.," *Am J Physiol.*, Vol. 151, p. 612-620, 1947.
96. Lacey, S.H., et al., "The posterior deltoid to triceps transfer: A clinical and biomechanical assessment," *J Hand Surg.*, Vol. 13A, p. 542-547, 1986.
97. Smeulders, M.J., et al., "Overstretching of sarcomeres may not cause cerebral palsy muscle contracture," *J Orthop Res*, Vol. 22, p. 1331-5, 2004.
98. Ward, S.R., et al., "Are current measurements of lower extremity muscle architecture accurate?," *Clin Orthop Relat Res*, Vol. 467, p. 1074-82, 2009.
99. Delval, A., et al., "Kinematic angular parameters in PD: reliability of joint angle curves and comparison with healthy subjects.," *Gait and Posture*, Vol. 28, p. 495-501, 2008.
100. Seven, Y.B., N.E. Akalan, and C.A. Yucesoy, "Effects of back loading on the biomechanics of sit-to-stand motion in healthy children.," *Human Movement Science*, Vol. 27, p. 65-79, 2008.
101. Lieber, R.L. and J. Friden, "Intraoperative measurement and biomechanical modeling of the flexor carpi ulnaris-to-extensor carpi radialis longus tendon transfer," *Journal of Biomechanical Engineering*, Vol. 119, p. 386-391, 1997.
102. Lieber, R.L. and J. Friden, "Musculoskeletal balance of the human wrist elucidated using intraoperative laser diffraction.," *Journal of Electromyography and Kinesiology*, Vol. 8, p. 93-100, 1998.
103. Lieber, R.L., et al., "Biomechanical properties of the brachioradialis muscle: Implications for surgical tendon transfer.," *J Hand Surg Am.*, Vol. 30, p. 273-282, 2005.
104. Maganaris, C.N., "Force-length characteristics of the in vivo human gastrocnemius muscle," *Clin Anat*, Vol. 16, p. 215-223, 2003.
105. Yucesoy, C.A., G.C. Baan, and P.A. Huijing, "Epimuscular myofascial force transmission occurs in the rat between the deep flexor muscles and their antagonistic muscles," *Journal of*

- Electromyography and Kinesiology, p. in press, 2009.
106. Ates, F., P.A. Huijing, and C.A. Yucesoy. "The role of muscle related fascial tissues in length-history effects causing decreased active muscle force particularly at low lengths." in Second International Fascia Research Congress. Amsterdam, the Netherlands. 2009.
 107. Yucesoy, C.A., G. Baan, and P.A. Huijing, "Epimuscular myofascial force transmission occurs in the rat between the deep flexor muscles and their antagonistic muscles," *J Electromyogr Kinesiol*, Vol. 20, p. 118-26, 2010.
 108. Maas, H., et al., "Myofascial force transmission between a single muscle head and adjacent tissues: length effects of head III of rat EDL," *J Appl Physiol*, Vol. 95, p. 2004-13, 2003.
 109. Yucesoy, C.A., et al., "Mechanisms causing effects of muscle position on proximo-distal muscle force differences in extra-muscular myofascial force transmission," *Med Eng Phys*, Vol. 28, p. 214-26, 2006.
 110. Herzog, W., et al., "Mysteries of muscle contraction.," *Journal of Applied Biomechanics*, Vol. 24, p. 1-13, 2008.
 111. Huijing, P.A., "Muscle as a collagen fiber reinforced composite: a review of force transmission in muscle and whole limb," *J Biomech*, Vol. 32, p. 329-45, 1999.
 112. Lipscomb, A.B., et al., "Evaluation of hamstring strength following use of semitendinosus and gracilis tendons to reconstruct the anterior cruciate ligament.," *Am J Sports Med.*, Vol. 10, p. 340-342, 1982.
 113. Yasuda, K., et al., "Graft site morbidity with autogenous semitendinosus and gracilis tendons.," *Am J Sports Med.*, Vol. 23, p. 706-714, 1995.
 114. Maeda, A., et al., "Anterior cruciate ligament reconstruction with multistranded autogenous semitendinosus tendon.," *Vol. 24*, p. 504-509, 1996.
 115. Ohkoshi, Y., et al., "Changes in muscle strength properties caused by harvesting of autogenous semitendinosus tendon for reconstruction of contralateral anterior cruciate ligament.," *Arthroscopy.*, Vol. 14, p. 580-584, 1998.
 116. Biewener, A.A., "Biomechanical consequences of scaling," *J Exp Biol*, Vol. 208, p. 1665-76, 2005.
 117. Biewener, A.A. and R. Blickhan, "Kangaroo rat locomotion: design for elastic energy storage or acceleration?," *J Exp Biol*, Vol. 140, p. 243-55, 1988.

118. Biewener, A.A., et al., "Muscle forces during locomotion in kangaroo rats: force platform and tendon buckle measurements compared," *J Exp Biol*, Vol. 137, p. 191-205, 1988.
119. O'Dwyer, N., P. Neilson, and J. Nash, "Reduction of spasticity in cerebral palsy using feedback of the tonic stretch reflex: a controlled study," *Dev Med Child Neurol*, Vol. 36, p. 770-86, 1994.
120. Yucesoy, C.A., et al., "Measurement of human gracilis muscle isometric forces as a function of knee angle, intraoperatively," *J Biomech*, Vol. 43, p. 2665-71, 2010.
121. Rosenbaum, P.L., et al., "Prognosis for gross motor function in cerebral palsy: creation of motor development curves," *JAMA*, Vol. 288, p. 1357-63, 2002.
122. Palisano, R., et al., "Development and reliability of a system to classify gross motor function in children with cerebral palsy," *Dev Med Child Neurol*, Vol. 39, p. 214-23, 1997.
123. Katz, K., A. Rosenthal, and Z. Yosipovitch, "Normal ranges of popliteal angle in children," *J Pediatr Orthop*, Vol. 12, p. 229-31, 1992.
124. Miller, F., et al., "Soft-tissue release for spastic hip subluxation in cerebral palsy," *J Pediatr Orthop*, Vol. 17, p. 571-84, 1997.
125. Neter, J., et al., *Applied Linear Statistical Models*. Irwin, Homewood, IL. 1996.
126. Ettema, G.J.C., G. Styles, and V. and Kippers, "The moment arms of 23 muscle segments of the upper limb with varying elbow and forearm positions: Implications for motor control. ," *Human Movement Science*, Vol. 17, p. 201-220. 1998.
127. Kuechle, D.K., et al., "The relevance of the moment arm of shoulder muscles with respect to axial rotation of the glenohumeral joint in four positions," *Clin Biomech (Bristol, Avon)*, Vol. 15, p. 322-9, 2000.
128. Lance, J.W., Spasticity: disordered motor control, R.G. Feldman, R.R. Young, and W.P. Koella, Editors. 1980, Year Book Medical Publishers: Chicago. p. 485-95.
129. Fergusson, D., B. Hutton, and A. Drodge, "The epidemiology of major joint contractures: a systematic review of the literature," *Clin Orthop Relat Res*, Vol. 456, p. 22-9, 2007.
130. Marty, G.R., L.S. Dias, and D. Gaebler-Spira, "Selective posterior rhizotomy and soft-tissue procedures for the treatment of cerebral diplegia," *J Bone Joint Surg Am*, Vol. 77, p. 713-8, 1995.
131. Rose, J. and K.C. McGill, "Neuromuscular activation and motor-unit firing characteristics in cerebral palsy," *Dev Med Child Neurol*, Vol. 47, p. 329-36, 2005.

132. Stackhouse, S.K., S.A. Binder-Macleod, and S.C.K. Lee, "Voluntary muscle activation, contractile properties, and fatigability in children with and without cerebral palsy," *Muscle & Nerve*, Vol. 31, p. 594-601, 2005.
133. Riad, J., et al., "Are muscle volume differences related to concentric muscle work during walking in spastic hemiplegic cerebral palsy?," *Clin Orthop Relat Res*, Vol. 470, p. 1278-85, 2012.
134. Makihara, Y., et al., "Decrease of knee flexion torque in patients with ACL reconstruction: combined analysis of the architecture and function of the knee flexor muscles," *Knee Surg Sports Traumatol Arthrosc*, Vol. 14, p. 310-7, 2006.
135. Delp, S.L., et al., "Hamstrings and psoas lengths during normal and crouch gait: implications for muscle-tendon surgery," *J Orthop Res*, Vol. 14, p. 144-51, 1996.
136. Mohagheghi, A.A., et al., "In vivo gastrocnemius muscle fascicle length in children with and without diplegic cerebral palsy," *Dev Med Child Neurol*, Vol. 50, p. 44-50, 2008.
137. Shortland, A.P., et al., "Architecture of the medial gastrocnemius in children with spastic diplegia," *Dev Med Child Neurol*, Vol. 44, p. 158-63, 2002.
138. Lieber, R.L. and J. Friden, "Spasticity causes a fundamental rearrangement of muscle-joint interaction," *Muscle Nerve*, Vol. 25, p. 265-70, 2002.
139. Ponten, E., S. Gantelius, and R.L. Lieber, "Intraoperative muscle measurements reveal a relationship between contracture formation and muscle remodeling," *Muscle Nerve*, Vol. 36, p. 47-54, 2007.
140. Huijing, P.A., "Epimuscular myofascial force transmission: a historical review and implications for new research. International Society of Biomechanics Muybridge Award Lecture, Taipei, 2007," *J Biomech*, Vol. 42, p. 9-21, 2009.
141. Yucesoy, C.A., "Epimuscular myofascial force transmission implies novel principles for muscular mechanics," *Exerc Sport Sci Rev*, Vol. 38, p. 128-34, 2010.
142. Huijing, P.A., et al., "Effects of knee joint angle on global and local strains within human triceps surae muscle: MRI analysis indicating in vivo myofascial force transmission between synergistic muscles," *Surg Radiol Anat*, Vol. 33, p. 869-79, 2011.
143. Ates, F., Y. Temelli, and C.A. Yucesoy, "Human spastic Gracilis muscle isometric forces measured intraoperatively as a function of knee angle show no abnormal muscular mechanics,"

- Clin Biomech (Bristol, Avon), 2012.
144. Meijer, H.J., J.M. Rijkelijhuizen, and P.A. Huijing, "Myofascial force transmission between antagonistic rat lower limb muscles: effects of single muscle or muscle group lengthening," *J Electromyogr Kinesiol*, Vol. 17, p. 698-707, 2007.
 145. McMulkin, M.L., et al., "Range of motion measures under anesthesia compared with clinical measures for children with cerebral palsy," *J Pediatr Orthop B*, Vol. 17, p. 277-80, 2008.
 146. Brouwer, B., et al., "Reflex excitability and isometric force production in cerebral palsy: the effect of serial casting," *Dev Med Child Neurol*, Vol. 40, p. 168-75, 1998.
 147. Damiano, D.L., et al., "Spasticity versus strength in cerebral palsy: relationships among involuntary resistance, voluntary torque, and motor function," *Eur J Neurol*, Vol. 8 Suppl 5, p. 40-9, 2001.
 148. Wiley, M.E. and D.L. Damiano, "Lower-extremity strength profiles in spastic cerebral palsy," *Dev Med Child Neurol*, Vol. 40, p. 100-7, 1998.
 149. Gribble, P.L., et al., "Role of cocontraction in arm movement accuracy," *J Neurophysiol*, Vol. 89, p. 2396-405, 2003.
 150. Hansen, S., et al., "Coupling of antagonistic ankle muscles during co-contraction in humans," *Exp Brain Res*, Vol. 146, p. 282-92, 2002.
 151. Damiano, D.L., et al., "Muscle force production and functional performance in spastic cerebral palsy: relationship of cocontraction," *Arch Phys Med Rehabil*, Vol. 81, p. 895-900, 2000.
 152. Ikeda, A.J., et al., "Quantification of cocontraction in spastic cerebral palsy," *Electromyogr Clin Neurophysiol*, Vol. 38, p. 497-504, 1998.
 153. O'Sullivan, M.C., et al., "Abnormal development of biceps brachii phasic stretch reflex and persistence of short latency heteronymous reflexes from biceps to triceps brachii in spastic cerebral palsy," *Brain*, Vol. 121 (Pt 12), p. 2381-95, 1998.
 154. Poon, D.M. and C.W. Hui-Chan, "Hyperactive stretch reflexes, co-contraction, and muscle weakness in children with cerebral palsy," *Dev Med Child Neurol*, Vol. 51, p. 128-35, 2009.
 155. Khot, A., et al., "Adductor release and chemodenervation in children with cerebral palsy: a pilot study in 16 children.," *J Child Orthop*, Vol. 2, p. 293-299, 2008.
 156. Saraph, V., et al., "The Baumann procedure for fixed contracture of the gastrosoleus in cerebral palsy. Evaluation of function of the ankle after multilevel surgery.," *J Bone Joint Surg Br.*, Vol.

- 82, p. 535-540, 2000.
157. Baddar, A., et al., "Ankle and knee coupling in patients with spastic diplegia: effects of gastrocnemius-soleus lengthening," *J Bone Joint Surg Am*, Vol. 84-A, p. 736-44, 2002.
 158. Nather, A., G.E. Fulford, and K. Stewart, "Treatment of valgus hindfoot in cerebral palsy by peroneus brevis lengthening," *Dev Med Child Neurol*, Vol. 26, p. 335-40, 1984.
 159. Tidball, J.G., "Myotendinous junction injury in relation to junction structure and molecular composition," *Exerc Sport Sci Rev*, Vol. 19, p. 419-45, 1991.
 160. Hawkins, D. and M. Bey, "Muscle and tendon force-length properties and their interactions in vivo," *J Biomech*, Vol. 30, p. 63-70, 1997.
 161. Berthier, C. and S. Blaineau, "Supramolecular organization of the subsarcolemmal cytoskeleton of adult skeletal muscle fibers. A review," *Biol Cell*, Vol. 89, p. 413-34, 1997.
 162. Street, S.F., "Lateral transmission of tension in frog myofibers: a myofibrillar network and transverse cytoskeletal connections are possible transmitters," *J Cell Physiol*, Vol. 114, p. 346-64, 1983.
 163. Street, S.F. and R.W. Ramsey, "Sarcolemma: transmitter of active tension in frog skeletal muscle," *Science*, Vol. 149, p. 1379-80, 1965.
 164. Yucesoy, C.A., "Epimuscular myofascial force transmission implies novel principles for muscular mechanics.," *Exercise and Sport Science Reviews*, Vol. 38, p. 128-134, 2010.
 165. Carvalhais, V.O., et al., "Myofascial force transmission between the latissimus dorsi and gluteus maximus muscles: An in vivo experiment," *J Biomech*, Vol. 46, p. 1003-7, 2013.
 166. Bojsen-Moller, J., et al., "Intermuscular force transmission between human plantarflexor muscles in vivo," *J Appl Physiol*, Vol. 109, p. 1608-18, 2010.
 167. Oda, T., et al., "In vivo behavior of muscle fascicles and tendinous tissues of human gastrocnemius and soleus muscles during twitch contraction," *J Electromyogr Kinesiol*, Vol. 17, p. 587-95, 2007.
 168. Zwick, E.B., et al., "Medial hamstring lengthening in the presence of hip flexor tightness in spastic diplegia," *Gait Posture*, Vol. 16, p. 288-96, 2002.
 169. Huijing, P.A. and G.C. Baan, "Extramuscular myofascial force transmission within the rat anterior tibial compartment: Proximo-distal differences in muscle force," *Acta Physiologica Scandinavica*, Vol. 173, p. 1-15, 2001.

170. Rijkelijhuizen, J.M., et al., "Myofascial force transmission also occurs between antagonistic muscles located within opposite compartments of the rat lower hind limb," *J Electromyogr Kinesiol*, Vol. 17, p. 690-7, 2007.
171. Maas, H. and T.G. Sandercock, "Are skeletal muscles independent actuators? Force transmission from soleus muscle in the cat," *J Appl Physiol*, Vol. 104, p. 1557-67, 2008.
172. Yucesoy, C.A., et al. "MRI analyses show in vivo occurrence of myofascial force transmission". in XXIII International Society of Biomechanics Congress. Brussels, Belgium,. 2011.
173. Smeulders, M.J., et al., "Progressive surgical dissection for tendon transposition affects length-force characteristics of rat flexor carpi ulnaris muscle," *J Orthop Res*, Vol. 20, p. 863-8, 2002.
174. Huijing, P.A. and G.C. Baan, "Myofascial force transmission: muscle relative position and length determine agonist and synergist muscle force," *J Appl Physiol*, Vol. 94, p. 1092-107, 2003.
175. Lieber, R.L., "Muscle fiber length and moment arm coordination during dorsi- and plantarflexion in the mouse hindlimb," *Acta Anatomica*, Vol. 159, p. 84-89, 1997.
176. Yu, W.S., et al., "Thumb and finger forces produced by motor units in the long flexor of the human thumb," *J Physiol*, Vol. 583, p. 1145-54, 2007.
177. Zatsiorsky, V.M., Z.M. Li, and M.L. Latash, "Enslaving effects in multi-finger force production," *Exp Brain Res*, Vol. 131, p. 187-95, 2000.
178. Benjamin, M., "The fascia of the limbs and back - a review," *J Anat*, Vol. 214, p. 1-18, 2009.
179. Jaspers, R.T., et al., "Acute effects of intramuscular aponeurotomy on rat gastrocnemius medialis: force transmission, muscle force and sarcomere length," *J Biomech*, Vol. 32, p. 71-9, 1999.
180. Hagbarth, K.E., G. Wallen, and L. Lofstedt, "Muscle spindle activity in man during voluntary fast alternating movements," *J Neurol Neurosurg Psychiatry*, Vol. 38, p. 625-35, 1975.
181. Wilson, L.R., S.C. Gandevia, and D. Burke, "Discharge of human muscle spindle afferents innervating ankle dorsiflexors during target isometric contractions," *J Physiol*, Vol. 504 (Pt 1), p. 221-32, 1997.
182. Yucesoy, C.A., Z. Seref-Ferlengez, and P.A. Huijing, "In muscle lengthening surgery multiple aponeurotomy does not improve intended acute effects and may counter-indicate: an assessment by finite element modelling," *Comput Methods Biomech Biomed Engin*, Vol. 16, p. 12-25,

- 2013.
183. Burke, D., et al., "The responses of human muscle spindle endings to vibration during isometric contraction," *J Physiol*, Vol. 261, p. 695-711, 1976.
 184. Kawano, F., et al., "Tension- and afferent input-associated responses of neuromuscular system of rats to hindlimb unloading and/or tenotomy," *Am J Physiol Regul Integr Comp Physiol*, Vol. 287, p. R76-86, 2004.
 185. Feldman, A.G., "Once more on the equilibrium-point hypothesis (λ model) for motor control," *J Mot Behav*, Vol. 18, p. 17-54, 1986.
 186. Latash, M.L., J.P. Scholz, and G. Schoner, "Motor control strategies revealed in the structure of motor variability," *Exerc Sport Sci Rev*, Vol. 30, p. 26-31, 2002.
 187. Latash, M.L., J.P. Scholz, and G. Schoner, "Toward a new theory of motor synergies," *Motor Control*, Vol. 11, p. 276-308, 2007.
 188. Latash, M.L., "Motor synergies and the equilibrium-point hypothesis," *Motor Control*, Vol. 14, p. 294-322, 2010.
 189. Jaspers, R.T., et al., "Healing of the aponeurosis during recovery from aponeurotomy: morphological and histological adaptation and related changes in mechanical properties," *J Orthop Res*, Vol. 23, p. 266-73, 2005.
 190. Sperry, R.W., "The problem of central nervous reorganization after nerve regeneration and muscle transposition," *Q Rev Biol*, Vol. 20, p. 311-69, 1945.
 191. Slawinska, U. and S. Kasicki, "Altered electromyographic activity pattern of rat soleus muscle transposed into the bed of antagonist muscle," *J Neurosci*, Vol. 22, p. 5808-12, 2002.
 192. Asakawa, D.S., et al., "In vivo motion of the rectus femoris muscle after tendon transfer surgery," *J Biomech*, Vol. 35, p. 1029-37, 2002.
 193. Granata, K.P., M.F. Abel, and D.L. Damiano, "Joint angular velocity in spastic gait and the influence of muscle-tendon lengthening," *J Bone Joint Surg Am*, Vol. 82, p. 174-86, 2000.
 194. Buurke, J.H., et al., "Influence of hamstring lengthening on muscle activation timing," *Gait Posture*, Vol. 20, p. 48-53, 2004.
 195. Saraph, V., et al., "Multilevel surgery in spastic diplegia: evaluation by physical examination and gait analysis in 25 children," *J Pediatr Orthop*, Vol. 22, p. 150-7, 2002.
 196. Cosgrove, A.P. and H.K. Graham, "Botulinum toxin A prevents the development of contractures

- in the hereditary spastic mouse," *Dev Med Child Neurol*, Vol. 36, p. 379-85, 1994.
197. Fock, J., et al., "Functional outcome following Botulinum toxin A injection to reduce spastic equinus in adults with traumatic brain injury," *Brain Inj*, Vol. 18, p. 57-63, 2004.
 198. Cardoso, E.S., et al., "Botulinum toxin type A for the treatment of the spastic equinus foot in cerebral palsy," *Pediatr Neurol*, Vol. 34, p. 106-9, 2006.
 199. Criswell, S.R., B.E. Crowner, and B.A. Racette, "The use of botulinum toxin therapy for lower-extremity spasticity in children with cerebral palsy," *Neurosurg Focus*, Vol. 21, p. e1, 2006.
 200. Herzog, W. and D. Longino, "The role of muscles in joint degeneration and osteoarthritis," *J Biomech*, Vol. 40 Suppl 1, p. S54-63, 2007.
 201. Longino, D., C. Frank, and W. Herzog, "Acute botulinum toxin-induced muscle weakness in the anterior cruciate ligament-deficient rabbit," *J Orthop Res*, Vol. 23, p. 1404-10, 2005.
 202. Longino, D., T.A. Butterfield, and W. Herzog, "Frequency and length-dependent effects of Botulinum toxin-induced muscle weakness," *J Biomech*, Vol. 38, p. 609-13, 2005.
 203. Ettema, G.J. and P.A. Huijting, "Properties of the tendinous structures and series elastic component of EDL muscle-tendon complex of the rat," *J Biomech*, Vol. 22, p. 1209-15, 1989.
 204. Strumpf, R.K., J.D. Humphrey, and F.C. Yin, "Biaxial mechanical properties of passive and tetanized canine diaphragm," *Am J Physiol*, Vol. 265, p. H469-75, 1993.
 205. Scott, S.H. and G.E. Loeb, "Mechanical properties of aponeurosis and tendon of the cat soleus muscle during whole-muscle isometric contractions," *J Morphol*, Vol. 224, p. 73-86, 1995.
 206. Williams, P.E. and G. Goldspink, "The effect of denervation and dystrophy on the adaptation of sarcomere number to the functional length of the muscle in young and adult mice," *J Anat*, Vol. 122, p. 455-465, 1976.
 207. Monti, R.J., et al., "Mechanical properties of rat soleus aponeurosis and tendon during variable recruitment in situ," *J Exp Biol*, Vol. 206, p. 3437-45, 2003.
 208. Maganaris, C.N. and J.P. Paul, "In vivo human tendon mechanical properties," *J Physiol*, Vol. 521 Pt 1, p. 307-13, 1999.
 209. Passerieux, E., et al., "Physical continuity of the perimysium from myofibers to tendons: involvement in lateral force transmission in skeletal muscle," *J Struct Biol*, Vol. 159, p. 19-28, 2007.
 210. Nishimura, T., A. Hattori, and K. Takahashi, "Arrangement and identification of proteoglycans

- in basement membrane and intramuscular connective tissue of bovine semitendinosus muscle," *Acta Anat (Basel)*, Vol. 155, p. 257-65, 1996.
211. Huijing, P.A., G.C. Baan, and G.T. Rebel, "Non-myotendinous force transmission in rat extensor digitorum longus muscle," *J Exp Biol*, Vol. 201, p. 683-91, 1998.
 212. Turkoglu, A.N., P.A. Huijing, and C.A. Yucesoy. "Assessment of Principles of Effects of Botulinum Toxin on Mechanics of Isolated Muscle Using Finite Element Modeling". in *Proceedings of the International Society of Biomechanics XXIIIrd Congress*. Brussels, Belgium. 2011.
 213. Yucesoy, C.A. and P.A. Huijing, "Specifically Tailored Use of the Finite Element Method to Study Muscular Mechanics within the Context of Fascial Integrity: The Linked Fiber-Matrix Mesh Model," *International Journal for Multiscale Computational Engineering*, Vol. 10, 2012.
 214. Englund, E.K., et al., "Combined diffusion and strain tensor MRI reveals a heterogeneous, planar pattern of strain development during isometric muscle contraction," *Am J Physiol Regul Integr Comp Physiol*, Vol. 300, p. R1079-90, 2011.
 215. Lowe, K., I. Novak, and A. Cusick, "Low-dose/high-concentration localized botulinum toxin A improves upper limb movement and function in children with hemiplegic cerebral palsy," *Dev Med Child Neurol*, Vol. 48, p. 170-5, 2006.
 216. Graham, H.K., et al., "Recommendations for the use of botulinum toxin type A in the management of cerebral palsy," *Gait Posture*, Vol. 11, p. 67-79, 2000.
 217. Russman, B.S., A. Tilton, and M.E. Gormley, Jr., "Cerebral palsy: a rational approach to a treatment protocol, and the role of botulinum toxin in treatment," *Muscle Nerve Suppl*, Vol. 6, p. S181-93, 1997.
 218. Koman, L.A., et al., "Management of cerebral palsy with botulinum-A toxin: preliminary investigation," *J Pediatr Orthop*, Vol. 13, p. 489-95, 1993.
 219. Borodic, G.E., et al., "Histologic assessment of dose-related diffusion and muscle fiber response after therapeutic botulinum A toxin injections," *Mov Disord*, Vol. 9, p. 31-9, 1994.
 220. Finol, H.J., D.M. Lewis, and R. Owens, "The effects of denervation on contractile properties of rat skeletal muscle," *J Physiol*, Vol. 319, p. 81-92, 1981.
 221. Dodd, S.L., et al., "Botulinum neurotoxin type A causes shifts in myosin heavy chain composition in muscle," *Toxicon*, Vol. 46, p. 196-203, 2005.

222. Fortuna, R., et al., "Changes in contractile properties of muscles receiving repeat injections of botulinum toxin (Botox)," *J Biomech*, Vol. 44, p. 39-44, 2011.
223. Lukban, M.B., R.L. Rosales, and D. Dressler, "Effectiveness of botulinum toxin A for upper and lower limb spasticity in children with cerebral palsy: a summary of evidence," *J Neural Transm*, Vol. 116, p. 319-31, 2009.
224. Molenaers, G., et al., "Long-term use of botulinum toxin type A in children with cerebral palsy: treatment consistency," *Eur J Paediatr Neurol*, Vol. 13, p. 421-9, 2009.
225. Wong, V., "Use of botulinum toxin injection in 17 children with spastic cerebral palsy," *Pediatr Neurol*, Vol. 18, p. 124-31, 1998.
226. Sutherland, D.H., et al., "Double-blind study of botulinum A toxin injections into the gastrocnemius muscle in patients with cerebral palsy," *Gait Posture*, Vol. 10, p. 1-9, 1999.
227. Koman, L.A., et al., "Botulinum toxin type A neuromuscular blockade in the treatment of lower extremity spasticity in cerebral palsy: a randomized, double-blind, placebo-controlled trial. BOTOX Study Group," *J Pediatr Orthop*, Vol. 20, p. 108-15, 2000.
228. Love, S.C., et al., "The effect of botulinum toxin type A on the functional ability of the child with spastic hemiplegia a randomized controlled trial," *Eur J Neurol*, Vol. 8 Suppl 5, p. 50-8, 2001.
229. Cosgrove, A.P., I.S. Corry, and H.K. Graham, "Botulinum toxin in the management of the lower limb in cerebral palsy," *Dev Med Child Neurol*, Vol. 36, p. 386-96, 1994.
230. Ubhi, T., et al., "Randomised double blind placebo controlled trial of the effect of botulinum toxin on walking in cerebral palsy," *Arch Dis Child*, Vol. 83, p. 481-7, 2000.
231. Bakheit, A.M., et al., "A randomized, double-blind, placebo-controlled, dose-ranging study to compare the efficacy and safety of three doses of botulinum toxin type A (Dysport) with placebo in upper limb spasticity after stroke," *Stroke*, Vol. 31, p. 2402-6, 2000.
232. Bhakta, B.B., et al., "Impact of botulinum toxin type A on disability and carer burden due to arm spasticity after stroke: a randomised double blind placebo controlled trial," *J Neurol Neurosurg Psychiatry*, Vol. 69, p. 217-21, 2000.
233. Van Der Walt, A., et al., "A double-blind, randomized, controlled study of botulinum toxin type A in MS-related tremor," *Neurology*, Vol. 79, p. 92-9, 2012.
234. Billante, C.R., et al., "Comparison of neuromuscular blockade and recovery with botulinum

- toxins A and F," *Muscle Nerve*, Vol. 26, p. 395-403, 2002.
235. Cichon, J.V.J., et al., "The effect of botulinum toxin type A injection on compound muscle action potential in an in vivo rat model.," *Laryngoscope*, Vol. 105, p. 144-148, 1995.
236. Dimitrova, D.M., M.S. Shall, and S.J. Goldberg, "Short-term effects of botulinum toxin on the lateral rectus muscle of the cat.," *Experimental Brain Research*, Vol. 147, p. 449-455, 2002.
239. Ettema, G.J.C., G. Styles, and V. Kippers, "The moment arms of 23 muscle segments of the upper limb with varying elbow and forearm positions: Implications for motor control," *Human Movement Science*, Vol. 17, p. 201-220, 1998.
238. Kuechle, D.K., et al., "The relevance of the moment arm of shoulder muscles with respect to axial rotation of the glenohumeral joint in four positions.," *Clinical Biomechanics*, Vol. 15, p. 322-329, 2000.
239. Yucesoy, C.A., Ö.E. Arıkan, and F. Ateş, "BTX-A Administration to the Target Muscle Affects Forces of All Muscles Within an Intact Compartment and Epimuscular Myofascial Force Transmission," *Journal of Biomechanical Engineering*, Vol. 134, p. 111002-1-9, 2012.
240. Frasson, E., et al., "Spread of botulinum neurotoxin type a at standard doses is inherent to the successful treatment of spastic equinus foot in cerebral palsy: short-term neurophysiological and clinical study," *J Child Neurol*, Vol. 27, p. 587-93, 2012.
241. Kuehn, B.M., "Studies, reports say botulinum toxins may have effects beyond injection site," *JAMA-Journal of the American Medical Association*, Vol. 299, p. 2261-2263, 2008.
242. Borodic, G.E., et al., "Botulinum A toxin for the treatment of spasmodic torticollis: dysphagia and regional toxin spread," *Head Neck*, Vol. 12, p. 392-9, 1990.
243. Yaraskavitch, M., T. Leonard, and W. Herzog, "Botox produces functional weakness in non-injected muscles adjacent to the target muscle.," *Journal of Biomechanics*, Vol. 41, p. 897-902, 2008.
244. Sheean, G.L., "Botulinum treatment of spasticity: why is it so difficult to show a functional benefit?," *Curr Opin Neurol*, Vol. 14, p. 771-6, 2001.
245. Dietz, V., J. Quintern, and W. Berger, "Electrophysiological studies of gait in spasticity and rigidity. Evidence that altered mechanical properties of muscle contribute to hypertonia," *Brain*, Vol. 104, p. 431-49, 1981.
246. Tardieu, C., et al., "Toe-walking in children with cerebral palsy: contributions of contracture

- and excessive contraction of triceps surae muscle," *Phys Ther*, Vol. 69, p. 656-62, 1989.
247. Kwon, D.R., et al., "Spastic cerebral palsy in children: dynamic sonoelastographic findings of medial gastrocnemius," *Radiology*, Vol. 263, p. 794-801, 2012.
 248. Sheehan, D.C. and B.B. Hrapchak, *Theory and Practice of Histotechnology*. Columbus, OH: Battelle Memorial Institute. 1987.
 249. Bancroft, J.D. and M. Gamble, *Theory and practice of histological techniques*. 6th ed. Philadelphia:: Churchill Livingstone/Elsevier. 2008.
 250. Misiaszek, J.E. and K.G. Pearson, "Adaptive changes in locomotor activity following botulinum toxin injection in ankle extensor muscles of cats," *J Neurophysiol*, Vol. 87, p. 229-39, 2002.
 251. Duchen, L.W., "Changes in motor innervation and cholinesterase localization induced by botulinum toxin in skeletal muscle of the mouse: differences between fast and slow muscles," *J Neurol Neurosurg Psychiatry*, Vol. 33, p. 40-54, 1970.
 252. Borodic, G.E., et al., "Botulinum a toxin for spasmodic torticollis: multiple vs single injection points per muscle," *Head Neck*, Vol. 14, p. 33-7, 1992.
 253. Chin, T.Y., et al., "Accuracy of intramuscular injection of botulinum toxin A in juvenile cerebral palsy: a comparison between manual needle placement and placement guided by electrical stimulation," *J Pediatr Orthop*, Vol. 25, p. 286-91, 2005.
 254. Wissel, J., et al., "European consensus table on the use of botulinum toxin type A in adult spasticity," *J Rehabil Med*, Vol. 41, p. 13-25, 2009.
 255. Carli, L., C. Montecucco, and O. Rossetto, "Assay of diffusion of different botulinum neurotoxin type a formulations injected in the mouse leg," *Muscle Nerve*, Vol. 40, p. 374-80, 2009.
 256. Hyman, N., et al., "Botulinum toxin (Dysport) treatment of hip adductor spasticity in multiple sclerosis: a prospective, randomised, double blind, placebo controlled, dose ranging study," *J Neurol Neurosurg Psychiatry*, Vol. 68, p. 707-12, 2000.
 257. Hamdy, R.C., et al., "Safety and efficacy of botox injection in alleviating post-operative pain and improving quality of life in lower extremity limb lengthening and deformity correction," *Trials*, Vol. 8, p. 27, 2007.
 258. Fortuna, R., et al., "The effects of electrical stimulation exercise on muscles injected with botulinum toxin type-A (botox)," *J Biomech*, Vol. 46, p. 36-42, 2013.

259. Lim, E.C., A.M. Quek, and R.C. Seet, "Botulinum toxin-A injections via electrical motor point stimulation to treat writer's cramp: pilot study," *Neurol Neurophysiol Neurosci*, p. 4, 2006.
260. Picelli, A., et al., "Botulinum toxin type A injection into the gastrocnemius muscle for spastic equinus in adults with stroke: a randomized controlled trial comparing manual needle placement, electrical stimulation and ultrasonography-guided injection techniques," *Am J Phys Med Rehabil*, Vol. 91, p. 957-64, 2012.
261. Sutherland, D.H. and J.R. Davids, "Common gait abnormalities of the knee in cerebral palsy," *Clin Orthop Relat Res*, p. 139-47, 1993.
262. Hagglund, G. and P. Wagner, "Spasticity of the gastrosoleus muscle is related to the development of reduced passive dorsiflexion of the ankle in children with cerebral palsy: a registry analysis of 2,796 examinations in 355 children," *Acta Orthop*, Vol. 82, p. 744-8, 2011.
263. Bourbonnais, D. and S. Vanden Noven, "Weakness in patients with hemiparesis," *Am J Occup Ther*, Vol. 43, p. 313-9, 1989.
264. Koman, L.A., B.P. Smith, and J.S. Shilt, "Cerebral palsy," *Lancet*, Vol. 363, p. 1619-31, 2004.
265. Cote, T.R., et al., "Botulinum toxin type A injections: adverse events reported to the US Food and Drug Administration in therapeutic and cosmetic cases," *J Am Acad Dermatol*, Vol. 53, p. 407-15, 2005.
266. Mahant, N., P.D. Clouston, and I.T. Lorentz, "The current use of botulinum toxin," *J Clin Neurosci*, Vol. 7, p. 389-94, 2000.
267. Thacker, B.E., et al., "Passive mechanical properties and related proteins change with botulinum neurotoxin A injection of normal skeletal muscle," *J Orthop Res*, Vol. 30, p. 497-502, 2012.
268. Dengler, R., et al., "Local botulinum toxin in the treatment of spastic drop foot," *J Neurol*, Vol. 239, p. 375-8, 1992.
269. Marsden, J., et al., "Muscle paresis and passive stiffness: key determinants in limiting function in Hereditary and Sporadic Spastic Paraparesis," *Gait Posture*, Vol. 35, p. 266-71, 2012.
270. Park, G.Y. and D.R. Kwon, "Sonoelastographic evaluation of medial gastrocnemius muscles intrinsic stiffness after rehabilitation therapy with botulinum toxin a injection in spastic cerebral palsy," *Arch Phys Med Rehabil*, Vol. 93, p. 2085-9, 2012.
271. Colovic, H., et al., "Estimation of botulinum toxin type A efficacy on spasticity and functional outcome in children with spastic cerebral palsy," *Biomed Pap Med Fac Univ Palacky Olomouc*

- Czech Repub, Vol. 156, p. 41-7, 2012.
272. Miscio, G., et al., "Botulinum toxin in post-stroke patients: stiffness modifications and clinical implications," *J Neurol*, Vol. 251, p. 189-96, 2004.
 273. Haubruck, P., et al., "Botulinum neurotoxin a injections influence stretching of the gastrocnemius muscle-tendon unit in an animal model," *Toxins (Basel)*, Vol. 4, p. 605-19, 2012.
 274. Mannava, S., et al., "Contributions of neural tone to in vivo passive muscle-tendon unit biomechanical properties in a rat rotator cuff animal model," *Ann Biomed Eng*, Vol. 39, p. 1914-24, 2011.
 275. Desloovere, K., et al., "The effect of different physiotherapy interventions in post-BTX-A treatment of children with cerebral palsy," *Eur J Paediatr Neurol*, Vol. 16, p. 20-8, 2012.
 276. Williams, S.A., et al., "Combining strength training and botulinum neurotoxin intervention in children with cerebral palsy: the impact on muscle morphology and strength," *Disabil Rehabil*, 2012.
 277. Bandholm, T., et al., "Neurorehabilitation with versus without resistance training after botulinum toxin treatment in children with cerebral palsy: a randomized pilot study," *NeuroRehabilitation*, Vol. 30, p. 277-86, 2012.
 278. Yasar, E., et al., "The efficacy of serial casting after botulinum toxin type A injection in improving equinovarus deformity in patients with chronic stroke," *Brain Inj*, Vol. 24, p. 736-9, 2010.
 279. Kanellopoulos, A.D., et al., "Long lasting benefits following the combination of static night upper extremity splinting with botulinum toxin A injections in cerebral palsy children," *Eur J Phys Rehabil Med*, Vol. 45, p. 501-6, 2009.
 280. Maas, H. and P.A. Huijting, "Mechanical effect of rat flexor carpi ulnaris muscle after tendon transfer: does it generate a wrist extension moment?," *J Appl Physiol*, Vol. 112, p. 607-14, 2012.
 281. Delp, S.L., D.A. Ringwelski, and N.C. Carroll, "Transfer of the rectus femoris: effects of transfer site on moment arms about the knee and hip," *J Biomech*, Vol. 27, p. 1201-11, 1994.
 282. Ateş, F., P.A. Huijting, and C.A. Yucesoy, "Previous muscular activity at high length yields sizable history effects causing decreased muscle force particularly at low lengths," *Second International Fascia Research Congress*, Vol. Amsterdam, the Netherlands, 2009.

283. Abbott, B.C. and X.M. Aubert, "The force exerted by active striated muscle during and after change of length," *J Physiol*, Vol. 117, p. 77-86, 1952.
284. Lieber, R.L. and S.C. Bodine-Fowler, "Skeletal muscle mechanics: implications for rehabilitation," *Phys Ther*, Vol. 73, p. 844-56, 1993.
285. Kreulen, M. and M.J. Smeulders, "Assessment of Flexor carpi ulnaris function for tendon transfer surgery," *J Biomech*, Vol. 41, p. 2130-5, 2008.
286. Meijer, H.J., G.C. Baan, and P.A. Huijting, "Myofascial force transmission is increasingly important at lower forces: firing frequency-related length-force characteristics of rat extensor digitorum longus," *Acta Physiol (Oxf)*, Vol. 186, p. 185-95, 2006.
287. Fung, Y.C., *Biomechanics: Mechanical Properties of Living Tissues*. Second Edition ed.: Springer. 1993.
288. Best, T.M., et al., "Characterization of the passive responses of live skeletal muscle using the quasi-linear theory of viscoelasticity," *J Biomech*, Vol. 27, p. 413-9, 1994.
289. Giles, J.M., A.E. Black, and J.E. Bischoff, "Anomalous rate dependence of the preconditioned response of soft tissue during load controlled deformation," *J Biomech*, Vol. 40, p. 777-85, 2007.
290. Einat, R. and L. Yoram, "Recruitment viscoelasticity of the tendon," *J Biomech Eng*, Vol. 131, p. 111008, 2009.
291. Schatzmann, L., P. Brunner, and H.U. Staubli, "Effect of cyclic preconditioning on the tensile properties of human quadriceps tendons and patellar ligaments," *Knee Surg Sports Traumatol Arthrosc*, Vol. 6 Suppl 1, p. S56-61, 1998.
292. Cheng, S., E.C. Clarke, and L.E. Bilston, "The effects of preconditioning strain on measured tissue properties," *J Biomech*, Vol. 42, p. 1360-2, 2009.
293. Lokshin, O. and Y. Lanir, "Viscoelasticity and preconditioning of rat skin under uniaxial stretch: microstructural constitutive characterization," *J Biomech Eng*, Vol. 131, p. 031009, 2009.
294. Palmer, M.L., et al., "Non-uniform distribution of strain during stretch of relaxed skeletal muscle fibers from rat soleus muscle," *J Muscle Res Cell Motil*, Vol. 32, p. 39-48, 2011.
295. Safran, M.R., et al., "The role of warmup in muscular injury prevention," *Am J Sports Med*, Vol. 16, p. 123-9, 1988.

296. McArdle, F., et al., "Preconditioning of skeletal muscle against contraction-induced damage: the role of adaptations to oxidants in mice," *J Physiol*, Vol. 561, p. 233-44, 2004.